Theoretical Foundations for Quantum Measurement in a General Relativistic Framework

Thesis by
Belinda Heyun Pang

In Partial Fulfillment of the Requirements for the
Degree of
Doctor of Philosophy in Physics

CALIFORNIA INSTITUTE OF TECHNOLOGY
Pasadena, California

2018
Defended May 29, 2018

Belinda Heyun Pang
ORCID: 0000-0002-5697-2162

ACKNOWLEDGEMENTS

Ends and beginnings follow in fractals,
everything's between.

I'd like to thank my advisor Yanbei Chen for his highly insightful guidance throughout the course of my research, and my family for being the fundamental constant.

And, not least, all the people who were here in this time between.

ABSTRACT

In this work, we develop theoretical formulations to analyze experimentally relevant quantum measurement schemes in a general relativistic framework, and discuss their implications versus the Newtonian or non-relativistic viewpoints. Specifically, we address (i) matter waves in simple free fall, (ii) the Mach-Zehdner atom interferometer with light-matter interaction and (iii) optomechanical systems. The motivation is to explore the regime of physics where gravity and relativistic effects become pertinent for quantum experiments due to the increase in system size and complexity. Such experiments may illuminate a way forward to reconcile the independently successful but apparently paradoxical theories of gravity and quantum mechanics, where sound theoretical foundations are necessary to help guide the search for new physics at their interface.

PUBLISHED CONTENT AND CONTRIBUTIONS

B.Pang, F. Y. Khalili, Y. Chen. Universal Decoherence under Gravity: A perspective through the equivalence principle. *Phys. Lett. Rev*, 117, 2016 DOI: 10.1103/PhysRevLett.117.090401.

B.H.P and Y.C conceived the idea, formulated the mathematical approach, and wrote the manuscript. B.H.P performed the calculations. F.Y.K offered physical insight.

TABLE OF CONTENTS

LIST OF ILLUSTRATIONS

Chapter 1

INTRODUCTION

As ongoing experimental efforts push increasingly massive systems into the quantum regime, there has been great interest in using quantum mesoscopic systems as a testbed for previously unobserved effects. One particular area of interest has been to study the quantum-classical transition, and, as part of that investigation, to look for fundamental sources of decoherence. The idea that decoherence provides a partial a bridge between the quantum and classical worlds has been developed by Wigner, Walls, Milburn, Albrecht, Hu, and Zurek among others, with the essential idea being that no system is truly closed. The claim that a quantum state evolves unitarily according to Schroedinger's equation assumes that one can completely account for all interacting degrees of freedom (dof's). If so, then there exists a pure quantum state which describes their collective behaviour, which does indeed evolve unitarily until measurement (itself a conundrum that is related to the disconnect between the quantum and classical regimes). However, as a system grows in complexity and dof's, this assumption begins to fail. If we want to limit our attention to only a subregion of the total Hilbert space, for example the spatial distribution of a large molecule subject to thermal fluctuations, radiation, bombardment by air molecules etc., then we are looking at *open quantum system*. In such a system, one can suppose that the state under study is entangled with other degrees of freedom that we do not observe, which we call its environment. The total state of the system and environment evolves unitarily and between them exist quantum correlations. If we wish now to observe the system alone, we must average over all possible states of the environment about which we have no information, and this loss of information is precisely the decoherence effect. Thus, a state initially in a quantum superposition will over time become instead a statistical ensemble. The timescale of quantum decoherence grows with the complexity of our quantum state, which is consistent with our experience that we do not observe quantum superpositions in our daily lives. It must be noted that decoherence does not entirely solve the problem of the quantum-classical transition, since it can only make the claim and an ensemble of identically prepared pure states will, due to decoherence, become a probabilistic mixture of classical states, and it does not tell us which only of the classical states we will observe in any particular instance. Nevertheless, it is an important and very

useful starting point.

A natural question to ask is then how well we can isolate a system from the environment. Can we systematically identify and shield our system from external dof's, and if so, is the lack of superimposed cats simply the result of non-optimal experimental conditions? For many physicists, this scenario seems implausible enough to motivate the search for fundamental decoherence mechanisms that cannot be eliminated even in the ideal case. For this purpose, gravity holds great appeal. For one, gravitational forces scales with mass and is therefore consistent with our intuition that macroscopic objects are classical. Additionally, Einstein's theory of gravity as the curvature of spacetime is not an environment that can be controlled or eliminated, and is therefore a natural candidate for a universally decohering mechanism.

Intimately related to decoherence is quantum measurement, which in our use refers to precision measurements of classical variables using quantum limited devices, where measurement errors are attributed to quantum uncertainty. Understanding and controlling quantum noise has enabled the detection of minute signals that can have drastic implications for our understanding of physics, nature, and the universe, with one of the most important examples to date being LIGO's detection of gravitational waves [1]. In terms of quantum noise properties, LIGO (Laser Interferometer Gravitational-Wave Observatory) is in essence an optomechanical system which detects perturbations in spacetime, and whose detections have been consistent with Einstein's theory of general relativity. Beyond observing astrophysical events in the far reaches of our universe, there is also hope of using LIGO to probe the nature of gravity and constrain alternative theories for clues in the search for a theory of everything.

Understanding the role of gravity in quantum decoherence and the quantum measurement of gravitational signals is fundamentally the same problem, at the heart of which is the effect of gravitational interactions on quantum systems. Since general relativity is our best model for gravity, an important theoretical task in this effort is to formulate quantum dynamics in a relativistically consistent way. Therein lies both the challenge and the excitement, as there are many unanswered questions and paradoxical ideas when one tries to think about quantum mechanics in tandem with general relativity. For example, a quintessential feature of quantum states is that they can be highly nonlocal, whereas one might reasonably claim that general relativity is a theory of local observers and local frames. As such, how quantum systems behave in gravity is not very well understood outside of the Newtonian limit. Furthermore,

gravity's fundamental nature remains mysterious due to the elusiveness of a full quantum theory. Thus, at the interface of quantum mechanics and gravity arises many unknowns which invites phenomenological proposals and offers the possibility of exotic effects, such the idea of probing Planck scale physics using optomechanics [55], a formulation of Einstein's Equivalence principle for quantum systems [78], the possibility of observing gravitationally induced decoherence on Earth [57], or whether spacetime can be in a superposition [50]. These exciting questions are subject of much interest and discussion as experiments progress tantalizingly close to regimes that would allow for testing.

While there are many puzzling questions when one tries to reconcile general relativity with quantum mechanics, the requirement of consistency with what is well known and accepted in both theories must still constrain frameworks which try to make predictions without violating what experiments have already confirmed. This is not always a straightforward issue, since the equations which govern the dynamics of the complex or macroscopic systems of tabletop experiments must be some form of effective or phenomenological theory in order for those equations to be at all useful. For example, it is not feasible to model the interaction of an atom with an electromagnetic field by writing down the full Lagrangian of all the fundamental fields. Instead, one models the atom as a two-level system and writes down the Jaynes Cummings Hamiltonian where the atom interacts of the EM field through a magnetic or electric dipole moment. The formulation of such frameworks is often guided by intuition and experimental results as opposed to a first principles approach. However, where there is less empirical data and where our intuition might fail (often the two are correlated), it becomes more important to ground theoretical predictions on first principles to the extent possible, precisely because one is trying to understand previously untested regimes and make potential modifications to existing theories. To account for the appearance of a new, previously unobserved effects, it is worthwhile to understand if such effects could have been predicted by the established frameworks prior to proposing modifications. Then one can be more reasonably certain if what is observed is new physics that requires changes to our understanding or nature, or if the outcome is a previously unobserved prediction from an existing framework.

Of course, general discussions of matter's interaction with gravity are by its nature limited to very simple models such as scalar fields, which are frequently insufficient to describe the behaviour of table top experiments. Therefore, to bring these general

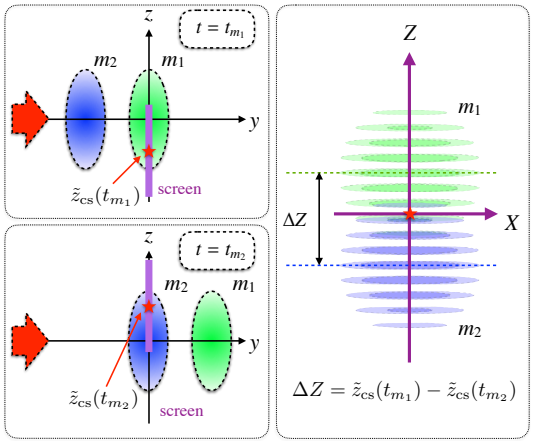

Figure 1.1: Detection results for a matter wave interferometry experiment involving molecules with internal states, where each internal state configuration is a component of the total quantum wavepacket. Snapshots taken at the times of arrival t_{m_1} and t_{m_2} for two different components (separation between the packets highly exaggerated). Positions of the screen differ at these moments (with central pixel labeled by red star whose trajectory is given by $\tilde{z}_{cs}(t)$), causing a shift in the interference pattern registered by the screen, which is best viewed in the central pixel's proper reference frame (right panel).

discussions to a more experimentally relevant regime, a preliminary step is to consider the case by case basis. There are two cases of particular interest due to the many proposals precisely aimed at use them for experimental tests of gravity: matter waves or atom interferometry and optomechanics. These form the focus of our discussions.

1.1 Covariant Formulation of Quantum Free Fall Experiements

In the spirit of maintaining consistency between the search for new physics and established theory, Chapters 2 and 3 of this thesis offers a Lorentz covariant formulation of quantum free fall experiments in line with relativistic principles. Free fall experiments involving quantum systems form the main thrust of gravity testing using quantum mechanics (examples include [12, 45, 60]) due to its relevance for testing the various formulations of equivalence principles which underpins the theory of general relativity. The motivation for this framework was to study whether and in what way a uniform gravitational field will cause decoherence in complex quantum matter, which is a very interesting idea proposed by Pikovski et. al in [57] that would have significant implications for our understanding of fundamental decoherence and the quantum-classical transition. Specifically, they proposed a thought experiment

of interfering matter waves consisting of complex molecules, which in this context means that it has internal degrees of freedom, and calculated a loss of interference fringe visibility for the matter wave evolving under gravity, which they interpret as decoherence. As we will discuss in Chapter 2, our Lorentz covariant formulation takes the point of view the molecules evolve in flat space and that gravity is accounted for by the motion of the detector. This formulation leads us to the same result as in [57] for loss of fringe visiblity, but lends itself to a *kinematic* interpretation of the result, which clarifies the source of dephasing as the shifting of the detector over the measurement time, such that different portions of the molecule imprints its signal at shifted locations on the detector (Fig. 1.1). This point of view posits that gravity is irrelevant for dephasing, since all that is necessary is relative motion between the molecules the the detector, and furthermore that quantum coherence is not irrevocably lost since full fringe visibility can be recovered if the relative motion is canceled at the time of detection (for example, if the detector was also allowed to free fall). In other words, we propose that while dephasing occurs, decoherence does not, and this interpretation has significantly different implications. While this framework was applied in the context of Pikovski's thought experiment, the ideas are quite general and can be extended to analyze existing and proposed free fall experiments which hope to measure relativistic effects.

As an extension of the work in the above relativistic treatment of pure free fall (no other interactions until measurement), in Chapter 3 we consider the atom interferometry experiments of Kasevich, Chu, Peters, Mueller, and others [35, 45, 53], which, in addition to free fall, also involves light-atom interactions. Our work provides a rigorous framework for (i) analyzing relativistic corrections to atom interferometry and quantifying the errors introduced in the approximations made in previous and often cited treatments [23, 63], which seem to be the basis for many theoretical extensions proposing to test relativistic effects [45, 60, 73]; and (ii) allow an extension to a full quantum treatment of light, which may be used to study possible back-action noise of these devices.

1.2 Optomechanics from First Principles

In the field of quantum measurement, there has been a strong push in optomechanics community over the past few years to achieve quantum limited devices for use in sensing and other applications, and there is significant interest in whether these devices are capable of measuring relativistic effects or new physics. However, to our knowledge, a first principles of the optomechanics Hamiltonian has not yet

been done, and the Hamiltonian currently in use is constructed out of the known behaviour of these systems. To date, the most foundational justification was made by C.K Law in [40], in which he constructed a Lagrangian from *a priori* equations of motion. However, it seems that in order to test for new physics, one must begin without assumptions the system's dynamics. To this end, in Chapter **??** we begin with an action and derive the equations of motion as a consequence of the variational principle. The Hamiltonian we obtain in this way differs from Law's on the order of special relativistic effects. Our formulation also has the advantage of being modular, in the sense that interactions of the optomechanical system with other degrees of freedom can be tacked on so long as they written in the form of an action. We hope that this first principles approach might be useful to the optomechanics community as they consider the possibility of using their devices to probe new physics .

1.3 LIGO and Linearized Quantum Gravity

One of the most exciting results obtained from quantum limited measurement to date is the detection of gravitational waves by LIGO. LIGO is currently quantum noise limited at high frequencies, and planned upgrades will continue to push sensitivity towards and below the standard quantum limit (SQL) . Given its sensitivity, it is natural to wonder what sorts of bounds it might be able place on modifications to gravitational theory, including quantum gravity. The theoretical challenge here is that gravity is difficult to quantize in a Hamiltonian framework, and even in the linear regime its gauge degrees of freedom pose difficulties, particularly when one is interested in studying its effects on macroscopic matter which cannot be easily represented by scalar fields. However, the problem greatly simplifies in situations where one is able to gauge fix in the transverse-traceless (TT) gauge, and in Chapter 5 we argue that this applies for LIGO and present the canonical formulation of linearized quantum gravity interactions in this gauge. The equations of motion recover the classical limit, and we additionally find a backaction effect from the GWs onto the detector that can be identified with the classical radiation reaction potential. However, in order for this potential to affect a quantum degree of freedom while preserving the operator commutation relation, gravity itself must also be quantum. The backaction effect, albeit small, is a new feature that has not previously been considered for LIGO. Additionally, despite the backaction being traceable to classical radiation reaction, the necessity of it having a quantum origin when the potential is applied to a quantum system does not appear to have been previously discussed.

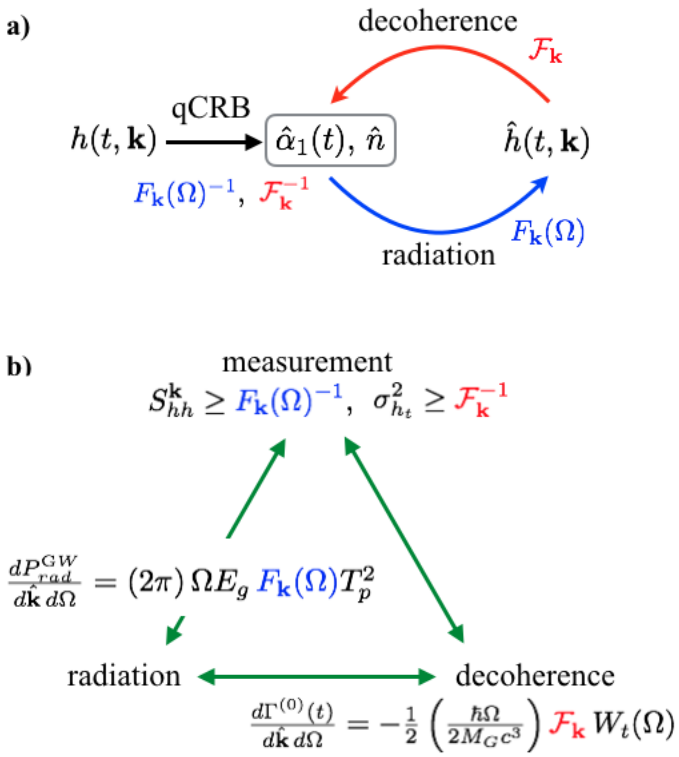

Figure 1.2: Figure a) elucidates the interactions between the GW field and the probe. For each k-mode we separate the GW field into a large classical amplitude $h(t,\mathbf{k})$ and quantum fluctuations $\hat{h}(t,\mathbf{k})$, and denote the probe degree of freedom by $\hat{\alpha}_1(t)$ (strongly pumped cavity) and $\hat{n}$ (no pumping) with the associated quantum Fisher information $F_{\mathbf{k}}(\Omega)$ and $\mathcal{F}_{\mathbf{k}}$. The action of the external classical amplitude $h(t,\mathbf{k})$ onto the probe is a measurement process characterized by the qCRB which is the inverse of the quantum Fisher information in either scenario, while action of the quantum fluctuations $\hat{h}(t,\mathbf{k})$ results in decoherence. The reverse quantum process in which the probe acts onto $\hat{h}(t,\mathbf{k})$ results in radiation. Figure b) quantifies the reciprocity relations between the three processes through the quantum Fisher information.

1.4 Reciprocity between Measurement and Decoherence

Earlier we mentioned that quantum measurement and decoherence are related, and we now elaborate on this remark. Simply stated, decoherence is the measurement of a system by an environment, which information is subsequently lost. There is thus a duality between measurement and decoherence in the sense that in the former the quantum state is the object *which measures* whereas in the latter it is the object *being measured*. However, quantum metrology mostly concerns itself with the measurement of classical quantities using a quantum state, in contrast to decoherence whose underlying mechanism is the tracing over of quantum correlations between

two fundamentally quantum systems. It is then interesting to ask what happens if we allow the signal being measured to have its own quantum fluctuations. Then it seems plausible that quantum correlations underlie both decoherence and measurement, and that there should exist a relations between measurement sensitivity and decoherence. In fact, as will be discussed in Chapter 6 , we find fundamental reciprocity relations between radiation, measurement, and decoherence for LIGO quantified by its quantum Fisher information (see Fig. (1.2)). That radiation should be related to decoherence is well known, but the link between measurement sensitivity of a quantum sensor and its decoherence due to the fluctuations of the signal field does not appear to have been previously studied. Although we derive these relations specifically for LIGO, we propose that similar relations hold generally for linear quantum measurement devices and a quantized signal field.

1.5 Outlook

As experimental progress continues towards testing gravitational effects on quantum matter, it is important to have a theoretical framework for analyzing and interpreting these results. Due to our lack of previous experimental results and intuition concerning general relativistic effects on quantum systems, there has been some significant debate over how to interpret observed or predicted experimental results. For example, the author has been party to such a debate over the interpretation of whether or not uniform gravity can cause decoherence, with analyses offered from wide ranging perspectives, from questioning its compatibility with the Equivalence Principle [11, 48], to questioning the definition of relativistic center of mass coordinates [26, 65], or accepting the interpretation of decoherence and comparing it against competing decohering sources [16]. Another example is the debate over whether atom interferometry experiments can be reinterpreted to measure the gravitational redshift using the atom's Compton frequency ω_C as a clock frequency which gives measurements of proper time of $\Delta\tau \sim 1/\omega_C$ [45], with the relativistic analysis there contested against the non-relativistic analysis using Feynman's path integral formulation of quantum mechanics [73]. With experiments involving matter waves within theoretically predicted parameter regime to test quantum free fall [12, 60], atom interferometers proposed to measure gravitational waves [30], and great interest in using optomechanics to test spacetime quantization [55] (among other examples), it is vital that we understand the subtleties when gravity interacts with quantum matter using a careful theoretical approach, so that the observed effects can be correctly interpreted.

Chapter 2

UNIVERSAL DECOHERENCE DUE TO UNIFORM GRAVITY

B.Pang, F. Y. Khalili, Y. Chen. Universal Decoherence under Gravity: A perspective through the equivalence principle. *Phys. Lett. Rev*, 117, 2016 DOI: 10.1103/PhysRevLett.117.090401.

2.1 Preface

In this chapter we analyze from a relativistic viewpoint a proposed experiment to use matter wave interferometry for detecting decoherence in Earth's gravitational field The initial proposal is due to [57] and generated much interest among the quantum measurement community because it offered the idea that uniform gravity can cause unavoidable decoherence in quantum systems, and that furthermore this effect near the testable regime. In our analysis, we take the viewpoint consistent with Einstein's equivalence principle (EEP), which states the dynamics of a system as measured by stationary observer in a constant gravitational field is the same as an that measured by an accelerating observer in flat space (no gravity). From this perspective, we offer an alternative interpretation of the proposed effect which is grounded in the kinematics of the observer and not in gravity. The apparent loss of coherence is decoherence, i.e the loss of quantum information to the enivironment, but rather dephasing due non-optimal measurement. This chapter is based on published work [48] but includes sections on quantum decoherence and Einstein's equivalence principle to provide more context for our results.

2.2 Introduction

Exciting ideas have been proposed to explore the interplay between quantum mechanics and gravity using precision measurement experiments, for example testing the quantum evolution of self-gravitating objects [75], searching for modifications to the canonical commutation relation [55], and studying the propagation of quantum wavefunctions in an external gravitational field [14, 79]. There have also been proposals for the emergence of classicality through gravitationally induced decoherence, such as from an effective field theory approach [10, 28] or the Diósi-Penrose model [24, 51]. Pikovski et al. recently pointed out that a composite quantum particle, prepared in an initial product state between its "center of mass" and its

internal state, will undergo a decoherence process with respect to its spatial degrees of freedom in a uniform gravitational field — as exhibited by a loss of contrast in matter-wave interferometry experiments, whose loss depends on the gravitational acceleration g [57]. They attributed this effect to gravitational time dilation, and proposed this as a universal decoherence mechanism for composite particles. This interpretation has significant implications and has been the subject of lively debate [4, 11, 25, 56].

According to Einstein's Equivalence Principle (EEP), freely falling experiments cannot detect the magnitude of gravitational acceleration [71]. Of course, the thought experiment in Ref. [57] is not in free fall: although there is no physical detector in their setup, implicitly their detection process occurs in an accelerating lab. This means their result is not necessarily in contradiction with the EEP. Nevertheless, it is still interesting to explain why the dephasing, which takes place during the particle's *free* propagation, has a rate determined by gravity. Furthermore, since EEP implies that gravity is equivalent to acceleration, the idea of decoherence induced by uniform gravity suggests that the motion of an accelerated observer affects the evolution of a quantum system in such a way that causes decoherence, which is an idea that begs clarification.

At this point, we note that calculating the dephasing of wavefunctions in the Lab frame as in Ref. [57] mixes the observed effects due to propagation and those due to acceleration of the detection frame. In this paper, we will separate these two processes by providing a description of both the system and measurement process in free falling Lorentz frames which can be extended globally to Minkowski coordinates. In a Lorentz frame, the internal states of the composite particle do not interact with external potentials or each other, and are distinguished only by their rest mass m. Therefore we can treat each internal state as an independent, freely propagating particle species labeled by m. The particles are measured in a detector frame with relative motion, where specializing to a uniformly accelerating detector frame recovers the case of gravity. The overall measurement outcome is the trace over all species. Using this framework, we model a physical realization of the (1+1)d thought experiment of Ref. [57]. In (3+1)d, we consider a particle beam propagating along one direction, being measured by a screen travelling along an arbitrary trajectory in a transverse direction [Fig. 2.3]. Due to the mass dependence of de Broglie wave dispersion, where $\omega_k \approx k^2/2m$, the packets have different propagation velocities and will arrive at the detector at different times. This means

that the pattern registered by the *m*oving detector for each species will be spatially shifted along the direction of detector motion [Fig. 2.4]. This is equivalent to a mass dependent phase shift that will result in the blurring of interference fringes when all patterns are summed. Here, the motion of the detector will determine the size of spatial the shifts, and therefore determines how much blurring occurs. This explains the appearance of g in the dephasing rate of Ref. [57], since it controls the motion of the screen for the case of uniform gravity. In this view, the source of dephasing is mass dependent dispersion, which appears as a loss of quantum coherence due to a *k*inematic effect of detector motion. To emphasize that it is not gravitational, we predict dephasing even in the absence of gravity for a detector with uniform velocity. This insight allows us to understand the thought experiment of Ref. [57] without referring to time dilation: there, the interference pattern generated by each species has a mass dependent spatial wavevector, again due to dispersion. The dephasing is larger as one moves farther away from the center of the superposition. If we observe the state at a constant coordinate position in the Lab frame, then the effect of a moving Lab move farther away from its center. Mathematically, this corresponds to Ref. [57]'s calculation of the correlations between constant coordinate values z_1 and z_2, initially near the center, at some later time in the Lab frame. Therefore g again appears in the dephasing rate via the Lab frame's motion.

The Lorentz frame approach provides a simple way to understand the dephasing. However, a rigorous calculation requires a description of the system and measurement as Lorentz covariants, since Lorentz symmetry is a property required in our discussion of frame independent physics viewed by arbitrary observers. We develop our formalism in this fully relativistic way, although we find that relativistic effects are ignorable, and the non-relativistic limit completely reconstructs the effect found in Ref. [57]. In this analysis we have assumed EEP to hold. We point out comparison of this approach with an explicit treatment of gravity as an modified external force field offers possibilities to test for EEP violations in the quantum regime. For our calculations and results we have set $\hbar = c = 1$.

2.3 Einstein's Equivalence Principle

In this section we give a brief background on Einstein's equivalence principle with a focus on efforts to extend EEP into the quantum regime. Much of this information, particularly regarding the tests of classical EEP, can be found in [71].

The EEP is the underpinning of Einstein's theory of General Relativity and must

hold for any metric theory of gravity. It can separated into three components: 1) that the effects of gravity on a object is independent of its composition, or the Weak Equivalence Principle; 2) that local non-gravitational physics is independent of the velocity of the observer, otherwise known as Local Lorentz invariance (LLI); and 3) local non-gravitational physics is independent of the position of the observer in spacetime, otherwise known as Local Position Invariance (LPI). The three principles combined can be intuitively summarized by the following statement: that the outcomes of experiments in local gravity of magnitude g are the same as the outcomes of experiments occurring in the absence of gravity as measured by an observer accelerating at the same magnitude.

Since EEP must hold for general relativity, or indeed, for any metric theory of gravity, any violations would imply that GR is only an approximate theory and will fail in certain regimes. Therefore, test of EEP are crucial for those interested in alternative theories of gravity. Some classic experiments include the torsion balance experiment first conducted by Eötvös which looked for the difference between gravitational and inertial mass, or the Michelson-Morley experiment which tested Lorentz invariance. More recently, quantum experiments have been proposed for tests of EEP, such as matter wave interferometry to test WEP [12]. Atom interferometry experiments have also been proposed as a way to look for deviations in gravitational redshift [45] which, if found, can be attributed to LPI violation. The applicability of the proposed experiment as a measure of the gravitational redshift to the sensitivity claimed by the authors is a matter of some controversy [73]. We emphasize that the role of gravity in the analysis of these quantum experiments is classical the sense that the quantum particles fall along classical geodesics, and as such they are tests of the *classical* EEP using a quantum measurement device.

Increasingly, the interest in quantum mechanics and EEP has extended from the quantum measurement of a classical effect to the understanding of how EEP applies in the context of quantum theory. Some obvious issues arise in trying to reconcile quantum mechanics with GR, even aside from the challenges of quantizing gravity itself. For example, in quantum mechanics states of matter is fully described by its wavefunction which evolves according to Schroedinger's equation, neither of which is Lorentz invariant. Although quantum field theory provides a Lorentz invariant framework, its use has been large limited to describing the outcomes of scattering experiments of fundamental particles, and it is often unclear how to formulate interactions between macroscopic matter in the second quantization

formalism. Furthermore, Heisenberg's uncertainty principle and superpositions in quantum mechanics is in fundamental conflict with the idea of a local rest frame. For example, consider the quantum state in a superposition of position states, represented schematically as

$$|\psi\rangle = \frac{1}{\sqrt{2}}\left(|x_1\rangle + |x_2\rangle\right) \tag{2.1}$$

Where is its rest frame? If there are tidal forces over the extent of the wavefunction, how would the state evolve? Which geodesics would it follow?

As an example of this line of questioning, Viola and Onofrio [68] analyzed a gedanken experiment of weak equivalence principle for freely falling quantum objects. For classical objects, free fall experiments requires that two objects with different inertial masses be prepared at the same position and velocity, and their respective time of flights to a fixed location is recorded. The paths of the objects are given by

$$z_j(t) = z_0 + v_0 t - \frac{1}{2}\frac{m_g^{(j)}}{m_i^{(j)}} g t^2 \tag{2.2}$$

where $j = 1, 2$ is the object label, g is the magnitude of gravitational acceleration, m_i denotes inertial mass, and m_g denotes gravitational mass. Then, for $m_i^{(1)} \neq m_i^{(2)}$, the objects will nevertheless follow the same paths as long as gravitational and inertial masses are the same. Of course, in quantum mechanics position and momentum (velocity) must obey the uncertainty principle, and so the constraint for the quantum experiment is that the two quantum states must have the same initial expectation values for momentum and position, or

$$\langle \hat{z}(0)\rangle_{\psi_1} = \langle \hat{z}(0)\rangle_{\psi_2} \tag{2.3a}$$

$$\langle \hat{p}(0)\rangle_{\psi_1} = \langle \hat{p}(0)\rangle_{\psi_2} \tag{2.3b}$$

This above condition is rather subtle in quantum theory because, as noted in [68], differences in expectation values can arise from quantum coherence. For example, for a Schroedinger cat state involving a superposition of two spatially Gaussian states with coefficients c_+ and c_-, the expectation values for position and momentum depends on their relative phase as well as their magnitudes. Supposing however that the conditions in Eq. (2.3) are satisfied, Viola and Onofrio find that the time of flight distributions by the expectation value $T^{(j)}$ and standard deviation σ^j

$$T^{(j)} \pm \sigma^{(j)} = \sqrt{2\frac{m_i^{(j)}}{m_g^{(j)}}\frac{z_0}{g}} \pm \epsilon\frac{\hbar}{\Delta_0 m_g^{(j)} g} \tag{2.4}$$

where ϵ is a state dependent numerical factor (e.g. for either Gaussian or cat states) and Δ_0 is the initial spatial spread of the wavefunction. As seen in Eq. (2.4), when inertial and gravitational masses are equal the two objects will have the same average time of flight, even when the initial state is is a highly non-classical cat state, while their spread is mass dependent. Viola and Onofrio further argue that when $m_g = m_i$, the mass dependent spread can be attributed to the kinematic effect of a non-inertial observer.

In deriving Eq. (2.4), Viola and Onofrio used the standard Schroedinger's equation for evolution in a gravitational field with distinct inertial and gravitational masses.

$$i\hbar\frac{\partial}{\partial t}\psi(z,t) = \left(-\frac{\hbar^2}{2m_i}\partial_z^2 - m_g g z\right)\psi(z,t) \tag{2.5}$$

More recently, Zych and Bruckner [78] proprosed a quantum formulation of the equivalence principle whereby the rest, inertial, and gravitational masses are promoted to operators. This seems to be a phenomenological proposal based on the extension of the idea of rest mass and energy equivalence. Then, an energy eigenstate is not only associated with a rest mass value, but also and gravitational and inertial mass value, where all three parameters can be distinct. The corresponding rest, gravitational, and inertial mass operators would then be capable of addressing coherences between superposition of energy eigenstates with respect to their mass values.

The above proposals analyze quantum systems in Newtonian gravity using the standard picture of Schroedinger evolution, with phenomenological modifications to include relativistic effects (i.e mass energy equivalence) in the case of [78]. However, in the discussion of EEP it is also useful to see how quantum systems behave in the equivalent viewpoint, where the system is evolving in flat space with no gravitational forces, but the lab and measurement devices are accelerating, to compare the results when the Equivalence principle holds. For example, the predictions of [68] should be the same in both viewpoints when $m_i = m_g$, and those of [78] using their phenomenological Hamiltonian should be the same when each energy eigenstate have the same mass values (with Lorentz factors relating rest and inertial masses). The alternative viewpoint can be formulated using quantum field theory in flat space and, crucially, is consistent with Lorentz invariance, which underpins concepts such mass-energy equivalence and allows for a rigorous discussion of relativistic effects. Deviations between the two viewpoints when the equivalence principle should hold (i.e when inertial and gravitational masses are equal) indicates some violation of

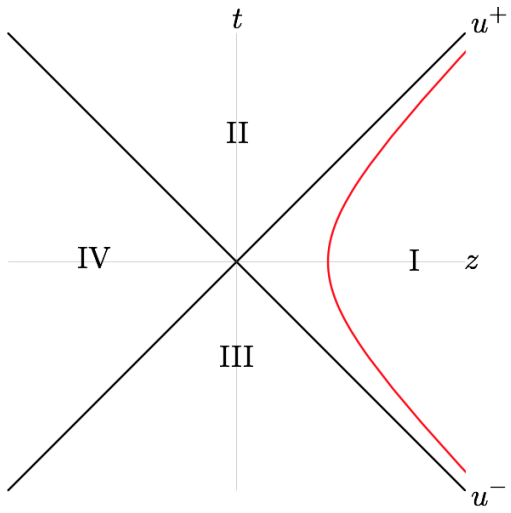

Figure 2.1: The trajectory of a uniformly accelerating observer (Rindler observer) embeds in Minkowski spacetime as a hyperbolic trajectory (red). Spacetime is separated in four regions by the null surfaces u^+ and u^-, which respectively are the future and past Cauchy horizons that divide spacetime into four regions: region I can exchange information with the Rindler observer; region II can receive but not send; region III can send but not receive; and region IV can neither send nor receive.

EEP that merits further study. Thus, investigations of general relativistic effects in quantum experiments, and in particular those that look for violations, should be conducted in parallel from both viewpoints the check for the consistency of the predictions or looks for the sources of contrast.

2.4 Newtonian Gravity as Flat Spacetime in an Accelerated Frame

The claim that in general relativity constant gravity is locally equivalent to an uniformly accelerating observer (also called a Rindler observer) in flat space can be mathematically substantiated by writing the metric for flat spacetime using the proper frame coordinates of the accelerating observer (Rindler metric).

In Minkowski coordinates $x^\mu = (t, x, y, z)$, the metric of flat spacetime is simply the Minkowski metric

$$ds^2 = -c^2dt^2 + dx^2 + dy^2 + dz^2 \tag{2.6}$$

In these coordinates, the trajectory $x_a^\mu(\tau)$ of a uniformly accelerating observer as a function of the observer's proper time τ is given by

$$[t_a(\tau), z_a(\tau)] = \left[\frac{c}{g}\sinh\left(\frac{g\tau}{c}\right), \frac{c^2}{g}\left(\cosh\left(\frac{g\tau}{c}\right) - 1\right)\right] \tag{2.7}$$

Its embedding in Minkowski space is shown in Fig.[2.4]. We've ignored the x, y directions because these are not the directions of observer motion and experiences no transformations. The above trajectory can be derived by noting that

$$\frac{dx^\mu}{d\tau} = u^\mu, \quad \frac{du^\mu}{d\tau} = a^\mu \tag{2.8}$$

and that there exist algebraic relations between the components of acceleration and velocity given by

$$\vec{u} \cdot \vec{u} = -1, \quad \vec{a} \cdot \vec{u} = 0, \quad \vec{a} \cdot \vec{a} = -g^2 \tag{2.9}$$

where the first two conditions in Eq. (2.9) always holds for any 4-velocity and the last condition is simply the statement that the acceleration is at constant value g. When evaluated in Minkowski coordinates with the Minkowski metric and the obtained relations are substituted into the differential equations in Eq. (2.8), along with the initial condition that $z_a(\tau) = 0$, one easily obtains the trajectory in Eq. (2.7), which we remark is hyperbolic

We now construct the observer's proper frame, by which we mean the following:

1. The basis vectors are orthonormal, meaning that $\vec{e}_\alpha \cdot \vec{e}_\beta = \eta_{\alpha\beta}$, where the subscript denotes *which* vector and not vector components.

2. The timelike vector is parallel to the observer's 4-velocity, or $\vec{e}_0 = \vec{u}$. This condition is equivalent to the claim that the observer must be at rest in the proper frame.

3. The basis vectors (or tetrad) must be non-rotating as it is transported along the observer's trajectory such that a gyroscope that the observer carries would remain stationary. For the accelerating observer, this condition means that the basis vectors follow the transport rule

$$\frac{d}{d\tau}\left(\hat{e}_\alpha\right)^\mu = \left(u^\mu a^\nu - u^\nu a^\mu\right)\left(\hat{e}_\alpha\right)_\nu \tag{2.10}$$

The three conditions above describe Fermi-Walker transport and give us the tetrad of the observer's proper frame at any point along its trajectory. Explicitly, the basis vectors in Minkowski coordinates have the following form

$$\begin{aligned}\left(\hat{e}_\tau\right)^\mu &= \left[\cosh\left(\frac{g\tau}{c}\right), \sinh\left(\frac{g\tau}{c}\right), 0, 0\right] \\ \left(\hat{e}_Z\right)^\mu &= \left[\sinh\left(\frac{g\tau}{c}\right), \cosh\left(\frac{g\tau}{c}\right), 0, 0\right]\end{aligned} \tag{2.11}$$

where τ and Z are labels in the proper frame. We can construct a coordinate system from the tetrad of the proper frame a spacetime point with Minkowski coordinates x^μ by noting the the spatial basis vectors at all points along the observers trajectory form spatial hypersurfaces which foliate the region of spacetime where the accelerating observer can send and receive information (the so-called Rindler wedge which is within a distant c^2/g from the observer). For an event within the wedge that occurs on the hypersurface at time τ, its coordinates are given by

$$x^\mu = \xi^k \left[\hat{e}_k(\tau)\right]^\mu + z_a^\mu(\tau) \tag{2.12}$$

where the k index runs over spatial dimension and ξ_k is the distance from the observer to the event along the spatial basis vector $\hat{e}_k(\tau)$. We now take the quantities (τ, ξ_k) which specify the event's spacetime location to be the coordinates of our proper frame. Substituting the expressions for $z_a^\mu(\tau)$ given in Eq. (2.7) and the basis vectors given in Eq. (2.11), the coordinate transformation from flat Minkowski $x^\mu = (t, x, y, z)$ to the observer's proper frame $X^\mu = (\tau, X, Y, Z)$ is straightforwardly given by

$$\begin{aligned} t &= \frac{c}{g}\left(1 + \frac{gZ}{c^2}\right)\sinh\left(\frac{g\tau}{c}\right) \\ z &= \frac{c^2}{g}\left(1 + \frac{gZ}{c^2}\right)\cosh\left(\frac{g\tau}{c}\right) - \frac{c^2}{g} \\ x &= X \\ y &= Y \end{aligned} \tag{2.13}$$

from which we obtain the form of the metric in the coordinates of the observer's proper frame

$$g_{\mu\nu} = \eta_{\rho\sigma}\frac{\partial x^\rho}{\partial X_\mu}\frac{\partial x^\sigma}{\partial X_\nu} \tag{2.14}$$

or explicitly

$$ds^2 = -c^2\left(1 + \frac{gZ}{c^2}\right)^2 d\tau^2 + dX^2 + dY^2 + dZ^2 \tag{2.15}$$

We emphasize that these coordinates do not cover all of spacetime. Referring to Fig.[2.4], a positively accelerating observer can only exchange information with events occurring in region I, and therefore the coordinates we've constructed is also only valid in this region and fail at distances $\sim c^2/g$. However, this is not a consideration for us since the experiment takes place well within the neighbourhood of the observer where the proper frame coordinates can be use.

Let us now compare this with the metric for a constant gravitational potential. The spacetime metric on Earth is given by the weak field limit of the Schwarzchild metric, which is the unique solution to Einstein's field equations for spherically symmetric vacuum up to one constant which bears the interpretation of mass. The full metric is given in Schwarzchild coordinates by:

$$ds^2 = -c^2\left(1 - \frac{R_S}{r}\right)dt^2 + \left(1 - \frac{Rs}{r}\right)^{-1} dr^2 + r^2 d\Omega^2, \quad R_s = \frac{2GM}{c^2} \tag{2.16}$$

where R_s is the Schwarzchild radius. In the weak field limit at $r \gg R_s$ the leading order correction is the R_s/r term in the g_{00} component (although the g_{rr} takes similar form, since it is the spatial component of the tensor it is $O(c^{-2})$ compared to g_{00}). Defining $\Phi = -GM/r$ we recognize that it is the Newtonian potential. Then, expanding Φ around $r_0 + Z$ for $Z \ll r_0$ and introducing the coordinates $\tau = t$, $X^2 + Y^2 + Z^2 = r^2$, we finally write

$$ds^2 \approx -c^2\left(1 + 2\frac{GM}{c^2 r_0^2}Z\right)d\tau^2 + dX^2 + dY^2 + dZ^2 \tag{2.17}$$

which is the same as the leading order expansion in gZ/c^2 of the metric in Eq. (2.15), with $g = GM/r_0$.

Here we have shown the the metric in the proper frame of an accelerated observer (in which the observer is at rest) is the same to leading order as the Schwarzchild metric outside a spherically symmetric mass, and thus the claim of EEP is mathematically substantiated. Although the Schwarzchild spacetime has curvature and is therefore fundamentally different from flat space, when considering constant local gravity the effects of curvature are ignored. The point here is that if we limit ourselves to a region where gravity is constant, then that region of spacetime is in fact flat and the different forms of the metric in Eqs. (2.6) and (2.17) are due to a *coordinate transformation*. An experiment which occurs in the weak field limit versus an experiment occurring in flat space being measured by a uniformly accelerating observer are simply different coordinate description of the same physics. Since any physical quantity must be coordinate invariant, the measurement outcomes obtained in either coordinate system must be the same if the EEP holds.

2.5 Quantum Decoherence

Since the focus of this work on the possibility of uniform gravity being a decoherence mechanism, it is useful to have a general discussion of quantum decoherence (in a nonrelativistic viewpoint) to give the reader some background of the concept.

Much of this discussion can be found in textbook resources on quantum noise and measurement such as [13]. Fundamentally, decoherence can be view as the loss of quantum information for a system entangled with an environment that has infinite degrees of freedom. While the total state vector (system plus bath) evolves unitarily, no experiment would have access to all the environmental degrees of freedom (dof's) necessary to reconstruct the complete quantum state, and instead limits its attention to a number of finite dof's (the system). Mathematically, the inability to measure the remaining degrees of freedom is represented by tracing over them. Thus, we may begin with the following pure quantum state of a system

$$|\psi(0)\rangle = \sum_n a_n |n\rangle \tag{2.18}$$

where $|n\rangle$ is a complete basis for the system's Hilbert space. Then the initial total quantum state (including the environment, or bath) is given by

$$\hat{\rho}(0) = \hat{\rho}(0)_s \otimes \hat{\rho}_B(0) = \sum_{m,n} a_m a_n^* |m\rangle\langle n| \otimes |\phi(0)\rangle\langle\phi(0)| \tag{2.19}$$

where ρ_B is the state of the bath at initial time, which we've assumed to be a pure state (this can be easily extended to mixed states). Suppose then that the total state evolves according to the Hamiltonian

$$H = H_s + H_B + H_{\text{int}} \tag{2.20}$$

and for simplicity, let us assume that the basis $|n\rangle$ we have chosen for the system's Hilbert space is backaction evading with respect to the interaction, so that $[\rho_s(0), H_{\text{int}}] = 0$. Then (in the interaction picture so $H_{\text{int}} \to H_I$) the total state evolves as

$$\rho(t) = \sum_{m,n} a_m a_n^* |m\rangle\langle n| \otimes |\phi_n(t)\rangle\langle\phi_m(t)| \tag{2.21}$$

We notice that the total state now is *entangled* and no longer separable into the form of a product state as in Eq. (2.19). The system has developed quantum correlations with the bath through their interaction, and its quantum state is now given by

$$\hat{\rho}_s(t) = \text{Tr}_B\{\hat{\rho}(t)\} = \sum_{nm} a_m a_n^* |m\rangle\langle n| \langle|\phi_m(t)|\phi_n(t)\rangle \tag{2.22}$$

where the quantum coherences represented by the off diagonal terms $a_m a_n^*$ is now weighted by the overlap $\langle\phi_m(t)|\phi_n(t)\rangle \leq 1$. Therefore, the quantum coherences decay, while the diagonal terms (which represent probabilities) are unaffected. The system is now a mixed state, as seen by the fact that $\text{Tr}[\hat{\rho}_s(t)^2] < 1$.

The above analysis illustrates the physical mechanism for decoherence. Often, approximations are made so that one can write down an evolution equations for the system state itself, without considering first the evolution of the total state and then tracing over the bath. In general, the time evolution of the system state in the present of coupling to an environment is represented by a non-unitary map of its density matrix, written in differential form as

$$\frac{d}{dt}\hat{\rho}_s = \mathcal{L}(t)\hat{\rho}_s(t) \tag{2.23}$$

with the solution

$$\hat{\rho}(t) = T\left[\exp\left(\int_{t_0}^{t} d\tau\ \mathcal{L}(\tau)\right)\right]\hat{\rho}(t_0) = V(t,t_0)\hat{\rho}_s(t_0) \tag{2.24}$$

where T is the time ordering operator. Under certain physical approximations, the map $V(t)$ has the semigroup property

$$V(t)V(t') = V(t+t') \tag{2.25}$$

which intuitively corresponds to the idea that the propagation of $\hat{\rho}_s$ over a certain time interval does not depend on the time at which the propagation occurs. In this case, the system's evolution can be written in what is called Lindblad form

$$\frac{d}{dt}\hat{\rho}_s = -i[H,\hat{\rho}_s] + \sum_k \gamma_k\left(\hat{L}_k\hat{\rho}_s(t)\hat{L}_k^\dagger - \frac{1}{2}\left\{\hat{L}_k^\dagger\hat{L}_k, \hat{\rho}_s(t)\right\}\right) \tag{2.26}$$

where $\hat{L}_k$ are known as the Lindblad, or jump, operators and γ_k is a decay rate associated with dissipation and decoherence, depending on whether they affect the diagonal or off-diagonal elements of the density matrix in a particular basis (e.g if $\left[\hat{L}_k, |n\rangle\langle n|\right] = 0$ then there is only pure decoherence in the $|n\rangle$ basis). We point out the Eq. (2.26) is local in time and has no reference to the external bath.

The series of approximations that can produce the Lindblad equation from Schroedinger's equation are as follows:

1. Weak coupling between the system and the bath, such that the evolution can be described perturbatively to second order in the interaction strength, as below (from Schroedinger's equation in the interaction picture)

$$\frac{d}{dt}\hat{\rho}_s(t) = -\int_0^t d\tau\ \mathrm{Tr}_B\left\{\left[\hat{H}_I(t),[\hat{H}_I(\tau),\rho_s(\tau)]\right]\right\} \tag{2.27}$$

where the interaction Hamiltonian has the general form (in the Schroedinger picture)

$$H_{\text{int}} = \sum_i \hat{A}_i \hat{B}_i, \quad H_I(t) = \hat{U}_0^\dagger(t) \hat{H}_{\text{int}} \hat{U}_0(t) \tag{2.28}$$

where $\hat{U}_0(t)$ is the evolution operator with respect to the free system and bath Hamiltonians.

2. A large reservoir for which can assume, when combined with the weak coupling assumption, that its interactions with the system does not effect its behaviour over coarse-grained timescales which are relevant to the experiment (i.e the timescale of system dynamics τ_s), so that $\hat{\rho}_B(t) = \hat{\rho}_B(0)$ and the total state of system and bath at anytime is approximately a product state

$$\hat{\rho}(t) \approx \hat{\rho}_s(t) \otimes \hat{\rho}_B \tag{2.29}$$

This above equation is known as the Born approximation. We point out that this does not mean the system and bath are not entangled - after all, the entanglement is necessary for decoherence. Rather, the Born approximation is the idea that the bath equilibrates upon perturbation on timescales $\tau_B \ll \tau_s$ such that one cannot resolve in time changes to its state.

3. The same underlying physical assumption of fast bath equilibrium times also gives us the Markov approximation, which replaces $\hat{\rho}_s(\tau)$ in Eq. (2.27) by $\hat{\rho}_s(t)$, so that the evolution is now local in time. The justification is that, because the bath equilibrates so quickly, it forgets about the system's history. Since apart from the bath, the system's time evolution is unitary and itself independent of its own history, then its evolution given interactions with a memoryless bath is likewise local in time.

4 . Finally, the assumption that $\tau_B \ll \tau_s$ allows us to extend the lower limit of integration $t = 0$ to $t \to -\infty$ since the initial state of the bath should not affect how the system evolves in the next time step. The approximations above are grouped together due to their reliance on the underlying assumption of Markovianity (along with weak coupling), and are together known as the Born-Markov approximations. They give us the Markovian master equation

$$\frac{d}{dt}\hat{\rho}_s(t) = -\int_0^\infty d\tau \ \text{Tr}_B \left\{ [H_I(t), [H_I(t-\tau), \hat{\rho}_s(t) \otimes \hat{\rho}_B]] \right\} \tag{2.30}$$

5. At this point, one can obtain the Lindblad equation if the bath is δ-function correlated, or

$$\mathrm{Tr}\left\{\hat{\rho}_B \hat{B}_i(t)\hat{B}_j(t')\right\} \propto \delta(t-t') \tag{2.31}$$

which implies that the bath has a white spectrum. However, this may not be the case for a general Markovian bath. To guarantee that Eq. (2.30) can take the Lindblad form of Eq. (2.26) for colored noise, one must additionally make the secular approximation in which one assumes that the system has eigenoperators $\hat{A}_j$ that have discrete frequencies ω_j for which $(\omega_j - \omega_{j'})\tau_B \gg 1$, and the rotating wave approximation that throws out any term oscillating at $\Delta\omega$. In this case, the Markovian master equation takes the form of Eq. (2.26) with

$$H \to \sum_j G(\omega_j)\hat{A}_j^\dagger \hat{A}_j, \quad \hat{L}_j \to \hat{A}_j \tag{2.32a}$$

where H represents a renormalization of the system's energy eigenstate (such as the Stark shift), with $S(\omega_j)$ given by the bath's correlation function, or

$$G(\omega_j) = \frac{1}{2i}\left[\Gamma(\omega_j) - \Gamma^*(\omega_j)\right] \tag{2.32b}$$

for

$$\Gamma(\omega_j) \equiv \int_0^\infty d\tau\ e^{i\omega_j\tau}\langle \hat{B}_j^\dagger(t)\hat{B}_j(t-\tau)\rangle \tag{2.32c}$$

The real part of Γ gives us the decay rate is the noise spectral density of the bath and gives us the decay rate

$$\gamma(\omega_j) = \Gamma(\omega_j) + \Gamma^*(\omega_j) \tag{2.32d}$$

We point out that we have made the additional assumption that the bath is stationary, or $[H_B, \hat{\rho}_B] = 0$ such that the bath correlation function depends only on the time difference.

It is important to note that the bath must have a continuum of modes in order for true decoherence to occur. For a finite number of modes, the bath operator can be written as (in some basis)

$$\hat{B}(t) = \sum_n^N \hat{b}_n e^{-i\omega_n t} \tag{2.33}$$

Then bath correlation function $\langle \hat{B}_j(t)\hat{B}_j(t-\tau)\rangle$ is essentially a finite sum over waves with different periodicities and is therefore itself periodic. The system state $\hat{\rho}_s$ then

has a finite Poincare recurrence time and no decoherence can have occurred, since decoherence is fundamentally an irreversible process.

In reviewing this formalism, we wanted to emphasize the underlying physical processes which cause decoherence, as well as the rather specific (albeit experimentally relevant) situations in which the Lindblad equation is a valid description of the system's evolution.

2.6 A summary of Pikovski's proposal

In this section we will summarize the proposal of Pikovski *et. al* in [57] and outline some of the questions it raised in the context of quantum decoherence and EEP discussed in the previous sections. Pikovski et. al considered composite particles involving internal degrees of freedom evolving under a uniform gravitational field. The internal degrees of freedom is described by the Hamiltonian H_0, and the total mass, by mass-energy equivalence, is given by

$$\hat{m}_{tot} = m_0 + \hat{H}_0/c^2 \tag{2.34}$$

where m_0 is some bare mass (i.e the rest mass of the particle in its ground state with respect to H_0). Since H_0 is an operator, the particle's rest mass becomes a degree of freedom in the total Hilbert space. Then the total composite particle evolves with the Hamiltonian

$$H = H_{cm} + H_0 + \left(m_0 + \frac{H_0}{c^2}\right) gx \tag{2.35}$$

where H_{cm} refers to the Hamiltonian for the center of mass (COM) degree of freedom. Then, proposing a diffraction type matter wave interferometry thought experiment whereby these composite particles are prepared in an initial superposition in position space and a thermal distribution with respect to the internal energy states, they obtain the result the the visibility $V(t)$ of the interference fringes will decay according to

$$V(t) \approx e^{-(t/\tau_{\text{dec}})^2} \tag{2.36}$$

for the decoherence timescale

$$\tau_{\text{dec}} = \sqrt{\frac{2}{M}} \frac{\hbar c^2}{k_b T g \Delta x} \tag{2.37}$$

where T is the equilibrium temperature of thermal internal state distribution and N is the number of internal degrees of freedom. Their interpretation of this loss of visibility is that the gravitational time dilation caused the spatial superposition

of the composite particle to decohere, and is a general effect not limited to matter wave interferometry, but applicable to any quantum particle with internal states. To paraphrase [57], a quantum particle travelling along a superposition of two worldlines accumulates phase according to their proper times. When the worldlines are along different heights in a gravitational potential, the proper times between the upper and lower paths are not equal, such that for the measurement time t the difference in proper time is given by $\Delta\tau = g\Delta z t/c^2$ and a corresponding phase difference of $\Delta\phi = m\Delta\tau$. Then, if the particle furthermore has internal energy states, the phase differences between the two paths are mass dependent. Without being able to distinguish between different mass states, one performs a trace over the internal state and the visibility is thus given by

$$V(t) = |\langle e^{iH_0\Delta\tau}\hbar\rangle| \tag{2.38}$$

where the average is taken over the internal dof's.

Here we comment that effectively, Pikovski et. al has separated the composite particle in a "system" degree of freedom (the center of mass), and the "bath" degree of freedom (the internal energy states). Indeed, in their paper they write down the following master equation [Eq. (6)]

$$\dot{\rho}_{cm}(t) \approx -\frac{i}{\hbar}\left[H_{cm} + \left(m_0 + \frac{E_0}{c^2}\right) gz, \rho_{cm}(t)\right] - \frac{\Delta E_0 g}{\hbar c^2} t\,[z,[z,\rho_{cm}]] \tag{2.39}$$

where

$$E_0 = \langle H_0\rangle, \quad \Delta E_0^2 = \langle H_0^2\rangle - \langle H_0\rangle^2 \tag{2.40}$$

which, by its Lindblad form, suggests that decoherence with respect to the position basis always occurs when internal states are involved, and is therefore universal. There is some question as to how to identify a COM degree of freedom for a composite particle[65], but supposing this is possible, there are a few questions that arise from Eq. (2.39). Referring back to the previous section which discussed the underlying physics for quantum decoherence, we point out that for the evolution of the system state to take the Lindblad form the bath must be 1) Markovian and weakly coupled and 2) either has a white noise spectrum or the secular approximation must apply and 3) must have a continuum of modes for true (irreversible) decoherence to occur. Failing to meet the first two conditions invalidates the derivation of the Lindblad equation from Schroedinger's equation. Failing to meet the third mean that coherence reappears on finite timescales. The third condition is less problematic because one can say the particle is so large that Poincarre recurrence occurs on

timescales unobservable in experiment. However, the first two merits some consideration. For the first condition, as pointed out by the authors themselves, "evolution in the presence of gravitational time dilation is inherently non-Markovian". The "bath" must remember the phase that it accumulated over the particle's trajectory, or in other words, it must remember the history of the system state. As for the second, the white noise spectrum is impossible for a finite number of modes. Even supposing the particle to be so large that the number of degrees of freedom is effectively infinite, it is difficult to see why in general the noise spectrum would not be colored, as this seems to be system dependent. If the spectrum is not white then the secular approximation, which requires the Lindblad operator to have a discrete spectrum, must hold, but clearly z is continuous.

The above discussion concerns technical details in deriving the decoherence effect. More fundamentally however, in view of the equivalence principle it is interesting to consider how a constant gravitational field can cause an irreversible change to the quantum state. In other words, since decoherence is the loss of information, how can the acceleration of an observer (which under EEP is equivalent to gravity) cause the quantum state to lose information? Therefore, it is worthwhile to understand whether and how the loss of visibility predicted in [57] appears in the equivalent viewpoint of an accelerating observer.

2.7 Relativistic Formulation of Quantum State Evolution and Measurement

In standard quantum mechanics, a complete description of any quantum system can be given by its wavefunction and evolved in time using Schroedinger's equation. Measurement is described by a positive operator-valued measure (POVM) such that the probability of obtaining the measurement outcome x for a quantum state ρ is given by

$$P(x) = \mathrm{Tr}(\rho E_x) \tag{2.41}$$

where E_x is Hermitian, positive, and complete. In the simplest case, a POVM is simply an orthogonal basis of the system and probability of measurement outcomes is the trace of the direct projection of the system state onto this basis. More generally, any POVM can be realized as the projection of a measurement device that is entangled with the system by unitary evolution onto an orthogonal basis spanning the device's Hilbert space. The POVM for an interference experiment whose outcome is the spatial distribution is the set of operators $\{|\mathbf{x}\rangle\langle\mathbf{x}|\}$ where $\mathbf{x}$ denotes position. However, in a relativistic setting the wavefunction, Schroedinger's equation, and the spatial POVM are all problematic because they violate Lorentz

invariance and cannot be applied if one wants to compare measurement outcomes between inertial and non-inertial frames. Therefore, our first task is to formulate a Lorentz covariant description of the system, its evolution, and the measurement process, and we do so in the Lorentz frame with Minkowski coordinates $x^\mu = (t, x, y, z) = (t, \mathbf{x})$.

Experimental setup in the Lorentz frame

In the non-inertial frame of the Earth based observer, the gravitational force acts along the z direction and the particles are prepared and detected by a stationary emitter and detector at a fixed distance L apart along the propagation direction y. When viewed in the Lorentz frame, this corresponds to an emitter and detector accelerating in the z-direction and at distance L apart along the y direction. The detector is a screen with extension in x and z, and we choose a particular pixel on the screen to be our local observer. We choose the Lorentz frame which at the initial time of the experiment $t = \tau = 0$ coincides with the proper frame of the central pixel (see section **??** for details), except for a translation along y of distance L (see Fig.[2.3]). Parametrizing its trajectory x^μ_{cs} by its proper time τ, we have

$$x^\mu_{cs}(\tau) = [t_{cs}(\tau), 0, L, z_{cs}(\tau)] \tag{2.42}$$

In section **??** that we've already established the equivalence between local gravity and observer motion. We now relax the assumption that the observer is uniformly accelerating to investigate the more general case. Suppose instead that in the Lorentz frame the observer has a general time dependent trajectory with an instantaneous 3-velocity $v(\tau)$, then at any moment along its trajectory the coordinate transformation between the Lorentz frame x^μ and the observer's proper frame $X^\mu = (\tau, X, Y, Z)$ is given by

$$x^\mu(\tau) = \Lambda^{-1}[v(\tau)]^\mu{}_\nu X_\nu + x_{cs}(\tau), \quad \tau := \tau(t) = [t_{cs}(\tau)]^{-1} \tag{2.43}$$

or more explicitly

$$x^\mu(\tau, X, Y, Z) = \left[t_{cs}(\tau) + v\gamma Z/c^2, X, Y + L, z_{cs}(\tau) + \gamma Z\right] \tag{2.44}$$

where we have the Lorentz factor $\gamma = \left(\sqrt{1 - v^2/c^2}\right)^{-1}$.

Correspondingly, the basis vectors of the observer's tetrad $\{\hat{e}_\mu\}$ is given by

$$\hat{e}_\nu(\tau) = \Lambda^{-1}[v(\tau)]^\mu{}_\nu \hat{g}_\mu \tag{2.45}$$

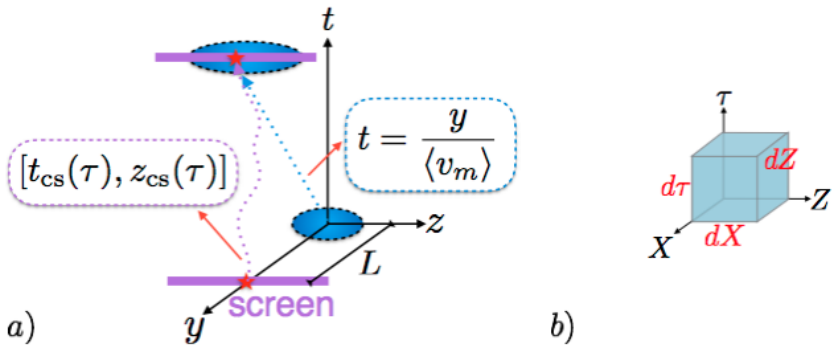

Figure 2.2: Figure a) shows the spacetime trajectory of the central pixel on the screen, which we choose to be our local observer with arbitrary motion along z parametrized by its proper time, given in Minkowski coordinates by $x^{\mu}_{cs}(\tau)$. The screen is located a distance L away from the screen in the y direction, which is also the propagation direction of the quantum particles (represented by the blue ellipses). The particles have localized wavepackets and a well defined average momentum, which determines their mass dependent propagation velocity v_m, and the particles' trajectories are straight lines in spacetime in the $t - y$ plane. Figure b) shows a pixel on the screen in the central pixel's proper frame with coordinates (τ, X, Y, Z) and parametrized by labels (X, Z). Its differential spacetime volume spanned by the vectors $d\tau\vec{\partial}_{\tau}$, $dX\vec{\partial}_{X}$, $dZ\vec{\partial}_{Z}$. The measurement observable is the integral of the probability 4-current over the differential volume for each pixel (X, Z), which represents the number of particles which pass across each pixel over the time of the experiment and gives us the detected distribution over the observer's spatial coordinates.

where $\hat{g}_{\mu}$ are the Minkowsi basis vectors. One can check that $\{\hat{e}_{\mu}\}$ satisfy the requirements of the proper frame tetrad. Then, the coordinate transformation in Eq. (4.12) to transform the metric as in Eq. (2.14), we find that the metric in the proper frame of an observer with arbitrary motion is

$$ds^2 = -c^2\left(1 + \frac{g(\tau)Z}{c^2}\right)^2 d\tau^2 + dX^2 + dY^2 + dZ^2 \tag{2.46a}$$

for the proper acceleration

$$g(\tau) = \sqrt{-\eta_{\mu\nu}\left(\frac{d^2}{d\tau^2}x^{\mu}_{cs}(\tau)\right)\left(\frac{d^2}{d\tau^2}x^{\nu}_{cs}(\tau)\right)} = \gamma^2\frac{dv}{d\tau} \tag{2.46b}$$

The motion of the central pixel (observer) in Minkowski space and its relative position to the particle emitter is shown in Fig.[2.7a]

Evolution of a composite particle in the Lorentz frame

Having established the experimental setup in the Lorentz frame, we give a Lorentz covariant description of the composite particle. We can always diagonalize the internal energy Hamiltonian H_0 in the rest frame of the particle such that the internal states evolve independently (we acknowledge the the rest frame of a quantum particle is not well defined, but how the internal energy states depend on the position and momentum is not relevant to our problem, and for simplicity we define the H_0 eigenstates in the rest frame of a Gaussian wavepacket using its average position and momentum). Then, modelling each internal state as a different particle species with rest mass $m = \bar{m} + \delta m$ as an independent Klein Gordon field and the Lagrange density

$$\mathcal{L}_m = -\frac{1}{2}\left[\partial_\mu \phi_m \partial^\mu \phi_m + m^2\phi^2\right] \tag{2.47}$$

Solving for $\delta\mathcal{L}_m/\delta\phi_m = 0$ and promoting the field to the operator, we can write down the mode expansion

$$\hat{\phi}_m(\mathbf{k}) = \int \frac{d^3\mathbf{k}}{\sqrt{(2\pi)^3 2\omega_m(\mathbf{k})}}\left[\hat{a}_m(\mathbf{k})e^{ik_\mu x^\mu} + h.c\right] \tag{2.48}$$

where $\hat{a}_m(\mathbf{k})$ has a particle interpretation and is normalized to satisfy

$$\left[\hat{a}_m(\mathbf{k}), \hat{a}^\dagger_{m'}(\mathbf{k}')\right] = \delta_{mm'}\delta^3(\mathbf{k}-\mathbf{k}') \tag{2.49}$$

with the relativistic dispersion relation

$$\omega_m(\mathbf{k}) = \sqrt{m^2c^4 + (\hbar\mathbf{k})^2c^2} \tag{2.50}$$

which we emphasize is mass dependent. Without loss of generality, a single particle state for species m is given by

$$|\Psi_m\rangle = \int \frac{\mathrm{d}^3\mathbf{k}}{\sqrt{(2\pi)^3}}\, f_m(\mathbf{k})\hat{a}^\dagger_m(\mathbf{k})|0\rangle \tag{2.51}$$

where $\hat{a}^\dagger_m(\mathbf{k})$ creates a momentum eigenstate in the quantization frame with eigenvalue $\mathbf{k}$. The state vector $|\Psi\rangle$ is a Lorentz invariant quantum state and and exists everywhere in the spacetime region between the future light cone of the preparation event and the past light cone of the measurement event. We can map the quantum state to the familiar quantum mechanical wavefunction in the non-relativistic (NR) limit when g_m is limited to values of $\hbar|\mathbf{k}| \ll mc$ so that

$$\omega_m(\mathbf{k}) \approx \frac{mc^2}{\hbar} + \frac{\hbar\mathbf{k}^2}{2m} \tag{2.52}$$

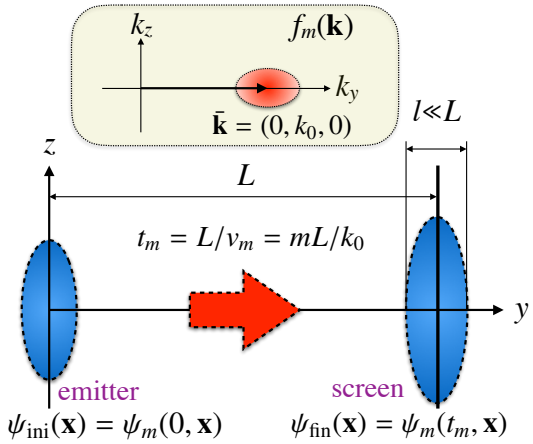

Figure 2.3: Propagation of a wavepacket for species m from the emitter to the screen in the Lorentz frame. For each m, the same initial wavefunction leads to the same measured wavefunction on the $y = L$ plane (where the screen is located), but the arrival time of the packets depend on m. Here the screen is moving along z. The inset illustrates that $f_m(\mathbf{k})$ is localized around $\bar{\mathbf{k}}$. For snapshots in time, see left panels of Fig. 2.4.

and define the NR field operator $\hat{\Phi}_m(t, \mathbf{x})$ as

$$\hat{\Phi}_m(t, \mathbf{x}) = \lim_{NR} e^{imc^2 t/\hbar} \sqrt{2m}\, \hat{\phi}_m(t, \mathbf{x}) \tag{2.53}$$

$$= \int \frac{d^3\mathbf{k}}{\sqrt{(2\pi)^3}} \left[\hat{a}_m(\mathbf{k}) e^{i(\mathbf{k}\cdot\mathbf{x} - \hbar\mathbf{k}^2 t/2m)} + h.c \right] \tag{2.54}$$

The operator $\hat{\Phi}(t, \mathbf{x})$ is orthogonal and complete over the spatial hypersurface at time t on the Hilbert space of single particle states, satisfying

$$\int d^3\mathbf{x}\, \hat{\Phi}(t, \mathbf{x})|0\rangle\langle 0|\hat{\Phi}(t, \mathbf{x}) = \hat{\mathbb{I}}, \quad \langle 0|\hat{\Phi}(t, \mathbf{x})\hat{\Phi}(t, \mathbf{x}')|0\rangle = \delta^3(\mathbf{x} - \mathbf{x}') \tag{2.55}$$

allowing us to identify

$$\hat{\Phi}(t, \mathbf{x})|0\rangle = |\mathbf{x}\rangle \tag{2.56}$$

where $|\mathbf{x}\rangle$ is the quantum mechanical position basis ket on the spatial hypersurface at time slice t. Then we define the wavefunction in the usual way

$$\psi_m(t, \mathbf{x}) = \langle 0|\hat{\Phi}_m(t, \mathbf{x})|\Psi_m\rangle = \int \frac{d^3\mathbf{k}}{(2\pi)^3}\, f_m(\mathbf{k}) e^{i\mathbf{k}\cdot\mathbf{x}} e^{-i\frac{\hbar\mathbf{k}^2 t}{2m}} \tag{2.57}$$

noting that $f_m(\mathbf{k})$ is the Fourier transform of $\psi_m(0, \mathbf{x})$ and represents the non-relativistic momentum distribution, or

$$f_m(\mathbf{k}) = \int d^3\mathbf{x}\, \psi_m(0, \mathbf{x}) e^{-i\mathbf{k}\cdot\mathbf{x}} \tag{2.58}$$

Conversely, given the form of the initial wavefunction $\psi_m(0, \mathbf{x})$ in the particle emitter frame, we can find $f(\mathbf{k})$ using Eq. (2.58) and identify the state vector $|\Psi_m\rangle$. Suppose then that the initial state of composite particle is a *direct-product* state between the internal and translational modes of the composite particle. The translational mode corresponds to the "center of mass" degree of freedom of Ref. [57], and contains all the information about the particle's location. Therefore, all species share the same initial wavefunction, or $\psi_m(0, \mathbf{x}) = \psi_{\text{ini}}(\mathbf{x})$ (Fig. 2.3), which means that $f_m(\mathbf{k})$ likewise is the same for all species. We note that here and in our paper [48] we use slightly different normalization conventions for the mode operator $\hat{a}$, so that certain quantities appear different. The physical results are unchanged.

We consider the case where $\psi_{\text{ini}}(\mathbf{x})$ is spatially localized around the origin and $f_m(\mathbf{k})$ is localized near $\bar{\mathbf{k}} = (0, k_0, 0)$ (inset of Fig. 2.3). This means that the wavepacket for species m will propagate along y with mean velocity $v_m = k_0/m$, and its center will arrive at the screen at $y = L$ in time $t_m = mL/k_0$. Although time evolution entangles the internal and translational modes so that $\psi_m(t, \mathbf{x})$ is mass dependent, the wavefunctions at their respective t_m does not depend on mass

$$\begin{aligned}\psi_m(t_m, \mathbf{x}) &= \langle 0|\hat{\Phi}_m(t_m, \mathbf{x})|\Psi_m\rangle = \int d^3\mathbf{x}'\; T[\hat{\Phi}_m(t_m, \mathbf{x}), \hat{\Phi}_m(0, \mathbf{x}')]\psi_{\text{ini}}(\mathbf{x}') \\ &= \sqrt{\frac{k_0}{2\pi i L}} \int d^3\mathbf{x}' e^{-\frac{k_0(\mathbf{x}-\mathbf{x}')^2}{2iL}} \psi_{\text{i}ni}(\mathbf{x}') \equiv \psi_{\text{f}in} \end{aligned} \tag{2.59}$$

In other words, the mass dependence of propagation and time of arrival cancel each other, so that all species have the same wavefunction upon arrival at the screen. Therefore, the pattern registered by the screen for each species will be the same modulo the particular location they land on the moving screen. We point out the the evolution of the wavefunction is simply given by the non-relativistic limit of the Feynman propagator for the KG field.

The evolution in Eq. (2.59) already offers some intuition about the source of the dephasing: that although each species of particles has the same spatial distribution upon its arrival at the detector, the detector itself is moving in time. Since the particles arrive at different times, it will be detected by different regions of the detector. To show this result formally we must formulate measurement process.

Covariant observables for relativistic quantum measurement

Before writing down the measurement operators, let us give some physical intuition for what we wish to measure. The interference pattern is the spatial distribution of the interfering particles. Therefore for each species, we measure the number of

particles captured by the screen per area over the lifetime of the experiment. We call this quantity the areal density and denote it by σ_m, and our final outcome σ is the sum of σ_m over the mass distribution.

We now introduce the 4-current operator

$$\hat{j}^{\nu}_{m}(x^{\mu}) = i\left[\partial^{\nu}\hat{\phi}_{m,-}(x^{\mu})\right]\hat{\phi}_{m,+}(x^{\mu}) + h.c. \tag{2.60}$$

which satisfy

$$\langle\Psi|\partial_{\mu}\hat{j}^{\mu}|\Psi\rangle = 0 \tag{2.61}$$

and where we've defined $\hat{\phi}_{m,+}$ and $\hat{\phi}_{m,-}$ as the positive and negative frequency components of $\hat{\phi}_m$. We remark here that the current operators are well defined and represent the flow of probability because, since we are in a spacetime with a timelike Killing vector, there is an unambiguous separation of positive and negative frequency modes, which means that the conserved charge in an spacelike 3-volume (representing probability) is alway positive, or

$$Q := \int d\Sigma_0\ \langle\hat{j}^{0}(x^{\mu})\rangle \geq 0 \tag{2.62}$$

Then the number of particles in a spacetime volume V for state $|\Psi\rangle$ is given by the flux integral

$$N_m[V] = \int_V d\Sigma_{\nu}\langle\Psi_m|\hat{j}^{\nu}_{m}|\Psi_m\rangle\,. \tag{2.63}$$

Here $d\Sigma_{\nu}$ is the differential volume one form, which can be intuitively understood as the region in spacetime bounded by the coordinate vectors $\Delta\vec{x}_a$, $\Delta\vec{x}_b$, $\Delta\vec{x}_c$, where a, b, c label which vector and not vector components, in the limit that $\Delta \to 0$

$$d\Sigma_{\mu} = \epsilon_{\mu\alpha\beta\gamma}dx^{\alpha}_{a}dx^{\beta}_{b}dx^{\gamma}_{c} \tag{2.64}$$

where $\epsilon_{\mu\alpha\beta\gamma}$ is the Levi-Civita tensor and is given in a coordinate system with metric determinant $\det[g_{\rho\sigma}]$ by

$$\epsilon_{\mu\alpha\beta\gamma} = \sqrt{-\det[g_{\rho\sigma}]}\ \hat{\epsilon}_{\mu\alpha\beta\gamma}, \quad \hat{\epsilon}_{\mu\alpha\beta\gamma} = \pm 1 \tag{2.65}$$

where the $\pm$ sign is chosen depending on whether the indices are an even (+) or odd ($-$) permutation.

For N_m counted by a particular pixel on the screen, the volume V over which we integrate the current flux is spanned by differential volume one-form corresponding

to the pixel's proper area and proper time for which are given by the coordinates of its proper frame, whose relation to the Lorentz frame was obtained in Eq. (2.44) and whose metric is given by Eq. (2.46a). In the proper frame, pixels on the screen are parametrized spatially by (X, Z) with $Y = 0$, and the boundary of its volume one form is spanned by the 4-vectors $d\tau\vec{\partial}_\tau$, $dX\vec{\partial}_X$ and $dZ\vec{\partial}_Z$ (Fig.[2.7b]), where $\vec{\partial}_\mu$ are coordinate basis vectors. Then, expressed in proper frame coordinates where the determinant of the metric is $\det[g_{\rho\sigma}] = (1 + gZ/c^2)$, the differential volume one form is given by

$$d\Sigma_{\bar{\nu}}(X, Z) = \left[0, 0, (1 + gZ/c^2)dXdZd\tau, 0\right] \tag{2.66}$$

with the barred subscript $\bar{\nu}$ to indicate that the expression is in *proper frame coordinates*. We point out that X and Z are labels for the pixel while $d\tau$, dX and dZ are scalar quantities representing the differential proper lengths of the volume edges. Since only the Y component of the one-form is non-zero, transforming to the Minkowski frame becomes an easy task

$$d\Sigma_\nu = \frac{\partial X^{\bar{\mu}}}{\partial x^\mu} d\Sigma_{\bar{\mu}} = \frac{\partial Y}{\partial x^\mu} d\Sigma_Y = \delta_{y\nu}(1 + gZ/c^2)dXdZd\tau \tag{2.67a}$$

and therefore, in Minkowski coordinates

$$d\Sigma_\nu(X, Z) = \left[0, 0, (1 + gZ/c^2)dXdZd\tau, 0\right] \tag{2.67b}$$

which is the same form as in the proper frame coordinates. This is not surprising because only the volume element is directed along y which is not a direction of motion and therefore experiences no Lorentz contractions.

We point out that we in fact defined the proper volume for a pixel at (X, Z) with the proper time of the central pixel instead of with its own proper time. The is a subtlety in the physical interpretation of the experiment: whether the each pixel turns on or off according to its own proper time, or whether everything occurs at the same coordinate time. However, this makes no difference if we measure for long enough times that we sample the entire length of the packet (effectively for $\tau \in (-\infty, \infty)$).

Finally, we are ready to construct our Lorentz covariant observables for each particle species as the set of operators $\{\hat{\sigma}_m(X, Z)\}$

$$\begin{aligned} \hat{\sigma}_m(X, Z) &= \frac{1}{\Delta X \Delta Z} \int d\Sigma_\mu \, \hat{j}^\mu_m \left[x^\mu(\tau, X, 0, Z)\right] \\ &= \int d\tau \, \left(1 + gZ/c^2\right) \hat{j}^y_m \left[x^\mu(\tau, X, 0, Z)\right] \end{aligned} \tag{2.68}$$

where $\sigma_m(X, Z)$ is the number flux through the pixel averaged over its proper area $\Delta X \Delta Z$, and which we'll refer to as the *areal density*. The integration volume is the spacetime region that is spanned by the pixel from $t = 0$ to the end of the experiment, and we can extend the time limits to $\pm\infty$ with the assumption that the quantum states are localized and pass through the screen entirely over the measurement time.

The total measurement, corresponding to tracing over the internal energy states, is given by

$$\hat{\sigma}(X, Z) = \int dm\ P(m)\hat{\sigma}_m(X, Z) \tag{2.69}$$

where $P(m)$ is the probability distribution of the different masses.

Let's looks more closely at the integrand of $\hat{\sigma}_m(X, Z)$ and its operation on the quantum state we've prepared in Eq. (2.51), denoting the integrand by $\dot{\sigma}_m(X, Z)$ such that

$$\sigma_m(X, Z) := \langle \Psi_m | \hat{\sigma}_m(X, Z) | \Psi_m \rangle = \int d\tau\ \dot{\sigma}_m(X, Z) \tag{2.70}$$

We will now make some simplifying assumptions and calculate $\dot{\sigma}_m$. Since we are now taking the expectation value with respect to our NR quantum state with $\hbar|\mathbf{k}| \ll mc$, we take the NR limit $\hat{j}_y$, which now has the mode expansion

$$\hat{j}^y_m(x^\mu) = \int \frac{d^3\mathbf{k}}{(2\pi)^3 2mc} \int d^3\mathbf{k}'\ \hbar k_y\ \hat{a}_m(\mathbf{k})^\dagger \hat{a}_m(\mathbf{k}') e^{-i(k_\mu - k'_\mu)x^\mu} + h.c \tag{2.71}$$

If our state $|\Psi\rangle$ has momentum mostly along y and centered at $\hbar k_0$, so that $\sigma_k \ll k_0$ where σ_k is the spread in momentum, then with error $O(\sigma_k/k_0)$

$$\langle \hat{j}^y_m \rangle \approx \frac{\hbar k_0}{c} \langle \hat{\Phi}_{m-} \hat{\Phi}_{m+} \rangle \tag{2.72}$$

which gives us

$$\dot{\sigma}_m(\tau, X, Z) = v_m(1 + gZ)|\psi^2_m\left(x^\mu(\tau, X_s, 0, Z)\right)|, \quad v_m = \frac{\hbar k_0}{m} \tag{2.73}$$

for $\psi_m(t, \mathbf{x})$ is given by Eq. (2.57).

The integral over τ for $\sigma_m(X, Z)$ physically means that we are integrating the particle flux over the worldline of the pixel labeled by X, Z. Operationally it is simpler to perform the integral over t instead of τ, so let us reparametrize its worldline by t. In particular,

$$z_s(t, Z) = z_{cs}(t) + \frac{Z}{\gamma} + O\left(\frac{gZ^2}{c^2}\right). \tag{2.74}$$

and

$$\frac{dt}{d\tau} = \gamma\left(1 + gZ/c^2\right) \tag{2.75}$$

Eqs. (2.74) and (2.75) allows us to write

$$\sigma_m(X,Z) = \frac{v_m}{c}\int \gamma^{-1}\left|\psi_m^2\left[t, X, 0, z_{cs}(t) + \gamma^{-1}Z\right]\right|^2 dt \tag{2.76}$$

In principle, this is our measurement result including relativistic corrections in v/c. However, we can show that $\sigma_m(X,Z)$ take a much more intuitive form by making some assumptions about our experiment. First, we assume that the packet is localized within l along y, where $l \ll k_0/\sigma_k^2$ and that during this time the packet remains rigidly moving along y with v_m (in other words, there is negligible dispersion of the wavepacket over the measurement duration). Then, recalling the $t_m = L/v_m$ is the time of arrival at the screen of species m in the classical limit, we can write within error of $O(l\sigma_k^2/k_0)$

$$|\psi_m^2(t_m + \delta t, x, y, z)| = |\psi_{\text{fin}}^2(x, y - v_m\delta t, z)| \tag{2.77}$$

Note that we are assuming the packet experiences negligible dispersion over time l/v_m. Since we can safely assume that packet size $l \ll L$, this does not preclude the packet from the effects of dispersion over the propagation length as long as it remains localized at the time of detection. Furthermore, assuming that the velocity of the detector is approximately constant over measurement duration so that γ is constant, and changing the integration variable from δt to $y' = y - v_m\delta t$, we can rewrite Eq. (2.68) as

$$\sigma_m(X,Z) = \int dy'\ \gamma^{-1}\left|\psi_{\text{fin}}^2(X, -y', z_{cs}(t_m + y'/v_m) + \gamma^{-1}Z)\right| \tag{2.78}$$

This has the particularly straightforward interpretation that the screen pixel (X,Z) samples the wave packet along a spatial slice, parametrized by

$$[y,z] = \left[-y', z_{\text{cs}}(t_m + y'/v_m) + \gamma^{-1}Z\right] \tag{2.79}$$

From Eq. (2.78) we see that the spatial distribution at the moment of their detection *is the same for all species*. The mass dependence lies in *where* the wavepacket is sampled through both the position and angle of sampling as one integrates y' over the packet length. In fact, a simpler picture is possible whereby we ignore the angle of sampling. To see this and obtain a simple form for our final result, let's now take the NR limit and assume wavefunction separability (although we've been quite

careful up to this point in allowing for a relativistic trajectory for the detector, it turns out that this does not affect the dephasing result). Writing the product state $\psi_{\text{fin}}(x, y, z) = \psi^x_{\text{fin}}(x)\psi^y_{\text{fin}}(y)\psi^z_{\text{fin}}(z)$, we see that in the absence of entanglement among the three spatial degrees of freedom the integral over y' is simply unity, and we have

$$\sigma_m(X, Z) = |\psi^x_{\text{fin}}(X)|^2 \left|\psi^z_{\text{fin}}[\tilde{z}_{\text{cs}}(t_m) + Z]\right|^2 \tag{2.80}$$

where

$$\tilde{z}_{cs}(t) = z_{cs}[\tau(t)] \tag{2.81}$$

and is the parametrization of the central pixel's trajectory in Minkowski time. Eq. (2.80) is our general result in the NR limit for localized quantum states with a well defined average momentum and wavefunction separability. With these assumptions, the mass dependence on the detection result is well approximated by the position at which the pixel samples $|\psi^2_{\text{fin}}|$ at the particular time of arrival t_m for each species m. To elaborate, as the different species propagate toward the detector, their mass dependent dispersion given in Eq. (2.50) manifests in a mass dependent propagation velocity v_m, which causes the species to spread apart from each other along the propagation axis. Thus, each species different time of arrival at the screen with motion along z, which registers the pattern from the different species at a m-dependent spatial shift, as shown in Fig. 2.4. This mass dependence is shown explicitly in Eq. (2.80) through $\tilde{z}_{cs}(t_m)$.

Although it seems like we've imposed quite specific constraints on the quantum state in arriving at Eq. (2.80), our formulation of measurement involving the integration of a probability current over the spacetime region corresponding to a probe's trajectory can be generally applied to detection measurements in a relativistic framework. The essential point is that in general relativity, quantum measurement cannot be taken for granted as being a non-relativistic POVM. To model measurement, one must identify the physical invariant that corresponds to the observable, which requires one to account for the trajectory of the measurement device and its interactions with the measured state in a Lorentz covariant way.

Brief Comment on Observer-Dependent Vacuum

In our formulation we have not discussed the effect of observer dependent vacuum, which has been studied in [67] and in itself a very interesting problem. Summarizing briefly, it can be shown that a Rindler observer sees the Minkowski vacuum state as a thermal state. Heuristically, this effect can be understood from the fact that there

is a Killing horizon with respect to the Rindler's observer's timelike Killing vector $\vec{\partial}_\tau$, meaning that there are regions of spacetime to and/or from which the Rindler observer cannot send and/or receive information (Fig.[2.4]), as we mentioned in section 2.4 when we noted that a Rindler observer cannot construct a global coordinate system using his proper frame tetrad. Then, if one were to expand a massive scalar field into positive and negative frequency modes (in other words, into $\hat{b}$ and $\hat{b}^\dagger$), for the Rindler observer those modes will only have support in his accessible region of spacetime (region I in Fig.[2.4]), and it is clear that any function with support only in the region must be a superposition of left and right propagating plane waves, corresponding to positive and negative frequency Minkowski mode. Therefore, since a Rindler mode is a superposition of Minkowski creation and annihilation operators and vice versa, the Minkowski vacuum satisfying $\hat{a}_k|0\rangle$ must be a multiparticle state with respect to $\hat{b}_k$.

However, the blackbody radiation predicted to be observed by the Rindler observer with acceleration g travelling through Minkowski vacuum has temperature

$$T_R = \frac{\hbar g}{2\pi c k_B} \tag{2.82}$$

whereas massive particles have Compton frequency $\omega_C = mc^2/\hbar$. Then, the expected number of particles observed due to this effect is negligible:

$$\bar{n} = \frac{1}{e^{\hbar\omega_C/k_B T_R} - 1} \sim \frac{g\tau_C}{c} \ll 1, \quad \tau_C = \frac{1}{\omega_C} \tag{2.83}$$

2.8 Dephasing and Loss of Interference Fringe Visibility

To see how the velocity of the screen causes loss of fringe visibility, suppose now that ψ^z_{fin} contains an interference pattern with visibility V, so that locally around $z \approx \tilde{z}_{cs}(t_m)$ we have $|\psi^z_{\text{fin}}(z)|^2 \propto [1 + V\cos(\alpha z + \phi)]$, where α is the wavenumber of the spatial oscillation. We can ignore ϕ without loss of generality, and write

$$\sigma(Z) \propto \int P_m \left(1 + V\cos[\alpha z_{cs}(t_m) + Z]\right) dm \tag{2.84}$$

This is simply a sum of shifted cosines, which will result in a "fuzzy" interference pattern with a new visibility V' such that

$$\frac{V'}{V} = 1 - \frac{\alpha^2 \dot{\tilde{z}}^2_{\bar{m}} t^2_{\bar{m}}}{2}\left(\frac{\Delta m}{\bar{m}}\right)^2 \tag{2.85}$$

where Δm^2 is the variance of the mass distribution, $\bar{m}$ is the average mass and the $\bar{m}$ subscript is used denote quantities of the average mass particle. We emphasize

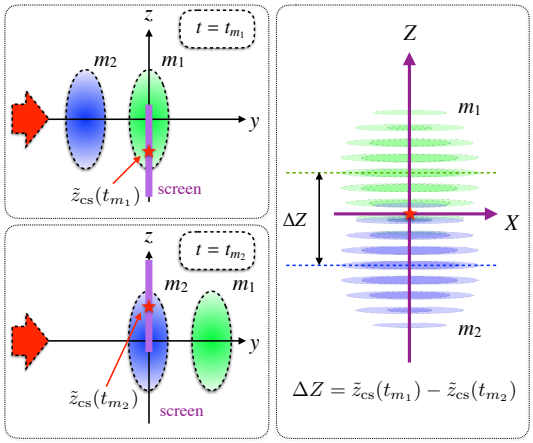

Figure 2.4: Snapshots taken upon arrival of m_1 and m_2 ($m_1 < m_2$) packets at the screen, at t_{m_1} (upper left panel) and t_{m_2} (lower left panel), respectively (separation between the packets highly exaggerated). Positions of the screen differ at these moments (with central pixel labeled by red star), causing a shift in the interference pattern registered by the screen, which is best viewed in the central pixel's proper reference frame (right panel).

that the loss of contrast we predict depends crucially on the transverse *velocity* of the screen at time $t_{\bar{m}}$, denoted by $\dot{\tilde{z}}_{\bar{m}}$, and has no dependence on the *acceleration*, or equivalently, on gravity.

Note that Eq. (2.85) assumes small differences in spatial shifts between species compared the coherence lengthscale, corresponding to short measurement times. But since the interference pattern is just the superposition of shifted cosines, for finite number of particle species, we can always find a time at which the oscillations for all species have cycled over an integer number of 2π. This will recover full fringe visibility, and is consistent with the point that a continuous spectrum of bath modes is necessary for true decoherence. Otherwise, the effect can only be interpreted as dephasing.

A Double Slit Experiment in a Uniformly Accelerating Lab

We now apply our model to the specific thought experiment of Ref. [57], where there is an initial spatial superposition of the translational mode so that $\psi_{\text{ini}}(x, y, z) \propto [\delta(z-z_1)+\delta(z-z_2)]$, and a thermal distribution at high temperature T of N harmonic DOF's, being measured by a detector with uniform acceleration g. From this, we calculate the parameters $V = 1$ and $\alpha = k_0(z_1 - z_2)/L$ from ψ_{fin}, $\tilde{z}_{cs}(t) = gt^2/2$ and $\dot{\tilde{z}}_{\bar{m}} = gt_{\bar{m}}$ from the detector motion, and $\Delta m = k_B T\sqrt{N}$ from the mass distribution.

Inserting these into our general result in Eq. (2.85), we find

$$V' = 1 - \frac{N}{2}\left[g(z_1 - z_2)k_B T\right]^2 t_{\bar{m}}^2 \tag{2.86}$$

which exactly reproduces the loss of contrast found in Ref. [57]. Using the insight that this is a kinematic effect which is due to a coordinate transformation, we now address this thought experiment without extension to our physical model to establish direct correspondance.

The (1+1)D thought experiment

We briefly state results from the thought experiment of Ref. [57] using our kinematic interpretation. Here, state preparation and detection occurs in two different Local Lorentz frames, which we denote by LLF-E for the emitter and LLF-D for the detector, with coordinates (t, z) and (τ, Z) respectively. Here, detection at time τ is an instantaneous evaluation of the particle's wavefunction in LLF-D. Mapping the initial wavefunction $\psi_m(0) \propto [\delta(z - z_1) + \delta(z - z_2)]$ in LLF-E to a state vector, we boost the field operator $\hat{\phi}_m$ by the instantaneous velocity v of LLF-D at detection time. The spatial distribution in LLF-D at τ for species m is then

$$|\psi_m(\tau, Z)|^2 \propto 1 - \cos\left[\frac{m}{\tau}\left(Z - z_c + v\tau\right)\Delta z\right] \tag{2.87}$$

where $\Delta z = z_2 - z_1$, and $z_c = (z_2 + z_1)/2$ is the center of the superposition. We point out that here the mass dependence lies in the spatial frequency of the interference cosine term, which again can be traced back to de Broglie wave dispersion. The effect of an accelerating detection frame that observes the system at the same coordinate point Z is to observe it at a point farther away from z_c as time increases. In the limit where the detector motion dominates such that $v\tau \gg Z - z_c$, such as when $Z \sim z_1, z_2$ for realizable massive superpositions, and for $v = g\tau$, we obtain the the same loss of contrast as in Ref [1].

Origin of the loss in visibility

While our predicted loss of visibility in Eq's. (2.86) for the Eq. (2.87) the same as that of Ref. [57] in the appropriate limits, we interpret this effect as being unrelated to gravity. The true source of dephasing is the mass dependent dispersion of de Broglie waves. In our experimental particle beam model, this manifests as mass dependent propagation velocities, causing the species to arrive at different times. This implies that a particular pixel on the moving screen is effectively evaluating $\psi_{\text{fin}}(\mathbf{x})$ at mass dependent positions along z as shown in Eq. (2.80) and in the left

panels of Fig. 2.4. On the screen itself, this means that different species land on different locations, resulting in mass-dependent shifts of their interference patterns along Z [Fig. 2.4, right panel], which in turn smears out the pattern. Pictured in the lab frame, packets of different species separate along y and drop onto the screen at different heights. The size of these shifts, and consequently the dephasing, depends on both the amount of time the species are allowed propagate, as well as the velocity of the screen at measurement time. In this way, the loss of visibility appears as a rate that is directly related to the transverse *velocity* of the detector [Eq. (2.85)], instead of *acceleration*. In the situation considered by Ref. [57], gravity happens to supply such a transverse velocity, thereby making the decrease in visibility dependent upon the gravitational acceleration. However, if we give the screen a uniform velocity in the Lab frame (with gravity) that matches the velocity at which the packets fall in the lab frame, there will be no loss of visibility. *Vice versa*, even in absence of gravity, any motion of the screen transverse to the beam's propagation direction as the packets land will lead to a loss of visibility. As for the thought experiment of Ref. [57], mass dependent wave dispersion implies greater dephasing among different species in regions farther away from the center of the initial superposition. Observing interference at constant lab coordinates equates to observing the system at a point whose distance from its center increases with time, resulting in an apparent dephasing "rate". Thus, our formalism offers an alternative perspective that the loss of visibility is a is a *kinematic effect* instead of a gravitational one.

2.9 Conclusions on Interpretation of Dephasing in Uniform Gravity

Having treated both the thought experiment of Ref. [57] and its possible physical implementation as a particle beam interferometry experiment, in both cases we offer the point of view that dephasing between different internal states do not arise from gravity, but instead from the mass dependence of their de Broglie waves' dispersion and the relative transverse motion of the detector. Furthermore, the dephasing we calculate from this perspective is the same as that predicted by Ref. [57] using their perspective of time dilation [1]. In these calculations, we have assumed EEP to be valid. The comparison of these two approaches - by treating gravity explicitly versus as acceleration - offers possibilities to study the implications of EEP in quantum systems and to test for its violations in this regime. To do this, we will have to

[1] The authors of Ref. [57] hold the position that the effect they describe is due to time dilation, and thus a different effect than discussed here.

consider a more general Hamiltonian in the Lab frame

$$\hat{H} = \hat{\mathbf{p}}^2/(2\hat{M}) + \hat{\mathbf{G}} \cdot \hat{\mathbf{x}} \tag{2.88}$$

where $\hat{\mathbf{G}}$, the gravitational force, is no longer given by $\hat{M}\mathbf{g}$, which would *a priori* be consistent with Weak Equivalence. In this case, the packets of multiple mass components will separate due to both the spectrums of $\hat{M}$ and $\hat{\mathbf{G}}$, and now gravity will cause packet separation in addition to the effect of mass. It is also plausible that preparation of novel quantum states can reveal more structures in the operator $\hat{\mathbf{G}}$ that could otherwise be revealed by a classical experiment [68, 78].

Chapter 3

RELATIVISTIC VIEWPOINT OF ATOM INTERFEROMETRY

3.1 Introduction

In this chapter we study the experiments of Kasevich, Peters, Chung, and Chu [35, 53] using a fully relativistic treatment in Minkowski spacetime, in which the emitters and receivers of light follow non-geodesic world lines. In these experiments, atoms having internal states are made to interfere in a gravitational field by splitting their wavefunction into different trajectories through the use of Raman pulses which act as photonic atom mirrors and beamsplitters. The phase accumulated is proportional to g of the gravitational acceleration. We analyze this system in a Lorentz covariant formalism assuming that g is constant. Our formalism shows that the resulting phase depends crucially on the initial phases of the laser pulses upon emission, and that the gravitational constant g appears because those phases are fixed to specific values at the moment of emission from accelerated emitters. More importantly, this work provides a rigorous framework for (i) analyzing relativistic corrections to atom interferometry and quantifying the errors introduced in the approximations made in previous and often cited treatments [23, 63], which seem to be the basis for many theoretical extensions proposing to test relativistic effects [45, 60, 73]; and (ii) allow an extension to a full quantum treatment of light including the atom?s back-action to light, which may be used to study possible back-action noise of these devices.

3.2 Experimental setup

As described in Ref. [54], the experimental setup corresponds to the following schematic: two level atoms may be in state $|a, k_0\rangle$ and $|b, k_b\rangle$, where a, b label the hyperfine level and k_0, k_b label the particle momentum. The atoms are shot up along the direction of the gravitational field z. Pulses may be applied to induce Raman transitions between the two states. In the simplest case, there are two pulses that are respectively co- and counter-propagating with respect to the atoms, where the co-propagating beam excites $|a, k_0\rangle$ to an intermediate state $|i\rangle$ upon absorption, and the counter-propagating beam induces $|i\rangle$ to decay to $|b, k_b\rangle$ upon emission. We shall call the co-propagating beam "beam 1" and the counter-propagating beam "beam 2". The two beams must be simultaneously present and within the linewidth of their transitions in order for the Raman transition to occur. Depending on the

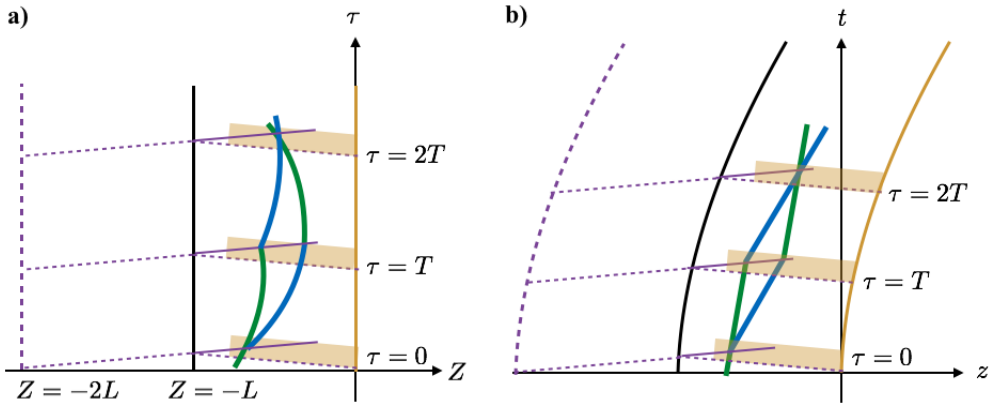

Figure 3.1: Spacetime diagrams of the atom interferometer experiment in Rindler (a) and Minkowski (b) coordinates, with flattened null rays to ease of representation. Emitters for both the co- and counterpropagating beams follow the same trajectory (yellow line), but the co-propagating beam (beam 1) only interacts with the atoms upon reflection at a surface located at constant $Z = -L$ due to Doppler shifting. Therefore, beam 1's emitter's effective trajectory (dotted purple line) is given by Eq. (3.4). Note that timing of the interaction is controlled by beam one, and that the pulses from beam 2 are broad enough that such that beams 1 and 2 overlap to induce atomic transitions for both paths.

duration of the pulse, the interaction can induce a beamsplitter effect whereby, for example

$$|a, k_0\rangle \to \frac{1}{\sqrt{2}} \left(|a, k_0\rangle + |b, k_b\rangle\right) \tag{3.1}$$

or a mirror effect, whereby

$$|a, k_0\rangle \to |b, k_b\rangle, \quad |b, k_b\rangle \to |a, k_0\rangle \tag{3.2}$$

In an interferometry experiment, the atomic state is typically prepared in $|a, k_0\rangle$. Then a first set of pulses is applied at $\tau = \tau_0$ in the local frame of the lasers in a beamsplitter type interaction so that there is now a superposition. The atoms propagate until $\tau = \tau_0 + T$, where a second set of Raman pulses is applied in a mirror type interaction, and finally last set of beamsplitter type pulses is applied at $\tau = \tau_0 + 2T$ to combine the two atomic beams. In the inertial frame, the atoms propagate freely while the emitters follows accelerating trajectories. In the setup we consider, which is essentially the experimental setup of [53], the two emitters follow the same trajectory and their pulses are emitted along the $-z$-direction simultaneously. At this point both laser beams are counter-propagating with respect to the atoms, but one beam is reflected at $Z = -L$ so that it becomes co-propagating. The co-propagating beam controls the timing the of transition, and

its photon only interacts with the atom after reflection, since it is otherwise Doppler shifted off resonance. We define the inertial frame to coincide with the proper frame of the emitters at $\tau = 0$, and the emitter trajectories embed in this frame as

$$(t_e(\tau), z_e(\tau)) = \left[\frac{1}{g}\sinh(g\tau), \frac{1}{g}\left(\cosh(g\tau) - 1\right)\right] \tag{3.3}$$

However, since beam 1 must be reflected before it interacts with the atom, its effective trajectory is (see Fig.[3.2])

$$(t_1(\tau), z_1(\tau)) = \left[\frac{1}{g}\sinh(g\tau), \frac{1}{g}\left(\cosh(g\tau) - 1\right) - 2L\right] \tag{3.4}$$

3.3 Covariant Action for Atom Propagation with Light-Atom Interaction

The standard non-relativistic analysis for this experiment categorizes the phase accumulated by each path of the atom into a laser phase and a propagation phase. The laser phase is that which is imprinted onto the atoms from the photon absorption and emission processes which occur during the transition between the two atomic states, while the propagation phase is due to the free evolution of the atoms between the light pulses. The two phases are considered to be separate contributions to the net phase shift. Here we present a formalism in the language of quantum fields that is relativistic and which accounts for the total evolution of the quantum state in the presence of light-atom interactions.

As delineated in Chapter 2, from the point of view of EEP, constant local gravity is equivalent to an accelerating observer, and therefore the above experiment can be viewed in Minkowski coordinates where the light emitters and detector have uniformly accelerating trajectories. Since there is only one relevant direction in the interferometry experiments, we work in (1+1)D space but refer to Lorentz invariant spacetime quantities as "four-vectors" or "four-volumes" and their spatial components as "three-vectors" or "3 volumes". We model the two atomic levels as massive scalar fields $\hat{\phi}_A$, $\hat{\phi}_B$. Additionally, we model each of the laser beams as an independent massless scalar fields $\hat{\phi}_1$, $\hat{\phi}_2$, propose an interaction Lagrangian of the form

$$S_{int} = g \int d\vec{x}\ \hat{\phi}_A(\vec{x})\,\hat{\phi}_B(\vec{x})\,\hat{\phi}_1(\vec{x})\,\hat{\phi}_2(\vec{x}) \tag{3.5}$$

Of course, properly speaking the laser beams are excitations of the electromagnetic vector field which couples to the charge currents of the atom, but Eq. (3.5) captures the nature of the interaction that induces the transition between the two modes without additional complications. We point out that this is an *effective* interaction

between two modes, and a more detailed description should involve a transition to an intermediate state. Let us furthermore assume the lasers beams are strongly pumped coherent states and experiences negligible backaction from its interaction with the atom. Therefore, the EM fields are free fields which can be expanded into freely propagating modes

$$\hat{\phi}_1 = \int \frac{dk}{\sqrt{2\omega_\gamma}} \left[\hat{a}(k)e^{i\vec{k}\cdot\vec{x}} + h.c\right] \tag{3.6a}$$

$$\hat{\phi}_2 = \int \frac{dk}{\sqrt{2\omega_\gamma}} \left[\hat{b}(k)e^{i\vec{k}_1\cdot\vec{x}} + h.c\right] \tag{3.6b}$$

where the notation $\vec{k}$ denotes a four-vector and the plain k denotes a three-vector, and where we have the dispersion relation

$$\omega_\gamma(k) = c|k| \tag{3.6c}$$

$$\left[\hat{a}(k), \hat{a}^\dagger(k')\right] = \left[\hat{b}(k), \hat{b}^\dagger(k')\right] = \delta(k - k') \tag{3.6d}$$

$$\tag{3.6e}$$

and similarly for $\hat{\phi}_2$, whose mode operators we denote by $\hat{b}(k)$, $\hat{b}^\dagger(k)$. For simplicity of notation, unless stated otherwise, we will not explicitly write any factors of 2π. Then, defining Fourier transforms of the atomic fields

$$\hat{\varphi}_A(\vec{k}) = \int d\vec{k}\, \hat{\phi}_A e^{-i\vec{k}\cdot\vec{x}} \tag{3.7a}$$

$$\hat{\varphi}_B^\dagger(\vec{k}) = \int d\vec{k}\, \hat{\phi}_B e^{i\vec{k}\cdot\vec{x}} \tag{3.7b}$$

Writing the interaction in terms of the Fourier components, we have

$$\begin{aligned} S_{int} = g \int d\vec{x} \langle\Psi_1|\hat{\phi}_1(\vec{x})|\Psi_1\rangle\langle\Psi_2|\hat{\phi}_2(\vec{x})|\Psi_2\rangle \\ \int d\vec{k}_A \int d\vec{k}_B\, \varphi_A(\vec{k_A})\varphi_B^\dagger(\vec{k_B}) e^{i\left(\vec{k}_A - \vec{k}_B\right)\cdot\vec{x}} \end{aligned} \tag{3.8}$$

Here we have taken the expectation values over the light fields under the assumption that the light's quantum state is not affected by the interaction, thereby ignoring any effects due to the quantum nature of the light beams. Assuming coherent laser beams, their states are in general given by

$$|\psi_1\rangle = \exp\left(\int dk \sqrt{2\omega_\gamma}\left[\alpha(k)\hat{a}(k)^\dagger - \alpha^*(k)\hat{a}(k)\right]\right)|0\rangle \tag{3.9a}$$

$$|\psi_2\rangle = \exp\left(\int dk\sqrt{2\omega_\gamma}\left[\beta(k)\hat{b}(k)^\dagger - \beta^*(k)\hat{b}(k)\right]\right)|0\rangle \tag{3.9b}$$

where the $\sqrt{2\omega}$ factor is a normalization chosen for convenience. Then, evaluating the expectation values in Eq. (3.8) with respect the laser states above, we find

$$\int \frac{dk_1}{\sqrt{2\omega_1}}\langle\psi_1|\hat{a}(k_1)e^{i\vec{k}_1\cdot\vec{x}}|\psi_1\rangle + c.c = \int dk_1 \left[\alpha(k_1)e^{i\vec{k}_1\cdot\vec{x}} + c.c\right] \tag{3.10a}$$

and similarly

$$\int \frac{dk_2}{\sqrt{2\omega_2}}\langle\psi_2|\hat{b}(k_2)e^{i\vec{k}_2\cdot\vec{x}}|\psi_1\rangle + c.c = \int dk_2 \left[\beta(k_2)e^{i\vec{k}_2\cdot\vec{x}} + c.c\right] \tag{3.10b}$$

Substitution of Eqs. (3.10) into the interaction term will result in four separate terms $\sim \alpha\beta$, $\alpha^*\beta$ and their complex conjugates. However, noting that the laser frequencies are tuned in the actual experiment so that the absorption of one photon is accompanied by the emission of another, we keep only the terms $\alpha^*\beta$, $\alpha\beta^*$ which represents this process, and subsequently the interaction becomes

$$S_{int} = g\int d\vec{x}\int d\mathcal{K}\ \varphi_A(\vec{k}_A)\,\varphi^\dagger(\vec{k}_B)\,\alpha(k_1)\beta^*(k_2)e^{i\left(\vec{k}_A-\vec{k}_B+\vec{k}_1-\vec{k}_2\right)\cdot\vec{x}} + h.c \tag{3.11}$$

We note that while the atomic operators $\varphi_{A,B}$ depends on the four-vector, the mode operators for the light field are, under our approximations, for a free field and have known dispersion relations given in Eq. (3.6c), and therefore the four-vector of the mode is completely specified by its three-vector.

Integrating S_{int} over the four-volume gives us the four-δ function corresponding the energy and momentum conservation for the scattering event

$$\int d\vec{x}\, e^{i\left(\vec{k}_A-\vec{k}_B+\vec{k}_1-\vec{k}_2\right)\cdot\vec{x}} = \delta^4\left(\vec{k}_A - \vec{k}_B + \vec{k}_1 - \vec{k}_2\right) \tag{3.12}$$

and we can subsequently integrate over k_1 and k_1 to obtain the form of the interaction term which involves only the atomic modes

$$\begin{aligned} S_{int} = g\Bigg\{&\int d\vec{k}_A\int d\vec{k}_B\ \varphi(\vec{k}_A)\varphi^\dagger(\vec{k}_B) \\ &\frac{1}{2}\alpha\left(\frac{k_B-k_A}{2}+\frac{\omega_B-\omega_A}{2}\right)\beta^*\left(\frac{k_B-k_A}{2}-\frac{\omega_B-\omega_A}{2}\right)+h.c\Bigg\} \end{aligned} \tag{3.13}$$

We note that at this point we do not yet have a dispersion equation relation the frequencies $\omega_{A,B}$ with the 3-momenta $k_{A,B}$, and for the moment the frequencies is simply the zeroth component of the four-vector not subject to "on-shell" constraints

(this is because we have interacting atomic modes and therefore do not in general have free particles that satisfy "on-shell" constraints).

The transformation into the Fourier space helped give us the energy-momentum conservation condition in Eq. (3.12). Having now incorporated this condition into the interaction term, we can transform back into the spatial domain. We note that the correlation function G depends only on the difference between $\vec{k}_A$ and $\vec{k}_B$, which means that the interaction between the atomic modes is local and has the form

$$S_{int} = g \int d\vec{x}\ \phi_A(\vec{x})\phi_B(\vec{x})\ \left[G(\vec{x}) + c.c\right] \tag{3.14}$$

where $G(\vec{x})$ contains information about the EM field

$$G(\vec{x}) = \frac{1}{2}\int d\vec{k}\ e^{i\vec{k}\cdot\vec{x}}\ \alpha\left[\frac{1}{2}(k+\omega)\right]\beta^*\left[\frac{1}{2}(k-\omega)\right] \tag{3.15}$$

where $\vec{k} = (\omega, k)$. As we will see, $G\vec{x}$ will determine the time of transition, which in turn affects the phase accumulation. The total action is then

$$S_{tot} = S_A^{(0)} + S_B^{(0)} + S_{int} \tag{3.16}$$

where $S_{A,B}^{(0)}$ are the free field actions for massive scalar fields $\phi_{A,B}$ with rest masses $m_{A,B}$. Having traced out the EM degrees of freedom, we now have a system consisting only of the two atomic modes.

3.4 Equations of Motion for Atomic Modes

So far the formalism is general except for the assumption that the light field is an approximately classical coherent state and experiences no backaction from the interaction, and that we have an effective two mode interaction (neglecting the intermediate mode). We can now derive equations of motion by making a further assumption that the atomic modes are perturbed adiabatically such that the fields can be expanded as

$$\phi_A(t,z) = \int \frac{dk}{2\omega_A}\left[\hat{A}(t,k)e^{-i\omega_A t + ikz} + h.c\right] \tag{3.17a}$$

$$\phi_B(t,z) = \int \frac{dk}{2\omega_B}\left[\hat{B}(t,k)e^{-i\omega_B t + ikz} + h.c\right] \tag{3.17b}$$

The assumption is that the full time evolution of the atomic modes is a perturbation to its free evolution, so that $A(t,k)$ and $B(t,k)$ are slowly varying and $\omega_{A,B}$ is the free field dispersion, given by

$$\omega_{A,B}(k) = \sqrt{m_{A,B}^2 + k^2} \tag{3.18}$$

for the rest mass $m_{A,B}$. It is therefore sufficient to label the modes by the three-vector k as we've done in Eq. (3.17b). Mathematically, the slowly varying condition on $A(t,k)$ stated as

$$\frac{\langle \dot{A}(t,k)\rangle}{\langle \hat{A}(t,k)\rangle} \ll \omega_A(k) \tag{3.19}$$

and similarly for $B(t,k)$. Finally, we note that this expansion assumes a clear separation between the positive and negative frequency modes (no squeezing), which is a valid physical condition for these experiments.

We point out that expanding the full field operator in this way and removing the free evolution from the modes, the operators $\hat{A}$, $\hat{B}$ correspond to *interaction picture operators*. To obtain their equations of motions, we first note that with the expansion in Eq. (3.17b) and the assumption in Eq. (3.19), we can write

$$\hat{A}(t,k) = i\int dz\left[e^{i\omega_A t - ikz}\partial_t\phi_A(t,z) - \left(\partial_t e^{i\omega_A t-ikz}\right)\phi_A(t,z)\right] \tag{3.20}$$

Here we remind the reader that the four-vector $\vec{k}$ satisfies the free field dispersion relation, and therefore the time derivative of $\hat{A}^\dagger$ evaluates to

$$\dot{\hat{A}}(t,k) = i\int dz\; e^{i\omega_A t-ikz}\left[-\partial_\mu\partial^\mu + m_A^2\right]\phi_A(t,z) \tag{3.21}$$

We note that the term in the integrand is the variation of the free action for ϕ_A, or

$$\frac{\delta S_A^{(0)}}{\delta\phi_A} = \left[\partial_\mu\partial^\mu - m_A^2\right]\phi_A \tag{3.22}$$

Then, since the physical field configuration must extremize the action, we have

$$\frac{\delta S_{tot}}{\delta\phi_A} = 0 = \frac{\delta S^{(0)}}{\delta\phi_A} + \frac{\delta S_{int}}{\delta\phi_A} \tag{3.23}$$

which implies

$$\left[-\partial_\mu\partial^\mu + m_A^2\right]\phi_A = \frac{\delta S_{int}}{\delta\phi_A} = g\phi_B(\vec{x})\left[G(\vec{x}) + c.c\right] \tag{3.24}$$

Substituting Eq. (3.24) into the equation of motion for $\hat{A}$ and following a similar procedure for B, we have

$$\dot{\hat{A}}(t,k) = ig\int dz\; e^{i\omega_A t-ikz}\phi_B(t,z)\left[G(t,z) + c.c\right] \tag{3.25a}$$

$$\dot{\hat{B}}(t,k) = ig\int dz\; e^{i\omega_B t-ikz}\phi_A(t,z)\left[G(t,z) + c.c\right] \tag{3.25b}$$

Using the expansion in Eqs. (3.17), we can express the equations of motion above in terms of mode operators, obtaining expressions involving terms $\sim BG,\ B^\dagger G + c.c$ for $\dot{A}$ and $\sim AG,\ A^\dagger G + c.c$ for $\dot{B}$, each associated with a phase term. We expect the laser beams to be tuned such that only the phase of the second term is small. Then, as we will see, the integration over z will ensure that all other terms are negligible. This is equivalent to the rotating wave approximation whereby fast rotating terms are discarded. Then, keeping only the term with small phase and performing a similar analysis for $\hat{B}^\dagger$, we obtain the final form of our general expression for the coupled equations of motion for the mode operators

$$\dot{\hat{A}}(t, k_A) = i \int \frac{dk_B}{2\omega_B} \hat{B}(t, k_B) F^*(k_A, k_B, t) \tag{3.26a}$$

$$\dot{\hat{B}}(t, k_B) = i \int \frac{dk_A}{2\omega_A} \hat{A}(t, k_A) F(k_A, k_B, t) \tag{3.26b}$$

where

$$F(k_A, k_B, t) = g e^{i(\omega_B - \omega_A)t} \int dz\ e^{-i(k_B - k_A)z} G(t, z) \tag{3.27}$$

for $G(t, z)$ given in Eq. (3.15), and represent the *spatial* Fourier transform of the combined EM fields.

Pulsed Light Interaction

To proceed further we need to include information about the laser beams and obtain an expression for $F(k_A, k_B, T)$. In such experiments, at least one light beam is usual pulsed to control the timing of the atomic transitions. We assume for our model that both beams are pulsed and emitted respectively at the spacetime coordinates (t_1, z_1) and (t_2, z_2) (we can take pulse length $\to \infty$ for a continuous beam), and that the beams are narrowly Gaussian distributed in frequency ω_1 and ω_2 respectively. Then, the co-propagating beam has

$$\alpha(\omega) = a(\omega) \exp\left[-\frac{(\omega - \omega_1)^2}{2\Delta_\alpha^2}\right] \exp[i\omega(t_1 - z_1)] \tag{3.28}$$

where $a(\omega)$ is a frequency dependent amplitude that also includes the normalization factor for the Gaussian, and is in general complex. Similarly, the counter-propagating beam has

$$\beta^*(\omega) = b^*(\omega) \exp\left[-\frac{(\omega - \omega_2)^2}{2\Delta_\beta^2}\right] \exp[-i\omega(t_2 + z_2)] \tag{3.29}$$

Then let us assume that $a(k)$, $b(k)$ are slowly varying in k-space compared to the widths $\Delta_{\alpha,\beta}$, such that the amplitudes are approximately constant over the frequency

range that has non-negligible contributions. Then, performing the inverse Fourier transform we find

$$\tilde{\alpha}(z-t) = \bar{\alpha}\exp\left\{-\frac{\Delta_\alpha^2}{2}\left[(z-z_1)-(t-t_1)\right]^2\right\} e^{-i\omega_1(t-z)}e^{i\omega_1(t_1-z_1)} \tag{3.30a}$$

$$\tilde{\beta}^*(z+t) = \bar{\beta}\exp\left\{-\frac{\Delta_\beta^2}{2}\left[(z-z_2)+(t-t_2)\right]^2\right\} e^{i\omega_2(t+z)}e^{-i\omega_2(t_2+z_2)} \tag{3.30b}$$

where $\bar{\alpha} \propto |a(\omega_1)|$ and $\bar{\beta} \propto |b^*(\omega_2)|$ are real quantities related to the amplitude of the coherent state around the peak frequencies. Substituting the above expression into Eq. (3.27) for $F(k_A, k_B, t)$ and assuming the the pulse length of the counter-propagating beam is much larger than that of the co-propagating beam, or $\Delta_\beta \ll \Delta_\alpha$, we find

$$F(k_A,k_B,t) = g\bar{\alpha}\bar{\beta}e^{i(\phi_1-\phi_2)}\exp\left[-\frac{(k_A-k_B+k_\gamma)^2}{2\Delta_\alpha}\right] \exp\left[-i(\omega_A-\omega_B+\omega_\gamma)t + i(k_A-k_B+k_\gamma)z_1(t)\right] \tag{3.31}$$

for

$$\omega_\gamma = \omega_1 - \omega_2, \quad k_\gamma = \omega_1 + \omega_2 \tag{3.32}$$

and where $z_1(t)$ is the position of the photon emitted at (t_1, z_1) given by

$$z_1(t) = z_1 + c(t-t_1) \tag{3.33}$$

with constant phases

$$\phi_1 = \omega_1(t_1 - z_1), \quad \phi_2 = \omega_2(t_2+z_2) \tag{3.34}$$

The approximation regarding the pulse lengths means that the timing of the interaction is determined by the co-propagating beam, since the counter-propagating beam is effectively continuous in comparison, and the interaction can only occur when both beams are present. This is apparent in Eq. (3.31) which only depends on Δ_α and (t_1, z_1). Eq. (3.31) also tells us that the difference in the three-momentum between modes A and B has to be around k_γ as a manifestation of momentum conservation, and also justifies discarding the "fast-rotating" terms. Since the light pulses contain different modes, the difference does not need to be exactly k_γ, but as $\Delta_\alpha \to \infty$ the Gaussian in the expression for F becomes a δ-function and $k_A - k_B = k_\gamma$ exactly.

Localized and Non-Relativistic Atomic States

We can now solve Eq. (3.26) by taking into account some features of the atomic quantum states. First, we assume that the spread of the atomic wavepacket in momentum space is much greater than that of the light pulse, we can evaluate the mode operators at the peak of the Gaussian in $F(k_A, k_B, t)$ and take them outside the integral, so that

$$\dot{\hat{A}}(t, k_A) = ig\hat{B}(t, k_A + k_\gamma) \int \frac{dk_B}{2\omega_B} F^*(k_A, k_B, t) \tag{3.35a}$$

$$\dot{\hat{B}}(t, k_B) = -ig\hat{A}(t, k_B - k_\gamma) \int \frac{dk_A}{2\omega_A} F(k_A, k_B, t) \tag{3.35b}$$

This approximation corresponds to the physical situation where the atomic wavepackets are much more spatially localized than that of the light pulse, so that the interaction can be approximated as occurring over the entire atomic wavepacket at the same time (in both the inertial and accelerated frames). Whereas in the general case, transitions between A and B occur between all k-modes, such that a single k-mode in A has some probability of transitioning to all k-modes in B and vice versa, under this approximation, transitions only occur between one pair of modes relative by the light wavevector k_γ.

We then assume that the atom is non-relativistic, so that $\hbar k \ll mc$ for both modes and we can expand the dispersion relations as

$$\omega_{A,B}(k) = m_{A,B}^2 + \frac{k^2}{2m_{A,B}} + O(v^2), \tag{3.36}$$

We also denote the difference in the Compton frequencies between the two modes as

$$\Omega_R = m_B - m_A, \quad m_B > m_a \tag{3.37}$$

and point out the ω_R is the resonant frequency of transition in the rest frame of the atom. Then, integrating over k_B (k_A) in Eq. (3.38), we finally obtain solvable equations of motion

$$\dot{\hat{A}}^\dagger(t, k) = ie^{-i\Delta_A t} f_A(t) e^{-i(\phi_1 - \phi_2)} \hat{B}(t, k + k_\gamma) \tag{3.38a}$$

$$\dot{\hat{B}}^\dagger(t, k + k_\gamma) = ie^{i\Delta_B t} f_B(t) e^{-i(\phi_1 - \phi_2)} \hat{A}(t, k) \tag{3.38b}$$

for

$$\Delta_{A,B} = \Omega_R - \omega_\gamma(1 - v_{A,B}) \tag{3.39}$$

and

$$f_{A,B}(t) = \frac{g\bar{\alpha}\bar{\beta}}{2m_{A,B}} \exp\left[-\frac{\Delta_\alpha^2}{2}(c - v_{A,B})^2(t - \tilde{t}_{A,B})^2\right] \tag{3.40}$$

where

$$v_A = \frac{k}{\bar{m}}, \quad v_B = \frac{k + k\gamma}{\bar{m}}, \tag{3.41}$$

and

$$\tilde{t}_{A,B} = \frac{t_1 - z_1}{1 - v_{A,B}} \tag{3.42}$$

To obtain the above we've introduced errors of$O(\Omega_R/\bar{m})$, which is very small when we assume negligible diffraction for the atomic wavepacket during the time of the experiment.

Let us now interpret these equations. As suggested by its notation, $\Delta_{A,B}$ represents the detuning of the laser frequencies from the rest frame resonance, with the Doppler shift properly accounted for. We note that the Doppler shift is with respect to the three-momentum of the mode and does not reference the velocity of the atom, meaning that each k-mode in the atomic wavepacket intoduces a different Doppler shift to the light frequency. This is a subtlety not typically accounted for, but of course is a small effect when the variance in momentum is small compared to its average value. The function $f_{A,B}(t)$ represents a time dependent frequency of transition, and selects for the value of t when the transition occurs. The width of the Gaussian in $f(t)$ is the time it takes for light to travel across the spatial extent of the pulse, and peak occurs at $t_{A,B}$ which is the time when the trajectory of the particle with three-momentum k starting from $z = 0$ meets trajectory of the photon emitted at (t_1, z_1).

Another point to note is that since the detuning and frequency functions depend on the value of k, they are not equal in the equations for motion for the mode pair $\hat{A}^\dagger(k)$ and $\hat{B}^\dagger(k + k_\gamma)$ with differences of $O(k_\gamma/m_{A,B})$. These differences stem from the the picture that for a $A \to B$ transition, the absorbed and emitted photons should be Doppler shifted with respect to the k-vector of the A state, while for the reverse transition they should be Doppler shifted with respect to that of the B state $k_B = k + k_\gamma$. However, we point out that this picture cannot be fully accurate without accounting for the intermediate state, and with the state error we evaluate the detuning and frequency functions at mode A's three-momentum k and drop the A, B subscripts on $\Delta,\ f(t), v, \tilde{t}$.

Solutions to Equations of Motion

The Eqs. (3.38) represents the final form of the equations of motion given our approximations regarding the light pulse and the atomic wavepackets. In fact, we can obtain the full time evolution of the modes with the Heisenberg picture mode

operators

$$A_H(t,k) = A(t,k)e^{-i\omega_A(k)t}, \quad B_H(t,k) = B(t,k)e^{-i\omega_B(k)t} \tag{3.43}$$

for which we obtain the equation pair

$$\dot{A}_H(t,k) = ie^{i\phi(t)}f(t)B_H(t,k+k_\gamma) - i\omega_A A_H(t,k) \tag{3.44a}$$

$$\dot{B}_H(t,k+k_\gamma) = ie^{-i\phi(t)}f(t)A_H(t,k) - i\omega_B B_H(t,k+k_\gamma) \tag{3.44b}$$

where $f(t)$ is defined in Eq. (3.40) and for the time dependent phase

$$\phi(t) = \Big[\omega_B(k+k_\gamma) - \omega_A(k) - \Omega_R + \omega_\gamma(1-v)\Big]\,t - (\phi_1 - \phi_2) \tag{3.45}$$

For a short and high intensity pulse centered at time $\tilde{t}_- \approx \tilde{t}$ with and ending at $\tilde{t} + \delta t$, the above pair of equations have the solutions [59] (dropping the H subscript and working now in the Heisenberg picture)

$$A(\tilde{t}+\delta t) = \Big[\cos(\bar{f}\delta t)A(\tilde{t}) + i\sin(\bar{f}\delta t)B(\tilde{t})e^{i\phi(\tilde{t})}\Big]\,e^{-i\omega_A\delta t} \tag{3.46a}$$

$$B(\tilde{t}+\delta t) = \Big[\cos(\bar{f}\delta t)B(\tilde{t}) + i\sin(\bar{f}\delta t)A(\tilde{t})e^{-i\phi(\tilde{t})}\Big]\,e^{-i\omega_B\delta t} \tag{3.46b}$$

where $\bar{f}$ is the average value of $f(t)$ over pulse duration given by

$$\bar{f} = \frac{1}{\delta t}\int dt\, f(t) \tag{3.47}$$

Here we've suppressed the momentum argument with the understanding that we are always referring to the two modes $A(t,k)$ and $B(t,k+k_\gamma)$. The solutions in Eqs. (3.46) have phase errors of $O(\Delta\times\delta t)$ and amplitude errors of $O(\Delta/\bar{f})$. We see from these equations that a photon mirror interaction is obtained for pulse duration $\bar{f}\delta t = \pi$, while a beamsplitter interaction is obtained for pulse duration $\bar{f}\delta t = \pi/2$.

3.5 Phase Shift in the Interferometry Experiment

For the experiment we can identify three pulse regions centered at $\tilde{t}^{\,i}$, $\tilde{t}^{\,ii}$, $\tilde{t}^{\,iii}$ that are of type beamsplitter, mirror, and beamsplitter respectively, and four propagation regions 0, I, II, III. In the initial propagation region, the operators are simply free field operators, or

$$A^{(0)}(t) = A_s e^{-i\omega_A t}, \quad B^{(0)}(t) = B_s e^{-i\omega_B t} \tag{3.48}$$

where the subscript s denotes the Schroedinger operator. These free operators then provide the initial values $A(\tilde{t}^{\,i}) = A^{(0)}(\tilde{t}^{\,i})$ and $B(\tilde{t}^{\,i}) = B^{(0)}(\tilde{t}^{\,i})$ in Eqs. (3.46) for the

first pulse. Then, denoting operators in the pulse region by A_i and B_i, we can obtain the mode operators in propagation region I by imposing the continuity conditions

$$A_I(\tilde{t}^i + \delta t) = A_i(\tilde{t}^i + \delta t), \quad B_I(\tilde{t}^i + \delta t) = B_i(\tilde{t}^i + \delta t) \tag{3.49}$$

The operators A_I and B_I then provide the initial values at the beginning of the second pulse at $\tilde{t}^{ii}$, and so on and so forth. Finally, in the last propagation region III where detection occurs we obtain

$$A_{III}(t) = \left[\frac{1}{2}e^{i\Phi}\left(1 + e^{i\Delta\phi}\right)A_s - \frac{i}{2}e^{i\Phi'}\left(1 - e^{i\Delta\phi}\right)B_s\right]e^{-i\omega_A t} \tag{3.50a}$$

$$B_{III}(t) = \left[\frac{i}{2}e^{-i\Phi'}\left(1 - e^{-i\Delta\phi}\right)A_s - \frac{1}{2}e^{-i\Phi}\left(1 + e^{i\Delta\phi}\right)B_s\right]e^{-i\omega_B t} \tag{3.50b}$$

where Φ, Φ' are unimportant overall phase shifts. To interpret these solutions, we point out that A_{III} and B_{III} are detected at the two different ports in a Mach-Zehdner geometry. For an initial single atom wavepacket prepared in the A state given by

$$|\psi\rangle = \int dk\, \sqrt{2\omega_A}\, Q(k) A_s^\dagger(k)|0\rangle \tag{3.51}$$

such that

$$\int dk |Q(k)|^2 = 1$$

(note that $A^\dagger|0\rangle$ states have normalization $2\omega_A$), then at the A-port one detects a particle with probability

$$\langle\psi| \int \frac{dk}{2\omega_A} A_{III}^\dagger(t,k) A_{III}(t,k)|\psi\rangle = \frac{1}{2} + \int dk |Q(k)|^2 \cos\Delta\phi(k) \tag{3.52a}$$

while at the B-port one detects a particle with probabilty

$$\langle\psi| \int \frac{dk}{2\omega_B} B_{III}^\dagger(t,k) B_{III}(t,k)|\psi\rangle = \frac{1}{2} - \int dk |Q(k)|^2 \cos\Delta\phi(k) \tag{3.52b}$$

where we have ignored errors of $O(\omega_\gamma/m_{A,B})$. The detected phase shift is averaged over all k-modes since the phase shift is k-dependent, as is clear from the expression

$$\begin{aligned}\Delta\phi(k) =& [-\Omega_R + \omega_\gamma(1 - v_k))]\left(\tilde{t}^{iii} - 2\tilde{t}^{ii} + \tilde{t}^i\right) \\ &- \left[(\phi_1 - \phi_2)^{iii} - 2(\phi_1 - \phi_2)^{ii} + (\phi_1 - \phi_2)^i\right]\end{aligned} \tag{3.53}$$

The k-dependence results from v_k which represents the Doppler shift on the laser frequency experienced by the different k-modes of the atomic states, and the superposition of momentum states in the atomic wavepacket evidently leads to a loss of

fringe visibility. However, for a narrow momentum distribution we can approximate $v_k \approx \bar{v}$, where $\bar{v}$ is the average velocity of the atom. When the laser beams are on resonance with respect to the average velocity, $-\Omega_R + \omega_\gamma(1-\bar{v})$ is precisely zero (recall that Ω_R is the resonant transition frequency in the atom's rest frame, while $\omega_\gamma(1-\bar{v})$ is the frequency of the laser beams shifted to the rest frame of the atom). Therefore, the total phase shift is given by

$$\Delta\phi = -\left[(\phi_1-\phi_2)^{iii} - 2(\phi_1-\phi_2)^{ii} + (\phi_1-\phi_2)^{i}\right] \tag{3.54}$$

which derives from the constant shifts in Eq. (3.34) and $(\phi_1 - \phi_2)$ depend on the spacetime points of emission of the co- and counter-propagating pulses given by (t_1, z_1) and $(t_2, z_2)$for each of the three pulses applied over the course of the experiment. In the described experimental setup, the emitters for the co- and counter-propagating beams follow the same trajectory given by Eq. (3.3) and emits pulses at proper times $\tau = \tau_0, \tau_0 + T, \tau_0 + 2T$. Since the co-propagating beam only interacts with the atom after being reflected at $Z = -L$ in the accelerating frame, its effective spatial coordinate in the accelerating frame is $Z = -2L$, as given by Eq. (3.4). Then corresponding Minkowski coordinates to leading order in $O(g)$ are

$$(t_1(\tau), z_1(\tau)) = \left(\tau, -2L + \frac{1}{2}g\tau^2\right) \tag{3.55}$$

$$(t_2(\tau), z_2(\tau)) = \left(\tau, \frac{1}{2}g\tau^2\right) \tag{3.56}$$

For each pulse we evaluate $(\phi_1 - \phi_2)$ at the spacetime coordinates given by Eq. (3.55) at the proper time of emission. Then Eq. (3.54) gives us

$$\Delta\phi = (\omega_1 + \omega_2)gT^2 \tag{3.57}$$

which is precisely the phase shift predicted in previous analyses [35].

3.6 Conclusions and Outlook

Using a Lorentz covariant formalism we have recovered the predictions that have been verified by the experiments of Kasevich, Peters, Chung, and Chu [35, 53] as a proof of principle, but the advantages to this framework has not been yet explored in this chapter. It provides a rigorous method for determining the approximations that must be made in order for the standard analysis to be valid, as well as a path for determining relativistic corrections and for incorporating the quantum fluctuations of light (which was here approximated as being classical, though the formalism is extendable to a full quantum treatment). Additionally, this formalism clarifies that

the source of the phase shift is neither due to propagation nor the phase of the laser beam at the point of interaction, but rather due to the initial conditions on the laser phase (specifically, that the laser phase is zero at the point of emission), which mean that the phase of each laser pulse must be carefully calibrated and should not depend on g (in the case where the laser frequency is Doppler shifted in a phase continuous way in the accelerating frame so as to be resonant with the free falling atoms, no phase shift will be detected [35]). As future work, it would be interesting to include a full quantum treatment for the laser beams and quantify the effect of its quantum fluctuations on the sensitivity of the atom interferometer as a quantum sensor, as well as compare the predictions of this framework to the frequently cited analyses [23, 63] with a particular regard towards relativistic corrections and a careful accounting of the errors introduced in the approximations implicit in those analyses.

Chapter 4

FIRST PRINCIPLES HAMILTONIAN FORMULATION OF OPTOMECHANICS

4.1 Preface

In this chapter we rigorously derive the Hamiltonian governing the dynamics for the optical field inside a Fabry Perot cavity interacting with a mechanical degree of freedom that changes its resonance condition, also known as the optomechanical interaction. For our problem we consider the simplest model where the mechanical degree of freedom is one of the cavity's mirrors, although experimental implementation of the optomechanical Hamiltonian has many variants. We show that our derivation is consistent with the current phenomenological formulation of the Hamiltonian, and discuss the applicability of our derivation to experimental variants. We also include a brief discussion of the advantages a rigorous derivation might have over the phenomenological formulation.

4.2 Introduction

The field of optomechanics has seen rapid experimental progress over the last decade. One main thrusts of these experiments is to observe quantum behaviour in macroscopic objects or to prepare macroscopic objects in quantum states. Some important results in this effort include the cooling of a nanomechanical resonator down to its quantum ground state [18], the observation of quantum coherent backaction force [58], and quantum squeezing of mechanical motion [74]. The motivation for studying optomechanical systems lies both in its potential for technological applications as well as for studying foundational questions in quantum mechanics. In terms of applications, there is active research in using optomechanical devices as an interface between different forms of quantum information carriers (i.e photons to phonon) to facilitate the sending, receiving, and storing quantum information [62, 76], as well as for use in ultra-weak force sensing [74]. As for fundamental physics, optomechanics allows one to study quantum behaviour on increasingly more massive scales, exhibiting the potential for bridging the quantum and classical regimes and offering the possibility of studying the quantum-classical transition. In this vein, optomechanical systems have been part of proposals to test spontaneous collapse models in which quantum superpositions localize in space at rates which depend on

some measure of macroscopicity, for example the mass density [9]. These models are phenomenological and motivated by the need to explain the randomness of the quantum measurement and the lack of observed quantum behaviour in ordinary experience, but has the advantage of being testable, and optomechanics experiments are approaching the regime to set bounds on model parameters. Additionally, the larger masses in optomechanical experiments lends itself naturally to studying the effects of gravity on quantum systems, leading to many proposals to test models of semiclassical or quantum gravity [75].

However, despite the interest in using optomechanics to study foundational questions in physics whose signatures often appear as very small effects, there has been no rigorous derivation of its Hamiltonian where both the cavity and mechanical modes are treated as dynamical degrees of freedom. To our best knowledge, the most foundationally motivated derivation constructs a Lagrangian from given equations of motion. While this formulation reproduces the linearized result and perturbative result that is consistent with experiment, it cannot address situations in which the optomechanical system interacts with other degrees of freedom whose effects on the optical and mechanical modes are not known *a priori* or phenomenologically, and must instead be derived from first principle, such as the case with weak quantum gravity. Therefore, it may be worthwhile to develop a formulation for the optomechanical system that lends itself more readily to the study of general interactions. Since the action provides the most fundamental description of any matter whether classical or quantum, we begin with the action and present a derivation of the optomechanical Hamiltonian where both the optical and mechanical modes are dynamical quantities and therefore free to interact, which facilitates the introduction of new interactions through the addition of the corresponding action terms.

4.3 Previous formulations

The optomechanical Hamiltonian for a cavity with a movable end mirror is given by

$$\hat{H} = \hbar\omega_0 \hat{a}^\dagger \hat{a} + H_q^{(0)} - \frac{\hbar\omega_0}{L}\hat{q}\hat{a}^\dagger\hat{a} \tag{4.1}$$

where L is the equilibrium length of the cavity and $\omega_0 = n\pi c/L,\ n \in \mathbb{Z}$ is the cavity resonance at equilibrium, and $H_q^{(0)}$ is the free Hamiltonian for the end mirror represented by its center of mass coordinate $\hat{q}$. The derivation of the interaction is most commonly presented as an expansion of the cavity's resonance frequency

about perturbation to its equilibrium length [8].

$$\omega(q) = \frac{\omega_0}{(1 + q/L)} \approx \omega_0 + q\frac{\partial\omega}{\partial q} + \frac{1}{2}q^2\frac{\partial^2\omega}{\partial q^2} + \ldots \tag{4.2}$$

This phenomenological derivation predicts results which are consistent with experiment, but it's unclear if it can be trusted at higher order of q/L or when considering relativistic effects. A more first principles approach is given by Law Ref. [40], whereby the electromagnetic field is constrained to satisfy the boundary conditions corresponding to perfectly reflective mirrors

$$A(t, 0) = A[t, q(t)] = 0 \tag{4.3}$$

where $q(t)$ is the full length of the cavity and time dependent. The field is then be decomposed into

$$A(t, x) = \sum_{n=1}^{\infty} Q_n(t)\sqrt{\frac{2}{q(t)}}\sin\left[\frac{n\pi x}{q(t)}\right], \quad n \in \mathbb{Z} \tag{4.4}$$

and further constrained to satisfy *a priori* equations of motion for the EM field and mirror position, given by

$$\frac{\partial^2 A(t, x)}{\partial x^2} = \frac{1}{c^2}\frac{\partial^2 A(t, x)}{\partial t^2} \tag{4.5a}$$

$$m\ddot{q} = -\frac{\partial V(q)}{\partial q} + \frac{1}{2}\left[\frac{\partial A(t, x)}{\partial x}\right]^2\Bigg|_{x=q(t)} \tag{4.5b}$$

Substituting Eq. (4.4) into Eq.s (4.5) results in coupled equations of motion for Q_n and q. Finally, a Lagrangian is constructed such to produce those equations of motion which contains all coordinates and velocities explicitly and canonical quantization proceeds in the usual way.

Evidently, the issue with this formulation is that the equations of motion must be known beforehand, which seems to be begging the question since, fundamentally, those equations should be obtained from the Lagrangian itself. Furthermore, the field $A(t, x)$ is confined within the cavity and therefore the wave equations is only valid in between the two mirrors. It is unclear how this consideration is reflected in the above derivation and whether it would lead to corrective effects. Possible issues regarding Eq. (4.5a) can be seem more clearly from revisiting the derivation of the Euler Lagrangian field equations, from which Eq. (4.5a) presumably follows. Suppose we have the action

$$S = \int d^4x\, \mathcal{L}\left(\phi, \partial_\mu\phi\right) \tag{4.6}$$

The variational principle states that the physical field configuration is an extremum of the action such that its first order perturbations vanish. Applying this, we find

$$\delta S\Big|_{\phi_{\text{soln}}} = 0 = \int d^4x \left\{ \left[\frac{\partial \mathcal{L}}{\partial \phi} - \partial_\mu \frac{\partial \mathcal{L}}{\partial(\partial_\mu \phi)} \right] \delta\phi + \partial_\mu \left(\frac{\partial \mathcal{L}}{\partial(\partial_\mu \phi)} \delta\phi \right) \right\} \Bigg|_{\phi_{\text{soln}}} \tag{4.7}$$

Under normal circumstances, the last term in Eq. (4.7) vanishes since it is a total divergence term and 4-current inside the divergence operator is evaluated at the boundary where $\delta\phi = 0$ (typically at infinity). Indeed, this procedure will give the wave equation in Eq. (4.5a) for a massless scalar field. However, in optomechanics we have a constrained problem where the constraint itself is a *dynamical quantity* that must be allowed to vary independently from A. We cannot set the total divergence term in Eq. (4.7) to zero at the boundary because the boundary is not fixed, and moreover must be allowed to vary over all possible values. Since the four divergence does not vanish, it seems that we cannot simply write down Eq. (4.5a) even with the caveat that it applies only inside the cavity.

In a more recent paper [36], Khorasani follows Law's approach but constructs a different Lagrangian out of the same equations of motion. This apparently is *not* an error in the calculations but is instead due to the fact that the Lagrangian is not fully constrained by equations of motion. The difference further highlights the need for a more consistent first principles approach.

4.4 Canonical Formulation from First Principles

The consistent way to apply the variational principle clearly requires us to define coordinates well defined endpoints where variations can be made to vanish. To this end, we introduce a "global" coordinate to represent excitations of a mode whose profile satisfies the boundary constraints in Eq. (4.3) while the coordinate is allowed to vary freely. In this way, the boundary conditions on the electromagnetic field are no longer boundaries on the action. Under this coordinate transformation, we obtain the Lagrangian without assuming *a priori* equations of motion.

We begin with the action of an unsourced EM field confined within two perfectly reflecting mirrors. Using Einstein summation notation and expanding denoting the vector potential by $\tilde{A}^\mu$, we write

$$L_{EM} = \int_{V_{\text{cav}}} d^3\mathbf{x} \left[-\frac{1}{4\mu_0} F_{\mu\nu} F_{\mu\nu} \right] = -\frac{1}{2\mu_0} \int_{V_{\text{cav}}} d^3\mathbf{x} \left[(\partial_i \tilde{A}_j)^2 - \frac{1}{c^2} \dot{\tilde{A}}_j^2 \right] \tag{4.8}$$

for $i \neq j$, where we've applied the Coulomb gauge and set $A^0 = 0$. The integration over space in confined to the volume within the cavity. Of course, the boundaries

of the cavity is only along one dimension, which we label x. We assume the light mostly propagates along the cavity axes, and therefore that the $\mathbf{k}$-vectors of the field have the property that $k_x \gg k_y,\, k_z$. Assuming that the transverse mode profile of the propagating field is approximately constant over the cavity length, we separate $\tilde{A}_j$ as follows

$$\tilde{A}_j(t, \mathbf{x}) = u(y, z)A(t, x) \tag{4.9}$$

Since the spatial variation of the mode profile is much smaller than the light propagation vector, or $\partial_{y,z}u(y, z) \ll |\mathbf{k}|$, we can write $(\partial_i \tilde{A}_j)^2 \approx u^2(y, z)(\partial_x A_j)^2$. The integrand in Eq. (4.8) is now a separable function of (y, z) and x and the integration over the transverse directions gives

$$\int_{-\infty}^{\infty} dxdy\ |u(y, z)|^2 \equiv \mathcal{U} \tag{4.10}$$

and the Lagrangian becomes

$$L_{EM} = \frac{\mathcal{U}}{2\mu_0} \int_0^{q(t)} dx \left[-(\partial_x A_j)^2 + \frac{1}{c^2}\dot{A}_j^2 \right], \quad j = x, y \tag{4.11}$$

The vector nature of the field is irrelevant and we continue our calculation by just considering one of the polarizations, which we denote by A. In a similar way to Ref. [36, 40] we decompose the EM field into modes which satisfy the boundary condition for perfectly reflecting mirrors given in Eq. (4.3). Additionally, for simplicity we assume a driven cavity at a particular resonance frequency so that the cavity contains only one mode. The EM is then written as

$$A(t, x) = \frac{c}{\sqrt{\omega_0 q}} \Phi(t) \sin(kx), \quad \frac{n\pi}{q(t)} \tag{4.12}$$

where ω_0 is the resonant frequency when $q(t) = L_0$. At this point, L_0 does not have a physical interpretation and is simply some constant value. The above decomposition is in fact a coordinate transformation, whereby the implicit dependence of $A(t, x)$ on coordinate L is made explicit. Substituting this form of $A(t, x)$ directly into L_{EM}, we obtain

$$L_{EM}\left(q, \dot{q}, \Phi, \dot{\Phi}\right) = \frac{\mathcal{U}}{2\mu_0\omega_0} \left[\frac{1}{2}\dot{\Phi}^2 - \frac{1}{2}\omega_q^2 \left(1 - \frac{1}{3}\frac{\dot{q}^2}{c^2} \right) \Phi^2 \right] \tag{4.13}$$

The above is an exact expression with $\omega_q = n\pi c/q$. We remark that the EM field is now represented by single coordinate Φ which represents the amplitude of a *global* mode, in contrast to Eq. (4.8) where the Lagrangian was given in terms of the *local*

field strength. Because the global mode includes information about the boundary, the auxiliary conditions in Eq. (4.3) and their effects on dynamics are built into the Lagrangian. To obtain the Hamiltonian we need to write down the full Lagrangian including the portion concerning the mirror motion.

To be consistent with relativistic term $\sim \dot{q}^2/c^2$ in L_{EM} we must also include special relativistic corrections in the mirror Lagrangian. For a particle not subject to external forces, its relativistic Lagrangian is given by

$$L_M = -mc\sqrt{-g_{\mu\nu}\dot{x}^\mu \dot{x}^\nu} \tag{4.14}$$

We assume that the system is in a static gravitational field and that the gravitational force is counteracted (e.g. by a table) so that we can set $g_{\mu\nu} = \eta_{\mu\nu}$. Additionally, we allow the possibility of external potential $V(q)$. Of course, in the relativistic formalism the potential must be given by the mirror's 4-vector, but we can say that we know the form of the potential in our local frame and furthermore that the only relevant forces are along the direction of the cavity axis. Then, defining $M_E = \mathcal{U}/2\mu_0\omega_0$ the total optomechanical Lagrangian becomes

$$L = -mc^2\sqrt{1-\frac{\dot{q}^2}{c^2}} - V(q) + \frac{1}{2}M_E\dot{\Phi}^2 - \frac{1}{2}M_E\omega_q^2\Phi^2\left[1-\frac{1}{2}\frac{\dot{q}^2}{c^2}\right] \tag{4.15}$$

At this point we'd like to take a slight detour and comment on Legendre transforms in the presence of weak velocity coupling of $O(\epsilon)$ or small non-quadratic velocity terms of $(O(\delta)$. In our case we have Φ coupled to $\dot{q}^2$ as well as the relativistic kinetic term, both of which will change the form of the canonical momentum. However, we can show that for $\epsilon,\ \delta \ll 1$ the difference in the Hamiltonian obtained by using the free versus exact canonical momenta is $O(\epsilon^2,\ \delta^2)$. To see this, let's write down a general Lagrangian with these types of terms

$$L_Q = \frac{1}{2}\alpha\dot{Q}^2 + gX + \alpha\frac{\beta}{s+2}\dot{Q}^{(s+2)}, \quad s \in \mathbb{Z},\ s > 0 \tag{4.16}$$

where α is a mass-like parameter and X is the interacting degree of freedom. We identify $gX = 2\epsilon/\alpha$ and $\beta\dot{Q}^s = \delta$ so that L_Q becomes

$$L_Q = \frac{\alpha}{2}(1+\epsilon)\,\dot{Q}^2 + \alpha\frac{\delta}{s+2}\dot{Q}^2 \tag{4.17}$$

The free and exact momenta are given by

$$P^{(0)} = \alpha\dot{Q} \tag{4.18a}$$

$$P = \alpha(1+\epsilon)\dot{Q} + \alpha\delta\dot{Q} = \alpha(1+\epsilon)\dot{Q} + \alpha\beta\dot{Q}^{(s+1)} \tag{4.18b}$$

We can solve for $\dot{Q}$ iteratively in terms of P and obtain

$$\dot{Q} = \frac{P}{\alpha(1+\epsilon)} - \frac{\beta}{(1+\epsilon)}\left[\frac{P}{\alpha(1+\epsilon)}\right]^{(s+1)} \tag{4.18c}$$

Then the Hamiltonian $H = P\dot{Q} - L[Q, \dot{Q}(P)]$ is given by

$$H = \frac{P^2}{2\alpha}(1-\epsilon) - \frac{\beta}{(s+2)}\left(\frac{P}{\alpha}\right)^s \frac{P^2}{\alpha} + O(\epsilon^2) + O(\epsilon\delta) + O(\delta^2) \tag{4.18d}$$

Conversely, if we simply used the form of the canonical momentum given by $P^{(0)}$ so that $\dot{Q} = P/\alpha$, we obtain the same result to the given order.

Returning to our problem, we see that the values for ϵ and δ are

$$\delta \sim \frac{\dot{q}^2}{c^2}, \quad \epsilon \sim \frac{M_E\omega^2\Phi^2}{mc^2} = \frac{E_{EM}}{mc^2} \tag{4.19}$$

where E_{EM} is the energy of the optical field which would be much smaller than the rest mass energy of an macroscopic mirror. Then the canonical momenta are

$$p = \frac{\partial L}{\partial \dot{q}} = m\dot{q}, \quad \Pi = \frac{\partial L}{\partial \dot{\Phi}} = M_E\Phi \tag{4.20}$$

giving the Hamiltonian

$$H = \frac{p^2}{2m} - \frac{p^4}{8m^3c^2} + V(q) + \frac{\Pi^2}{2M_E} + \frac{1}{2}M_E\omega_q^2\Phi^2\left[1 - \frac{1}{3}\frac{p^2}{m^2c^2}\right] \tag{4.21}$$

We can quantize here, but it is more useful to write H in a form that is consistent with formulations in the current literature. To this end, we introduce the canonical pair $\{\alpha_1, \alpha_2\}$ which represents the phase and amplitude of the cavity mode, and additionally transform into the frame that is co-rotating with ω_0 (this allows us to separate the fast and slow time dependences in the system). The new pair is related to $\{\Phi, \Pi\}$ by

$$\Phi = \sqrt{\frac{1}{\omega_0 M_E}}\left[\alpha_1\cos\omega_0 t + \alpha_2\sin\omega_0 t\right] \tag{4.22a}$$

$$\Pi = -\sqrt{\omega_0 M_E}\left[\alpha_1\sin\omega_0 t - \alpha_2\cos\omega_0 t\right] \tag{4.22b}$$

One can check that $\dot{\Phi} = \Pi/M_E$ in the above expressions as required. We use the type I generating function for the canonical transformation from $\{\Phi, \Pi\} \to \{\alpha_1, \alpha_2\}$ where

$$\frac{\partial F(\alpha_1, \Phi)}{\partial \alpha_1} = -\alpha_2, \quad \frac{\partial F(\alpha_1, \Phi)}{\partial \Phi} = \Pi \tag{4.23}$$

and the new Hamiltonian is

$$H_{\text{new}}(\alpha_1, \alpha_2) = H_{\text{old}}(\Phi, \Pi) - \frac{\partial F}{\partial t} \tag{4.24}$$

From now on we will denote H_{new} by H. Now we impose the canonical commutations relations

$$[\hat{p}, \hat{q}] = i\hbar, \quad [\hat{\alpha}_1, \hat{\alpha}_2] = i\hbar \tag{4.25}$$

and write the phase and amplitude in terms of raising and lowering operators

$$\hat{\alpha}_1 = \sqrt{\frac{\hbar}{2}}\left(\hat{a} + \hat{a}^\dagger\right), \quad \hat{\alpha}_2 = -\sqrt{\frac{\hbar}{2}}\left(\hat{a} - \hat{a}^\dagger\right), \tag{4.26}$$

so that $\left[\hat{a}, \hat{a}^\dagger\right] = 1$. We note that this is not a canonical transformation and therefore Eq. (4.26) can be substituted directly into H, which becomes

$$\begin{aligned} H = {} & \Gamma(\hat{p}, \hat{q})\left(\hat{a}^\dagger\hat{a} + \frac{1}{2}\right) + \frac{\hat{p}^2}{2m} - \frac{\hat{p}^4}{8m^3c^2} + V(\hat{q}) \\ & + \frac{1}{2}\Gamma(\hat{p}, \hat{q})\left[\left(\hat{a}^2 + \hat{a}^{\dagger 2}\right)\cos 2\omega_0 t - i\left(\hat{a}^2 - \hat{a}^{\dagger 2}\right)\sin 2\omega_0 t\right] \end{aligned} \tag{4.27}$$

where

$$\Gamma(\hat{p}, \hat{q}) = \frac{\hbar}{2\omega_0}\left[(\omega_{\hat{q}}^2 - \omega_0^2) - \frac{\omega_{\hat{q}}^2}{3}\frac{\hat{p}^2}{m^2c^2}\right] \tag{4.28}$$

Up to this point the only approximation we've made has been to discard terms of $O(\epsilon^2)$, $O(\delta^2)$, $O(\epsilon\delta)$ for ϵ, δ given in Eq. (4.19). There is also the implicit assumption that $\Delta\hat{q}/\hat{q} \ll \omega_{FSR}/\omega$ for the free spectral range ω_{FSR} of the cavity in order for the single mode model be valid. We see that the movable boundary mediates two-photon processes.

4.5 Approximations

We now assume that the mirror moves perturbatively about some equilibrium length which value we assign to L_0, and we redefine $\hat{q}$ to be the deviation from equilibrium so that $\hat{q}(t) \to \hat{q}(t) - L_0$. Recall that $\omega_0 = n\pi c/L_0$ and is now therefore the cavity resonance at equilibrium. Upon examining the Hamiltonian in Eq. (4.27) we see that pair creation and annhiliation processes occur at $2\omega_0$, or approximately twice the optical frequency compared to other dynamics, and we remove these terms using the Rotating Wave Approximation (RWA). To compare our derivation to the phenomenological formulation and the result obtained in Ref. [40], we expand H to

second order in $\hat{q}/L_0$ and obtain

$$H = \frac{\hat{p}^2}{2m}\left[1 - \frac{1}{4}\frac{\hat{p}^2}{m^2c^2} - \frac{1}{3}\frac{\hbar\omega_0\left(\hat{a}^\dagger\hat{a} + 1/2\right)}{mc^2}\right] + V(\hat{q}) \\ - \hbar\omega_0\left(\hat{a}^\dagger\hat{a} + \frac{1}{2}\right)\left[\frac{\hat{q}}{L_0} - \frac{3}{2}\frac{\hat{q}^2}{L_0^2}\right] \tag{4.29}$$

We remark that the vacuum energy of the EM mode appears in H, and when the field outside the cavity as well as all modes inside the cavity are considered these terms give the Casimir effect. It seems that in Eq. (4.29) there may be a relativistic correction to the Casimir effect due to the previously neglected interaction between the mirror's kinetic energy and the optical mode (which we will refer to as momentum-field coupling). This issue has not been carefully studied. Ignoring the vacuum effect, relativistic terms and keeping only to linear order in $\hat{q}/L_0$, our treatment agree with the previous derivations and experimental results.

4.6 Comparison with previous formulations

If we were to include the leading order relativistic correction and the second order term in $\hat{q}/L_0$ following the phenomenological formulation of Ref. [8] using the expansion for ω_{cav} given in Eq. (4.2), we would obtain

$$H_{\text{phen}} = \frac{\hat{p}^2}{2m}\left(1 - \frac{\hat{p}^2}{4m^2c^2}\right) - \hbar\omega_0\hat{a}^\dagger\hat{a}\left(\frac{\hat{q}}{L_0} - \frac{\hat{q}^2}{L_0^2}\right) \tag{4.30}$$

Comparing this to our result in Eq. (4.29), we see that the $\hat{q}^2/L_0^2$ terms differ by a factor of $3/2$ and, more interestingly, that the phenomenological formulation does not produce the $O(E_{EM}/mc^2)$ correction. The size of the E_{EM}/mc^2 term may be comparable or even exceed that of the $\hat{p}^4$ term and would be important in any experiment that concerns relativistic effects.

In Law's formulation the multimode Hamiltonian is given by (using our notation)

$$H_{\text{Law}} = \frac{1}{2m}\left(p + \frac{1}{q}g_{kj}\Pi_k\Phi_j\right)^2 + V(q) + \frac{1}{2}\sum_k\left[\frac{\Pi_k^2}{M_E} + \omega_k^2 M_E\Phi_k^2\right] \tag{4.31}$$

where $\omega_k = k\pi/q(t)$ for $k \in \mathbb{Z}$, and the dimensionless coefficients g_{kj} are given by

$$g_{kj} = \begin{cases} (-1)^{k+j}\frac{2kj}{j^2-k^2}, & k \neq j \\ 0, & k = j \end{cases} \tag{4.32}$$

In the single mode case and without relativistic correction, Eq. (4.31) gives our result in Eq. (4.21) but without the momentum-field coupling $H_{p\Phi}$

$$H_{p\Phi} = -\frac{1}{6}\frac{M_E\omega_q^2}{m^2c^2}p^2\Phi^2 \equiv -\frac{1}{6}g_{p\Phi}p^2\Phi^2 \tag{4.33}$$

Therefore, while Law's formulation produces the same second order position coupling as our result, it does not predict interactions between the mirror momentum and EM field.

In contrast, while exactly following Law's approach, Khorasani instead obtains for a single mode

$$H_{\mathrm{Kh}} = \frac{p^2}{2m} + V(q) + \frac{1}{2}\left[\frac{\Pi^2}{M_E} + \omega_q^2\Phi^2\right] - \frac{g_{p\Phi}}{24}\left(1 + \frac{3}{4}\frac{c^2}{\omega_q^2 q^2}\right)p^2\Phi^2 \tag{4.34}$$

in which the momentum-field coupling appears but with a numerical coefficient. Additionally, Khorasani did not include special relativistic kinetic effects which may be comparable to $H_{p\Phi}$.

To summarize, comparing our results to the three formulations from Ref. [8], Law, and Khorasani, all four agree at linear order in position coupling $\hat{q}/L_0$ and in the non-relativistic regime whose predictions have been confirmed by experiment. The single mode Hamiltonian from Law and Khorasani agree with our Hamiltonian at higher order position coupling, but Law's Hamiltonian does not include $H_{p\Phi}$ or any other relativistic correction. Khorasani's Hamiltonian has a term that is proportional to the $H_{p\Phi}$ that we derive but appears with a different numerical factor, and includes no other relativistic corrections.

4.7 Conclusion

The difficulty in canonical quantization of the optomechanical system resided in the fact that in this case $A(t, x)$ cannot follow its usual treatment as an independent field coordinate since it is implicitly dependent q. By identifying a global mode which contains information about boundary and making the corresponding coordinate transformation in Eq. (4.12), we were able to make explicit the formerly implicit dependence of $A(t, x)$ on q. While Ref. [40] also makes use of mode decomposition, the difference in the two approaches is that we did not use *a priori* equations of motion to construct a Lagrangian, and instead derived the equations from the Lagrangian itself.

Chapter 5

EFFECTS OF LINEAR QUANTUM GRAVITY ON LIGO

5.1 Preface

In this chapter we develop a canonical formulation of the LIGO's interactions with linear quantum gravity and study the implications of gravity's quantum nature on the LIGO detector. In contrast to the current detector-focussed perspective where the gravitational waves (GWs) are treated as an externally prescribed signal, we provide the more general viewpoint that the detected GWs are in fact large perturbations of the underlying field, whose quantum fluctuations couple to that of detector. This allows us to explore the full dynamics of the system comprising of both the detector and the GWs and the effects of their mutual interactions. This formulation provides a mathematical framework for discussions of quantum gravity in relation to LIGO or other optomechanical systems, including gravitationally induced decoherence in general relativistic theory and the detectability of gravitons, and can also be modified to study alternative theories of gravity for which an action exists.

5.2 Introduction

With LIGO's detection of gravitational waves [1], there's been interest in using the detector to study not only astrophysical sources, but the nature of gravity itself, including modified theories [3, 64, 77] and quantum gravity [2, 5, 7]. There are also important questions related to the quantum nature of the LIGO probe both in terms of the implications for its sensitivity as a measurement device [29, 43], as well as the possibility of it being a test bed to study the interplay of quantum mechanics and gravity. However, up to this point, the quantum interaction between gravitational waves and a LIGO-like (optomechanical) system has not been carefully studied from a general relativistic point of view, despite the interest in using optomechanical systems to study low energy gravity effects. To date, the literature comprises mainly of theoretical studies of its interaction with classical Newtonian gravity [34] and phenomenological models of quantum or semiclassical gravity [9, 39, 55, 75]. There are also general relativistic quantum formulations of weak gravity interactions with bosonic fields [6, 10, 47], but these treatments do not easily extend to more complex matter systems. In particular, Oniga et. al [46] derived the master equation for a bound scalar field, similar to an optical cavity, but in crucial contrast to LIGO's

operation did not allow for the boundary length to change. Furthermore, because these treatments focus on the decoherence to quantum matter, they take the view of the gravitational field purely as a constant temperature bath which does not experience perturbations from matter.

In this paper, we develop a canonical formulation of linear quantum gravity from Einstein's theory of general relativity interacting with a quantum LIGO-like system (probe) in processes involving gravitational waves (GWs), which in principle can be extended to study interactions of quantum LIGO with GWs from other gravitational theories derivable from the action principle, such as scalar-tensor theories [22]. In contrast to the conventional view of LIGO as a quantum probe for a classical and predetermined signal, in our formulation probe and the GW field are treated on equal footing as dynamical degrees of freedom in an enlarged Hilbert space. Importantly, this treatment allows the matter probe and GW field to act mutually on each other, in contrast to previous LIGO analyses where the GWs was treated as an external predetermined signal, or in previous analyses of weak quantum gravity acting on quantum matter where the gravitational field was assumed to be at constant thermal equilibrium and experiences no perturbation from its interaction. The GW→probe direction of interaction under unitary evolution recovers the same equations for LIGO's output field in the presence of a GW signal as was calculated previously [38], but due to our gauge choice it offers an alternative (though physically equivalent) perspective of the detection process. Conventionally, LIGO's GW detection is viewed in the Newtonian gauge, where the GW signal is understood to act as a strain force on LIGO's cavities' mirrors (test mass), whose motion then modulates the field inside the cavity. In our formulation in the TT gauge the GWs interact directly with the cavity field. While all measurable quantities are the same in either gauge, the latter facilitates an intuitive and straightforward derivation of the probe's ultimate quantum-limited measurement sensitivity, known as its quantum Cramer Rao bound (qCRB) [33], for which the test mass dynamics is shown to be irrelevant. In addition, the GW→probe direction can be formulated into a master equation for the quantum state of the probe, from which one obtains decoherence effects. Conversely, the probe→GW field direction of interaction recovers Einstein's field equations for the generation of GWs but where the stress-energy tensor $T_{\mu\nu}$ is quantum. These processes of measurement, decoherence, and radiation turn out to be fundamentally related, which will be the subject of the next chapter.

That the formalism in the classical limit recovers well known equations of GW

detection and generation provides a check on its validity, but it additionally predicts effects for which the quantum nature of the GW field becomes essential. Specifically, we find that the mutual interaction leads to quantum coherent backaction effects on the probe in such a way that requires quantum GW fluctuations to drive the probe's degrees of freedom in order to preserve the quantum commutation relations. Furthermore, these backaction effects can be shown to be equivalent to the radiation reaction damping that comes from classical corrections to the Newtonian potential [44]. This suggests that in order to include the effects of weak GR corrections to Newtonian potential on quantum matter without violating canonical quantization, those perturbations must themselves be quantum. Additionally, there is decoherence to the probe caused by GW vacuum fluctuations, which has no classical analogue.

This chapter is divided into the following sections: section II provides a description of the physical system along with definitions and notations used in this paper; in section III we explain our canonical formulation and derive from the action a quantum Hamiltonian governing the interaction between the probe and the GW field. In section IV, we write down the equations of motion, and in section V we discuss the backaction of GWs onto the probe.

5.3 Description of System

LIGO is a Michelson interferometer containing a Fabry-Perot cavity in each of its two arms. In its current operation, it additionally has a power recycling mirror to increase the power circulating inside the arm cavities, as well as a signal recycling mirror to increase the bandwidth of detection [1]. It has been shown that the antisymmetric mode of the interferometer which carries the GW signal and the quantum noises, including the power and signal recycling enhancements, can be mapped to a single detuned Fabry-Perot cavity with an effective input mirror and a perfectly reflective end mirror [15]. This introduces errors of $O(l_{SRC}/L)$ for signal recycling cavity length l_{SRC} and cavity arm length L, and so the assumption is valid when $l_{SRC} \ll L$ which is the case in experiment. Additionally, the effects of radiation pressure which drive both mirrors of the cavity can be attributed to the end mirror alone, holding the input mirror fixed, with errors of $\max\{\Omega L/c, T\}$ to input transmissivity T. Finally, we choose the cavity axis to be the x-direction along which we constrain the mirror motion described by its center of mass coordinate, thereby allowing us to model the mirror as massive point particle (valid for $t_m \ll \lambda_{GW}$ for mirror thickness t_m). In reality the LIGO mirrors are suspended pendulums, but the error in making this assumption is $O(q/l_p)$ where q is mirror displacement due to GW

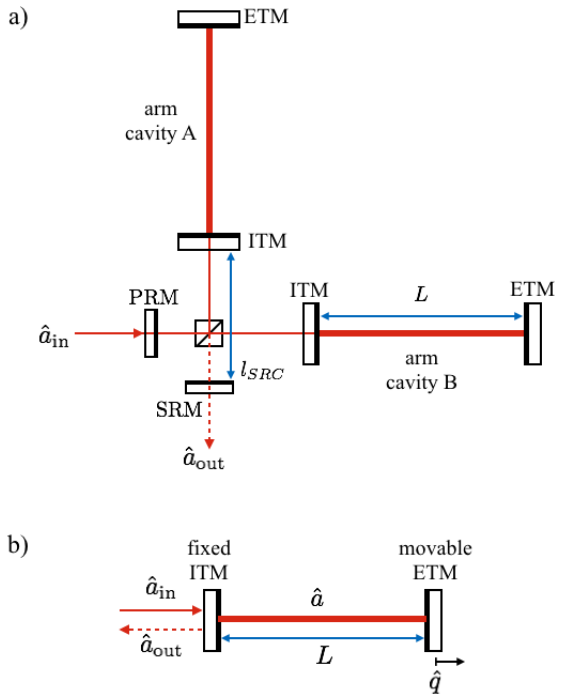

Figure 5.1: Schematic of LIGO's experimental setup. Figure a) shows the full Michelson interferometer in its current configuration with power and signal recycling mirrors (PRM and SRM) and the two Fabry-Perot arm cavities. Here L denotes the length of the arm cavity and l_{SRC} denotes the length of the signal recycling cavity (shown here not to scale). The arm cavities' input mirror (ITM) has transmissivity T and its end mirror (ETM) is perfectly reflective with $R = 1$. For low frequencies Ω of the GW wave such that $\Omega L/c \ll 1$ and for $T \ll 1$, $l_{SRC} \ll L$, the quantum inputs and outputs of the schematic in figure a) can be mapped to those of a single one-dimensional Fabry-Perot cavity shown in figure b).

and radiation pressure and l_p is the pendulum length. In summary, with the stated errors, the signal and quantum noise analysis for the LIGO Michelson interferometer can be mapped onto that for a single one-dimensional Fabry-Perot cavity and all the radiation pressure effect attributed to the end mirror. We choose the origin of our coordinate system to be the position of the input mirror, which means that it is also not affected by metric peturbations and we can therefore hold this coordinate fixed. We now have mapped LIGO to a basic optomechanical system [19].

For the gravitational field, we assume weak metric perturbations about flat spacetime, such that the metric $g_{\mu\nu} = \eta_{\mu\nu} + h_{\mu\nu}$, where $\eta_{\mu\nu}$ is the Minkowski metric with signature $(- + ++)$. Although LIGO operates in earth's gravitational field, this is a constant longitudinal component which is uncoupled from the dynamics of the perturbative field $h_{\mu\nu}$ and whose effect on the test masses are balanced by the tension

in the pendulums, and will therefore not affect our results.

Throughout this paper, unless otherwise stated, Greek indices $\mu, \nu \rho$ etc. (with the exception of λ) denote spacetime components of vectors and tensors; English alphabet indices i, j, k etc. denote purely spatial components; λ and ϵ denote graviton and photon polarizations respectively; boldface form $\mathbf{v}$ represents 3-vectors and $\vec{v}$ represents 4-vectors. We also use Einstein subscript summation notation where contraction is with respect to the background Minkowski metric (e.g $M_{\mu\nu}M^{\mu\nu}$). Repeated spatial indices denotes summation regardless of upper or lower position (e.g $v_i v_i$).

For terminology, "optical mode" refers to the optical field inside the Fabry-Perot cavity; "test mass" refers to the end mirror of the cavity; "probe" refers to the optomechanical system comprising of the optical mode, the test mass, and their interaction; "system" without a modifer refers to the GW field and the probe together; "pump field" refers to the optical input to the cavity and "output field" refers the cavity output on which measurement is performed.

5.4 Canonical Formulation

There are several approaches to the quantization of gravity, including covariant path integral quantization, canonical quantization, loop quantum gravity and string theory [37]. In our case, to study the interaction of weak gravity with macroscopic matter systems in finite time, the canonical formulation is most appropriate. Canonical quantization can be quite straightforward in systems with well-defined physical coordinates and velocities that appear in the Lagrangian in quadratic form, but here there are two difficulties. First is the fact that gravity has coordinate (or gauge) degrees of freedom which is mathematically reflected in the singularity of its Lagrangian. This means a physical state can be represented by several points in phase space. Dirac is credited with developing the Hamiltonian formulation of such gauge theories, in which the degeneracies in phase space due to gauge degrees of freedom can be eliminated by to restricting to a hypersurface which itself is foliated by gauge orbits. Quantization can proceed in the usual way by ignoring the existence of gauge freedom, but physical quantum states must satisfy constraint conditions which ensure that the physical Hilbert space slices across the gauge orbits [27]. Applying this approach to linearized gravity, Gupta derived a Hamiltonian for a pure gravitational field and the constraint conditions that must be satisfied by physical gravitational states. He also demonstrated that a pure gravitational field has only two

physical gravitons, although more exist in virtual states in the presence of interaction [32]. Although his methods are formally complete, in practice it is unclear how to apply them to solve for the actual states of matter and gravity. However, as will be demonstrated, these formal methods are not necessary for our purposes of studying the dynamics of gravitational wave interaction, and we argue that a simpler and more physically intuitive picture is sufficient in which only physical gravitons are involved in interactions and the gauge can be fixed prior to quantization, therefore requiring no restrictions on the Hilbert space. The second issue lies in deriving the optomechanical interaction, which is the interaction between the end mirror (test mass) of optical cavity in the LIGO interferometer and the optical mode it contains. This was discussed in detail in the previous chapter and we apply the results here.

Gauge Fixing for Gravitational Field

We begin with the linearized Einstein-Hilbert action for the metric in the harmonic gauge with $\partial_\mu h^{\mu\nu} = 0$, and write

$$S_{EH} = -\frac{c^4}{32\pi G}\int d^4x \left[\frac{1}{2}\partial_\mu h_{\alpha\beta}\partial^\mu h_{\alpha\beta} - \frac{1}{4}\partial_\mu h \partial^\mu h\right], \quad h = h^\rho_\rho \tag{5.1}$$

At this point the gauge is not yet fully fixed and there remains degeneracy in phase space. Under a gauge transformation where $x^\mu \to x^\mu - \xi^\mu(\vec{x})$ for some ξ_μ, the gravitational field transforms such that the polarization tensor for a graviton with 4-momentum $\vec{k}$ undergoes $\tau_{\mu\nu} \to \tau_{\mu\nu} + k_\nu\xi_\mu + k_\mu\xi_\nu$. The choice of the Lorentz gauge removes four degrees of freedom out of ten in the symmetric $h_{\mu\nu}$ tensor and constrains the vector field ξ^μ to satisfy $\Box\xi^\mu = 0$, but a single physical configuration can still be represented by an arbitrary choice of four coefficients. As remarked previously, one can nevertheless proceed to quantize by treating each component of the tensor $h_{\mu\nu}$ and its trace h as independent variables and then impose supplementary conditions on physical states. However, we argue that for our system the gauge may be fully fixed before quantization and consequently there would be no restrictions necessary on the physical Hilbert space. To elucidate, we are interested in leading order interactions of LIGO with gravitational waves, which means that the physical situations we consider will involve an absorbed (emitted) graviton propagating from (to) infinity, whose scattering amplitudes have Feynman diagrams with an external graviton line. The scattering amplitudes for these processes can generally be expressed as $M = \tau_{\mu\nu}\mathcal{M}^{\mu\nu}$ (or $M = \tau^*_{\mu\nu}\mathcal{M}^{\mu\nu}$ for outgoing), where $\tau_{\mu\nu}$ (or $\tau^*_{\mu\nu}$) is the unit polarization tensor for the external graviton and $\mathcal{M}^{\mu\nu}$ represents the amplitude for all other processes. Then, the Ward identity for a massless spin

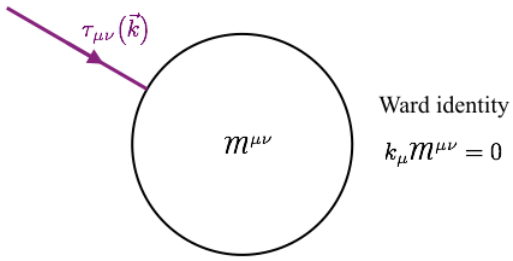

Figure 5.2: For processes involving an external graviton (incoming in the above) with 4-momentum k^ρ and polarization tensor $\tau_{\mu\nu}(k^\rho)$ interacting with matter, the scattering amplitude M can in general be decomposed into $M = \tau_{\mu\nu}\mathcal{M}^{\mu\nu}$, where $\mathcal{M}^{\mu\nu}$ represents all other interaction not including the external graviton. Under a gauge transformation the graviton's polarization tensor becomes $\tilde{\tau}_{\mu\nu} = \tau_{\mu\nu} + k_\mu\xi_\nu + k_\nu\xi_\mu$ for some 4-vector ξ^μ. The Ward identity states that $k_\mu\mathcal{M}^{\mu\nu} = 0$ which implies that $\tau_{\mu\nu}\mathcal{M}^{\mu\nu} = \tilde{\tau}_{\mu\nu}\mathcal{M}^{\mu\nu}$ and that the scattering amplitude M is invariant under gauge transformations of the external graviton. This justifies the restriction of the GW field to transverse traceless modes to leading order in GW interaction

2 particle, which follows either from Lorentz invariance or current conservation, states that $k_\mu\mathcal{M}^{\mu\nu} = 0$ for any null vector k^μ [52, 70].

Using this result, we see that the the scattering amplitude M is invariant under gauge transformations of the external graviton and any gauge we choose there will give the same results. Although the full graviton propagators of the theory are in general gauge dependent, we can ignore their contributions below $O(h^2)$. Therefore, we may impose any four additional constraints on $h_{\mu\nu}$ that is consistent with the Lorentz gauge to remove the four remaining gauge degrees of freedom, and we choose the transverse traceless (TT) conditions of $h_{\mu 0} = 0$ and $h^\mu_\mu = 0$. These conditions leave us with two total degrees of freedom for $h_{\mu\nu}$ corresponding the two physical gravitons in the plus and cross polarizations. The gauge is now fully fixed and $h_{\mu\nu}$ has only spatial components which can be expanded in the Fourier domain as

$$h^{TT}_{ij}(t,\mathbf{x}) = \int \frac{d^3\mathbf{k}}{\sqrt{(2\pi)^3}}\tau^\lambda_{ij}(\mathbf{k})h_\lambda(t,\mathbf{k})e^{i\mathbf{k}\cdot\mathbf{x}} \tag{5.2}$$

where the index $\lambda = +, \times$ denotes the polarization. The tensor $\tau^\lambda_{ij}(\mathbf{k})$ is the unit tensor for the $\mathbf{k}$-mode component, and satisfies orthogonality, transverse, and traceless conditions:

$$\tau^\lambda_{ij}\tau^{\lambda'}_{jk} = \delta_{\lambda,\lambda'}\delta_{ik}, \quad \mathbf{k}\cdot\boldsymbol{\tau}^\lambda(\mathbf{k}) = 0, \quad \mathrm{Tr}[\boldsymbol{\tau}^\lambda] = 0 \tag{5.3}$$

Finally, the Einstein Hilbert action can be rewritten as

$$S_{EH} = \frac{c^4}{32\pi G}\int dt \int_{\frac{1}{2}} d^3\mathbf{k}\left[\frac{1}{c^2}|\dot{h}_\lambda(t,\mathbf{k})|^2 - \mathbf{k}^2|h_\lambda(t,\mathbf{k})|^2\right] \equiv \int dt \int_{\frac{1}{2}} d^3\mathbf{k}\, \mathcal{L}^{(0)}_{GW}(t,\mathbf{k}) \tag{5.4}$$

We remark that h is related to h^* by

$$h^*_\lambda(t,\mathbf{k})\tau^\lambda_{ij}(\hat{\mathbf{k}}) = h_\lambda(t,-\mathbf{k})\tau^\lambda_{ij}(-\hat{\mathbf{k}}) \tag{5.5}$$

Therefore, summing $h_\lambda\tau^\lambda_{ij}$ over all of $\mathbf{k}$-space is physically equivalent to summing over $h_\lambda\tau^\lambda_{ij}$ and $h^*_\lambda\tau^\lambda_{ij}$ over half of k-space. The latter method allows us to treat h_λ and h^*_λ as independent degrees of freedom, in a similar approach to that of [20] for the Hamiltonian formulation of electrodynamics.

As a final remark, it is interesting to point out the relation between the Ward's identity used for scattering matrices and the supplemental conditions used to restrict the physical Hilbert space in the Hamiltonian formulation of linearized gravity. The supplementary conditions state that physical states must vanish when acted on by a set of superpositions of particular polarizations of the field operators (e.g $\left[\hat{a}_{3j} - \hat{a}_{0j}\right]|\psi\rangle = 0$). Such states can still have non-zero occupation of non-physical gravitons in an equal superposition ($|\psi\rangle = |1_{3j}\rangle - |1_{0j}\rangle$), but if so their norms will vanish (e.g $\langle\psi|\psi\rangle = 0$) due to the negative norm of $\hat{a}_{0j}$ [31]. Therefore, states which satisfy the supplementary conditions and have unit norm contains only physical gravitons. In comparison, the Ward identity states that $\mathcal{M}^{\mu\nu}$ must vanish when contracted with the polarization tensors of the same superposition of the fields in analogy to the supplementary conditions (e.g $\left[\tau^{\mu\nu}_{3j} - \tau^{\mu\nu}_{0j}\right]\mathcal{M}_{\mu\nu} = 0$, where the lower set of indices represents the polarization). Then it can be shown that averaging over the polarizations of the external graviton gives the transition probability $|M|^2 := \sum_{\lambda=+,\times}|\tau^\lambda_{\mu\nu}\mathcal{M}^{\mu\nu}|^2 = \mathcal{M}_{\mu\nu}\mathcal{M}^{\mu\nu}$, where the last equality makes use of the Ward identity which ensures that the scattering amplitudes corresponding production or absorption of non-physical gravitons that arises in the expression $\mathcal{M}_{\mu\nu}\mathcal{M}^{\mu\nu}$ (e.g $|\mathcal{M}^{3j}|^2$, $|\mathcal{M}^{0j}|^2$ etc.) will cancel each other, in analogy to the zero norm states.

Interaction between GW and Probe

The probe consists of the optical mode and the test mass, whose actions in perturbed spacetime can be written as $S_{\text{probe}} = S^\eta_{EM} + S^h_{EM} + S_q$, where S^η_{EM} was the EM action in Minkowski space and was defined in Eq. (4.8) and S^h_{EM} is the first order term in

the expansion of $S_{EM} \propto -\int d^4x\sqrt{-g}\; g_{\alpha\mu}g_{\beta\nu}F^{\mu\nu}F^{\alpha\beta}$, which we write below

$$\begin{aligned} S^h_{EM} &= \int dt\; L^h_{EM} \\ &= -\frac{1}{2\mu_0}\int_{V_{\rm cav}} d^4x\; h_{ij}\left[\frac{1}{c^2}\dot{\mathcal{A}}_i\dot{\mathcal{A}}_j - (\partial_i\mathcal{A}_k)(\partial_j\mathcal{A}_k) - (\partial_k\mathcal{A}_i)(\partial_k\mathcal{A}_j)\right] \end{aligned} \tag{5.6}$$

Similarly, we expand the action for the test mass $S_q = -mc\int d\tau$ to leading order in $h_{\mu\nu}$ and obtain

$$S_q = \frac{m}{2}\int dt\;\left[\dot{\mathbf{x}}_q^2 + h_{ij}(t,\mathbf{x}_q)\dot{x}^i_q\dot{x}^j_q\right] = \frac{m}{2}\int dt\;\dot{q}^2 \tag{5.7}$$

where to obtain the second equality we've ignored terms of $O(v^2/c^2)$ as well as the test mass's degrees of freedom of motion in the y, z directions, which are non-interacting and trivial. We denote the corresponding Lagrangian by $L^{(0)}_q = m\dot{q}^2/2$.

Thus, we find that the interaction between the GW and the probe only concerns the EM field, and, denoting this interaction by $L^{\rm int}_{GW}$, we have $L^{\rm int}_{GW} = L^h_{EM}$. In the previous chapter we detailed how to quantize the cavity modes and mirror motion of the optomechanical system. Reproducing this procedure and substituting h_{ij} in Eq. (5.6) by its expansion into transverse-traceless Fourier modes given in Eq. (5.2), we obtain

$$\begin{aligned} L^{\rm int}_{GW} = -\frac{\mathcal{U}}{2\mu_0}\int_{\frac{1}{2}} d^3\mathbf{k}\left[J_\lambda(\mathbf{k})h_\lambda(t,\mathbf{k}) + J^*_\lambda(\mathbf{k})h^*_\lambda(t,\mathbf{k})\right] \\ \left[\frac{1}{2\omega_0}\dot{\Phi}_i\dot{\Phi}_j - \frac{\omega_0}{2}\left(\Phi_i\Phi_j + \delta_{ix}\delta_{jx}\Phi_k^2\right)\right] \end{aligned} \tag{5.8}$$

where $J_\lambda(\mathbf{k})$ is a GW mode profile function, and is given by

$$J_\lambda(\mathbf{k}) = \frac{-i(e^{ik_xL}-1)}{k_xL}\frac{\tau^\lambda_{xx}(\mathbf{k})}{\sqrt{(2\pi)^3}} \tag{5.9}$$

We point out that only the xx component of the GW field interacts with our probe, which is the direction of propagation of the dynamical photons in the optical mode. The factor of $-i(e^{ik_xL}-1)/k_xL$ derives from the spatial variation of the gravitational wave over the spatial extent of the optical mode. For long wavelength GWs such as those from LIGO's astrophysical sources, $k_xL \ll 1$ and $J_\lambda(\mathbf{k})$ simply reduces to the interacting polarization tensor component. However, in order to study backaction due to GW radiation from LIGO itself, one must include this factor to ensure convergence, since the backaction effect requires that radiated GW vary over the length of the cavity.

Canonical Quantization

The full Lagrangian for the system is then

$$L = L_q^{(0)} + L_{EM}^{(0)} + \int dt \int_{\frac{1}{2}} d^3\mathbf{k}\, \mathcal{L}_{GW}^{(0)}(t,\mathbf{k}) + L_{OM} + L_{GW}^{int} \tag{5.10}$$

We then proceed with canonical quantization, first performing a Legendre Transform to identify conjugate pairs $\{h_\lambda(\mathbf{k}), \Pi_\lambda^*(\mathbf{k})\}$, $\{\Phi_i, \mathbb{P}_i\}$, $\{q, p\}$. We remark that although the photon polarization appear coupled in L_{GW}^{int} in Eq. (5.8), the interaction between the different polarization occur on much shorter timescales than those of interest. Performing the same canonical transformation on the cavity mode pair $\{\Phi, \Pi\} \to \{\alpha_1, \alpha_2\}$, we obtain the Hamiltonian

$$H = H_q^{(0)} + H_{GW}^{(0)} + H_{OM} + H_{GW}^{\text{int}} \tag{5.11}$$

Here $H_q^{(0)}$ and $H_{GW}^{(0)}$ are the free Hamiltonians for the test mass and metric perturbation respectively, and

$$H_{OM} = -\frac{\omega_0 \hat{q}}{2L}(\hat{\alpha}_1^2 + \hat{\alpha}_2^2) \tag{5.12}$$

is the optomechanical interaction, and H_{GW}^{int} is the interaction between the GW field and the probe, given by

$$H_{GW}^{\text{int}} = -\frac{\omega_0}{4}\left(\hat{\alpha}_1^2 + \hat{\alpha}_2^2\right) \int d^3\mathbf{k}\; J_\lambda(\mathbf{k}) \hat{h}_\lambda(t,\mathbf{k}) \tag{5.13}$$

We then quantize canonically by imposing the commutation relations

$$[\hat{q}, \hat{p}] = i\hbar \tag{5.14a}$$

$$[\hat{\alpha}_1, \hat{\alpha}_2] = i\hbar \tag{5.14b}$$

$$\left[\hat{h}_\lambda(\mathbf{k}), \hat{\Pi}_{\lambda'}^\dagger(\mathbf{k}')\right] = \left[\hat{h}_\lambda^\dagger(\mathbf{k}), \hat{\Pi}_{\lambda'}(\mathbf{k}')\right] = i\hbar\delta_{\lambda\lambda'}\delta^2(\mathbf{k}-\mathbf{k}') \tag{5.14c}$$

We remark that under the canonical transformation and the RWA, the polarizations are now independent, and we have therefore suppressed the its superscript.

In order to perform measurement on the probe state while maintaining a constant amplitude inside the cavity, we must relax the perfect reflectivity condition to couple the probe to an external pump field whose ingoing photons drive the optical mode and whose outgoing photons are measured by the photodetector. The outgoing photons may be also thought of as ancillae which ensures that the probe state

evolves unitarily during continuous measurement, obviating measurement based feedback. We enlarge our Hilbert space to include the external pump by adding

$$H_{\text{ext}} = i\sqrt{2\gamma}\left[\hat{a}^\dagger \hat{c}_{x=0} - \hat{a}\hat{c}^\dagger_{x=0}\right] - i\int_{-\infty}^{\infty} dx\ \hat{c}^\dagger_x \partial_x \hat{c}_x \tag{5.15}$$

to account for the interaction between the pump and probe (going directly to the interaction picture with respect to the free evolution of the pump field). Here $\hat{a}$, $\hat{a}^\dagger$ are raising and lowering operators of the optical mode, defined such that

$$\hat{\alpha}_1 = \sqrt{\frac{\hbar}{2}}\left(\hat{a} + \hat{a}^\dagger\right) \tag{5.16a}$$

$$\hat{\alpha}_2 = -i\sqrt{\frac{\hbar}{2}}\left(\hat{a} - \hat{a}^\dagger\right) \tag{5.16b}$$

Relaxing the condition of perfect reflectivity also allows LIGO to operate in the detuned configuration where the pump field has off resonant frequency $\omega_L = \omega_0 + \Delta$. The fast evolution in the canonical transformation of the cavity mode is then given by ω_L instead of the ω_0, and this results in an additional term in the Hamiltonian given by

$$H_\Delta = -\Delta\left(\hat{\alpha}_1^2 + \hat{\alpha}_2^2\right)/2 \tag{5.17}$$

Assuming large average amplitude inside the cavity, we linearize the Hamiltonian by writing $\hat{\alpha}_1 \to \bar{\alpha} + \delta\hat{\alpha}_1$ and $\hat{\alpha}_2 \to \delta\hat{\alpha}_2$. Then keeping only terms linear in small quantity δ in the interaction terms (which are already small), we write down the final form of our Hamiltonian:

$$\begin{aligned} H = H_q^{(0)} + H_{GW}^{(0)} + H_{\text{ext}} - \frac{\Delta}{2}\left(\hat{\alpha}_1^2 + \hat{\alpha}_2^2\right) \\ - \omega_0 \bar{\alpha}\hat{\alpha}_1\left[\frac{\hat{q}}{L} + \frac{1}{2}\int d^3\mathbf{k}\ J_\lambda(\mathbf{k})\hat{h}_\lambda(t,\mathbf{k})\right] \end{aligned} \tag{5.18}$$

where we take $\Delta \to 0$ to recover the tuned configuration.

For notational simplicity we denote the integral over GW k-modes by $\hat{h}(t)$, and point out that in the wave zone ($k_x L \ll 1$) $\hat{h}(t) = \hat{h}^{TT}_{xx}(t, \mathbf{0})$ according to Eq. (5.2). For a strong excitation of the GW field from an astrophysical event such as a BBH merger, we can separate the GW field into a large classical component along with quantum fluctuations and write $\hat{h}(t) \to h_s(t) + \hat{h}(t)$, and the interaction Hamiltonian becomes

$$H_{\text{int}} = -\frac{\omega_0 \bar{\alpha}\hat{\alpha}_1}{2}\left[h_s(t) + \hat{h}(t)\right] \tag{5.19}$$

We also point out that H_{ext} was not derived from a fundamental action and was added phenomenologically in accordance with the standard formulation for input-output theory in quantum optics [69]. The only concern here would be the interaction between the external pump and the GW field, but that interaction is negligible since the power in the pump without the amplification effects of a Fabry Perot cavity is orders of magnitude smaller than that of the optical mode.

5.5 Equations of Motion

We identify the input and output pump field from the external field operators $\hat{c}_x$ [19]

$$\hat{a}_{\text{ in}} = \hat{c}_{x=0^-}, \quad \hat{a}_{\text{ out}} = \hat{c}_{x=0^+}, \quad \hat{c}_{x=0} = \frac{\hat{c}_{x=0^-} + \hat{c}_{x=0^+}}{2} \tag{5.20}$$

and denote their corresponding amplitude and phase quadratures by $\hat{\alpha}^{(1,2)}_{\text{in}}$. From the Hamiltonian in Eq. (5.18) derive following Heisenberg EOM for the probe and the GW field. The test mass is simply driven by the radiation pressure force, and its EOM are

$$\dot{\hat{q}} = p/m, \quad \dot{\hat{p}} = \omega_0 \bar{\alpha} \hat{\alpha}_1 / L \tag{5.21}$$

The cavity mode carries the effects of both GWs and test mass motion in the phase quadrature. In the presence of detuning, the amplitude and phase quadratures rotate into each an analogy to a harmonic oscillator

$$\dot{\hat{\alpha}}_1 = -\Delta \hat{\alpha}_1 - \gamma \hat{\alpha}_1 + \sqrt{2\gamma}\hat{\alpha}^{(1)}_{\text{in}} \tag{5.22a}$$

$$\dot{\hat{\alpha}}_2 = \Delta_1 - \gamma \hat{\alpha}_2 + \sqrt{2\gamma}\hat{\alpha}^{(2)}_{\text{in}} - \frac{\omega_0 \bar{\alpha}}{2} \int d^3\mathbf{k}\; J_\lambda(\mathbf{k}) \hat{h}_\lambda(\mathbf{k}) - \frac{\omega_0 \bar{\alpha}}{L} \hat{q} \tag{5.22b}$$

Finally, the GWs modes evolve independently and is driven by the cavity mode amplitude

$$\dot{\hat{h}}_\lambda(\mathbf{k}) = \frac{1}{M_G} \hat{\Pi}_\lambda(\mathbf{k}) \tag{5.23a}$$

$$\dot{\hat{\Pi}}_\lambda(\mathbf{k}) = -\omega_k^2 M_G \hat{h}_\lambda(\mathbf{k}) + \frac{\omega_0 \bar{\alpha}}{2} J^*_\lambda(\mathbf{k}) \hat{\alpha}_1 \tag{5.23b}$$

where $\omega_k = c|\mathbf{k}|$ and we've defined $M_G = c^2/32\pi G$.

Discussion of GW Interaction

We point out that, as expected, in the TT gauge the metric perturbations do not affect the coordinate motion of a particle moving along a geodesic [44] to order (v^2/c^2), as evident in Eq. (5.7). Additionally, if the particles are initially at rest (such that $v = 0$), and experience no other forces, then linear metric perturbations will not

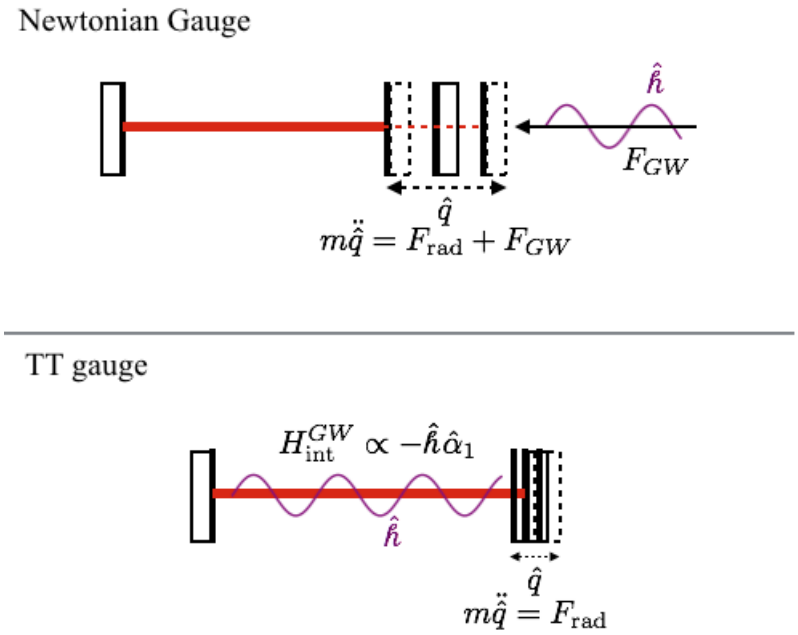

Figure 5.3: Representations of the GW interaction in the Newtonian versus TT gauges. In the Newtonian gauge, the gravitational wave exerts a strain force F_{GW} so the the test mass position is driven by both radiation pressure and gravitational wave forces. In contrast, in the TT gauge the GW interacts directly with the optical cavity mode and the test mass position is driven by radiation pressure forces alone. The two pictures are physically equivalent descriptions of the dynamics of a cavity whose mirrors fluctuate about their geodesic due to radiation pressure. In the presence of an incoming GW, geodesics of the two mirrors deviate and the proper length of the cavity changes. In the Newtonian gauge, the change in proper length is reflected in the test mass coordinate, while in the TT gauge this effect is directly accounted for by a phase shift in the cavity mode. The TT gauge viewpoint allows for a canonical description of the interaction.

affect coordinate motion for even appreciable values v/c. This is because the gauge symmetry for gravitational fields is a diffeomorphism, or a local symmetry, and so the coordinate length between two free falling particles is gauge dependent. The proper length, however, is a physical quantity and is the same in any gauge. It should be noted that for our system, the test mass in not actually a free falling particle since it interacts optomechanically with the optical mode. This means that its position coordinate may be affected by metric perturbations even in the TT gauge, and in fact are through the coupling of L_{OM} to h_{ij}. However, this term is of $O(hq/L)$, which is second order in small quantities and therefore ignored.

The reason for the different form of the equations of motion for matter interacting with GWs in different gauges can be quite simply seen through the interaction action

term $\int d^4x\ h_{\mu\nu}T^{\mu\nu}$. Upon a gauge transformation the metric perturbation changes $h_{\mu\nu} \rightarrow h_{\mu\nu} + \xi_{\mu,\nu} + \xi_{\nu\mu}$ while $T_{\mu\nu}$, being a physical quantity, remains unchanged. This means different terms appear in the interaction, thereby resulting in different EOM.

The consequence of the TT gauge choice is that in this picture, the GWs interact directly with the optical mode, in contrast to the standard view that GWs exert a strain force onto the test mass whose motion then causes a phase shift. The TT gauge view allows for straightforward derivation of the fundamental limit to measurement sensitivity for LIGO, as we will discuss in the next chapter.

5.6 GW Field Dynamics

Since our formalism treats the GW field and the probe on equal footing, the interaction between them is bidirectional, meaning that in addition to the Hamiltonian in Eq. (5.18) describing how the probe evolves under GW interaction, it also governs how the probe affects the dynamics of the GW field. In this section, we consider the latter relation. We will show that the solution to the GW field following our formalism and the EOM given in subsection 5.5 will reproduce the classical quadrupole moment formula for gravitational waves, derived from Einstein's classical field equations

$$h_{ij}^{TT}(t, \mathbf{x}) = \frac{2G}{c^4} \frac{\dot{I}_{ij}^{TT}(t - |\mathbf{x}|/c)}{|\mathbf{x}|} \tag{5.24}$$

This is unsurprising, but it serves as a demonstration of the equivalence in the relations between perturbative quantum gravity interacting with quantum matter and that of the classical scenario. This justifies the viewpoint that quantum fluctuations in stress-energy will radiate GW in the same way as classical matter, and furthermore, that non-classical states of quantum matter will result in non-classical states of GWs.

We will now solve the coupled EOM given in subsection 5.5 for the GW field. It is simplest to do this in the time frequency domain where we define the frequency Fourier pair

$$\hat{O}(\Omega) = \int_{-\infty}^{\infty} dt\ \hat{O}(t)e^{-i\Omega t}, \quad \hat{O}(t) = \int_{-\infty}^{\infty} \frac{d\Omega}{2\pi}\ \hat{O}e^{-i\Omega t} \tag{5.25}$$

Then, we have

$$\tau_{ij}(\mathbf{k})\hat{h}_\lambda(\Omega, \mathbf{k}) = \frac{\omega_0\bar{\alpha}}{2M_G} \frac{\tau_{ij}(\mathbf{k})J_\lambda(\mathbf{k})}{(\omega_k^2 - \Omega^2)}\hat{\alpha}_1(\Omega) \tag{5.26}$$

Since the probe is a Newtonian source, we can apply the slow motion condition and make the simplifying approximation that $|\mathbf{k}|L \ll 1$, such that $J_\lambda(\mathbf{k}) \to \tau_{xx}(\mathbf{k})/\sqrt{(2\pi)^3}$. Remembering that we are already in the TT gauge, the inverse spatial Fourier transform of Eq. (5.26) will give us the gauge fixed GW field in configuration space, or $\hat{h}^{TT}_{ij}(\Omega, \mathbf{x})$. We write

$$\hat{h}^{TT}_{ij}(\Omega, \mathbf{x}) = \frac{16\pi G}{c^2} \int \frac{d^3\mathbf{k}}{(2\pi)^3} \frac{\omega_0 \bar{\alpha} \hat{\alpha}_1(\Omega) \tau^\lambda_{ij}(\mathbf{k}) \tau^\lambda_{xx}(\mathbf{k}) e^{i\mathbf{k}\cdot\mathbf{x}}}{\omega^2 - \Omega^2} \tag{5.27}$$

It is possible to show that Eq. (5.27) can be written as

$$\hat{h}^{TT}_{ij}(\Omega, \mathbf{x}) = \frac{16\pi G}{c^2} \mathbb{L}^{TT}(\mathbf{x}) \left[\int \frac{d^3\mathbf{k}}{(2\pi)^3} \frac{\hat{T}_{ij}(\Omega, \mathbf{k}) e^{i\mathbf{k}\cdot\mathbf{x}}}{\omega_k^2 - \Omega^2} \right] \tag{5.28}$$

where $\hat{T}_{ij}(\Omega, \mathbf{k})$ is the time and spatial Fourier transform of the stress energy tensor of the probe, and, neglecting terms of $O(q/L)$ and $O(v^2/c^2)$, is simply the stress energy tensor of the optical mode $\hat{T}^{EM}$. It is given by the

$$\hat{T}_{ij}(\Omega, \mathbf{k}) = \hat{T}^{EM}_{ij}(\Omega, \mathbf{k}) = \delta_{ix}\delta_{jx} \frac{\omega_0 \bar{\alpha}}{c^2} \hat{\alpha}_1(\Omega) \tag{5.29}$$

The notation $\mathbb{L}^{TT}(\mathbf{x})$ is shorthand for the TT projection operator, which projects each Fourier component $\hat{T}_{ij}(\Omega, \mathbf{k})$ to its TT components with respect to propagation vector $\mathbf{k}$, and accounts for the presence of the polarization tensors in Eq. (5.27). Explicitly, this operation on some general tensor field $f_{ij}(\mathbf{x})$ is given by

$$\begin{aligned} \mathbb{L}^{TT}(\mathbf{x}) \left[f_{ij}(\mathbf{x}) \right] = \int d^3\mathbf{x}' \int d^3\mathbf{x}'' \Big[& \mathcal{P}_{il}(\mathbf{x}', \mathbf{x}'') \mathcal{P}_{jm}(\mathbf{x}', \mathbf{x}'') \\ & - \frac{1}{2} \mathcal{P}_{ij}(\mathbf{x}', \mathbf{x}'') \mathcal{P}_{mn}(\mathbf{x}', \mathbf{x}'') \delta^n_l \Big] f_{lm}(\mathbf{x}'') \end{aligned} \tag{5.30}$$

where $\mathcal{P}_{ij}(\mathbf{x}, \mathbf{x}')$ is the transverse projection operator for vector plane waves, such that $\int d^3\mathbf{x}' \mathcal{P}_{ij}(\mathbf{x}, \mathbf{x}') v_j e^{i\mathbf{k}\cdot\mathbf{x}'} = v^\perp_i e^{i\mathbf{k}\cdot\mathbf{x}}$, and is equal to

$$\mathcal{P}_{ij}(\mathbf{x}, \mathbf{x}') = \delta_{ij}\delta^3(\mathbf{x} - \mathbf{x}') - \partial_i G(\mathbf{x}, \mathbf{x}') \partial_{j'} \tag{5.31}$$

where $G(\mathbf{x}, \mathbf{x}') = -1/(4\pi|\mathbf{x} - \mathbf{x}'|)$ is the Green's function of the $\boldsymbol{\nabla}^2$ operator.

Examining Eq. (5.29), we note that $\hat{T}_{ij}(\Omega, \mathbf{k})$ in fact independent of $\mathbf{k}$. In fact, using the slow-motion condition, we can show that

$$\hat{T}_{ij}(\Omega, \mathbf{k}) = \int d^3\mathbf{x}\, \hat{T}_{ij}(\Omega, \mathbf{x}) \tag{5.32}$$

or that the Fourier **k**-mode of the stress energy tensor is equal to the the its own volume integral. Substituting this relation into Eq. (5.28), taking the long wavelength approximation such that kL
1, and performing the inverse transform to the time domain, we obtain our final expression for the GW field:

$$\hat{h}_{ij}^{TT}(t,\mathbf{x}) = \frac{4G}{c^2}\mathbb{L}^{TT}(\mathbf{x})\left[\frac{\int d^3\mathbf{x}'\ \hat{T}_{ij}(t-|\mathbf{x}|/c,\mathbf{x}')}{|\mathbf{x}|}\right] \tag{5.33}$$

which is equivalent to the mass quadrupole formula in Eq. (5.24) by stress-energy conservation [44]. Finally, we point that that since the argument of the TT projection operator $\mathbb{L}^{TT}$ depends only on the distance $r = |\mathbf{x}|$ under the long wavelength approximation, Eq. (5.30) reduces to a simple form, where it can be written in terms of transverse projection operator for radially traveling waves:

$$\mathbb{L}^{TT}\left[f_{ij}\right] = P_{il}f_{lm}P_{mj} - \frac{1}{2}P_{ij}\ \mathrm{Tr}\left\{\boldsymbol{Pf}\right\}, \quad P_{lm} = \delta_{lm} - \frac{x_l x_m}{r^2} \tag{5.34}$$

We have reproduced Einstein's equations for gravitational waves using a fully quantum formalism. This serves as a check to our formalism, as well as a theoretical basis for discussing quantum GW states generated by quantum matter.

5.7 Probe Dynamics

We now consider the other direction of the gravitational interaction and study the effects of GWs on probe dynamics, and in particular examine the implications of quantum GW fluctuations in signal detection and on the quantum state of the probe. We show that the backaction effects due to GW generation onto the probe necessarily introduce fluctuations from quantum GWs into the interferometer input, which points to the necessity of reformulating the bound for a signal when its own quantum fluctuations are taken into account. Additionally, we demonstrate reciprocity between maximum detection sensitivity and GW energy radiation, and offer the physical interpretation of LIGO as an antenna or a bidirectional transducer between photons and gravitons. Finally, we demonstrate decoherence to the probe by a GW bath, and point out the relationship between decoherence and the qCRB.

Probe EOM Solutions and GW Backaction

We choose $t = 0$ to be the initial time of the GW interaction and solve the EOM in subsection 5.5 in the Laplace domain, with the Laplace transform pair for some

time dependent operator $\hat{O}(t)$ being

$$\hat{O}(s) = \int_0^\infty dt\ \hat{O}(t)e^{-st}, \quad \hat{O}(t) = \frac{1}{2\pi i}\int_{-i\infty+\epsilon}^{i\infty+\epsilon} ds\ \hat{O}(s)e^{st} \tag{5.35}$$

where ϵ is determined by the region of convergence. In the Laplace domain, Eq. (5.27) becomes

$$\hat{h}_\lambda(s,\mathbf{k}) = \frac{s}{s^2+\omega_k^2}\hat{h}_\lambda(0,\mathbf{k}) + \frac{1}{M_G}\frac{\hat{\Pi}_\lambda(0,\mathbf{k})}{s^2+\omega_k^2} + \frac{\omega_0\bar{\alpha}}{2}\frac{1}{M_G}J_\lambda^*(\mathbf{k})\frac{\hat{\alpha}_1(s)}{s^2+\omega_k^2} \tag{5.36}$$

The first two terms of the Eq. (5.36) represent the input GW field, while the last term is the part of the GW field generated by the probe and will result in backaction effects. We assume that that probe is operating under steady state prior to GW interaction and therefore eliminate its initial state. Substituting $\hat{q}(s) = \omega_0\bar{\alpha}\,\hat{\alpha}_1/mLs^2$ into the EOM for the $\hat{\alpha}_2$ and solving the coupled equations for the optical mode quadratures in terms of the input fields, we obtain

$$\begin{pmatrix} s+\gamma & \Delta \\ -(1+\xi_B)\Delta & s+\gamma \end{pmatrix}\begin{pmatrix}\hat{\alpha}_1 \\ \hat{\alpha}_2\end{pmatrix} = \sqrt{2\gamma}\,\mathbb{I}\begin{pmatrix}\hat{\alpha}_{\text{in}}^{(1)} \\ \hat{\alpha}_{\text{in}}^{(2)}\end{pmatrix} + \frac{\omega_0\bar{\alpha}}{2}\begin{pmatrix}0\\1\end{pmatrix}\left(\hbar_s + \hat{\hbar}\right) \tag{5.37}$$

where ξ_B is the modification to optical mode response due to backaction from the test mass and GW field, and is given by

$$\xi_B(s) = \frac{1}{\Delta}\left(\frac{\epsilon_q}{s^2} + \epsilon_{GW}s\right) \tag{5.38}$$

for $\epsilon_q = (\omega_0\bar{\alpha})^2/mL^2$ and $\epsilon_{GW} = 8G(\omega_0\bar{\alpha})^2/15c^5$. We remark that for GW backaction we have only considered effects due to outgoing gravitational waves.The leading order Feynman diagrams for back action processes involve a graviton propagator between in and out matter states, which in principle should include contributions from longitudinal and timelike gravitons if we were to account for all gravitational effects. Restricting our attention to the TT modes ignores time-symmetric self-gravity effects such as the Newtonian self-potential, but those are well separated from the leading order time-asymmetric term that is the GW backaction.

Tuned Configuration

Let us first consider the implications of backaction in the tuned configuration by taking $\Delta \to 0$ and solving Eq. (5.37). We obtain the solutions

$$\hat{\alpha}_1 = \frac{\sqrt{2\gamma}}{s+\gamma}\hat{\alpha}_{\text{in}}^{(1)}, \quad \hat{\alpha}_2 = \frac{\sqrt{2\gamma}}{s+\gamma}\hat{\alpha}_{\text{in}}^{(2)} + \xi_B\frac{\sqrt{2\gamma}}{(s+\gamma)^2}\hat{\alpha}_{\text{in}}^{(1)} + \frac{\omega_0\bar{\alpha}}{2}\left(\hbar_s + \hat{\hbar}\right) \tag{5.39}$$

Explicitly, the backaction effect on measurement is given by the noise input-output relations, which derives from the EOM for the external pump field using the definitions for the input/output field in Eq. (5.20), and are given by $\hat{\alpha}^{(j)}_{\text{out}} = \hat{\alpha}^{(j)}_{\text{in}} - \sqrt{2\gamma}\hat{\alpha}_j$ for $j = 1, 2$. Substituting in the solutions for $\hat{\alpha}_j$, we find the following relations for the noise part of the output field

$$\hat{\alpha}^{(1)}_{\text{out}} = e^{2i\beta}\hat{\alpha}^{(1)}_{\text{in}}, \quad \hat{\alpha}^{(2)}_{\text{out}} = e^{2i\beta}\left[\hat{\alpha}^{(2)}_{\text{in}} - \left(\mathcal{K}_{pd} + i\mathcal{K}_{GW}\right)\hat{\alpha}^{(1)}_{\text{in}}\right] - \sqrt{2\gamma}\frac{\omega_0\bar{\alpha}}{2}\frac{\hat{h}}{s+\gamma} \tag{5.40}$$

where β is an uninteresting overall phase factor and $\mathcal{K}_{pd}$ and $\mathcal{K}_{GW}$ are the backaction terms due to the test mass and GWs respectively. Making the identification $s \to -i\Omega$, we have $\beta = \arctan(\Omega/\gamma) + \pi/2$ and

$$\mathcal{K}_{pd}(\Omega) = \frac{1}{m}\left(\frac{\omega_0\bar{\alpha}}{L}\right)^2 \frac{2\gamma}{\Omega^2(\gamma^2+\Omega^2)}, \quad \mathcal{K}_{GW}(\Omega) = \frac{2\Omega\gamma\epsilon_{GW}}{\gamma^2+\Omega^2} \tag{5.41}$$

The term $\mathcal{K}_{pd}$ is exactly the well known ponderomotive effect which causes a rotation and squeezing of the input noise ellipse, with rotation angle $\theta = \arctan(\mathcal{K}_{pd}/2)$, squeeze angle $\phi = \text{arccot}(\mathcal{K}_{pd}/2)/2$, and squeeze factor $r = \text{arcsinh}(\mathcal{K}_{pd}/2)$ [38]. On the other hand, the GW backaction is imaginary and therefore must be associated with additional fluctuations in $\hat{\alpha}^{(2)}_{\text{out}}$ in order for $\left[\hat{\alpha}^{(2)}_{\text{out}}(t), \hat{\alpha}^{(2)}_{\text{out}}(t')\right] = 0$, or else $\hat{\alpha}^{(2)}_{\text{out}}$ cannot be continuously measured without measurement backaction. Indeed, we see in Eq. (5.40) that there are fluctuations from the GW field which ensure that the output phase quadrature commute at different times, and additionally enlarges the total area of the output noise ellipse. Unfortunately, these additional fluctuations cannot be removed without access to quantum GW degrees of freedom and will therefore introduce additional noise, albeit at $O(\epsilon^2_{GW})$.

Comparison with the Newtonian Viewpoint

To understand the GW backaction more intuitively, we now go to the Newtonian gauge and show that the backaction effect derives from a correction to the Newtonian potential. In this gauge, the metric perturbations act as a gravitational force on the test mass, whose motion due to radiation pressure implies a time dependent quadrupole moment which radiates GWs. The leading order effect of the outgoing GWs results in a reaction potential Φ_{react} which in turn damps the motion of the test mass [44]. This effect is known as radiative damping, since the damping of test mass motion is interpreted as being due to the loss of energy in the form of GW radiation. To see this explicitly, we write the EOM of the test mass in the Newtonian gauge under

radiation pressure and the radiation reaction force:

$$\ddot{\hat{q}} = -\frac{\partial}{\partial x}\Phi_{\text{react}} + \frac{\omega_0\bar{\alpha}}{mL}\hat{\alpha}_1, \quad \Phi_{\text{react}}(\mathbf{x}) = \frac{G}{5c^5}\mathcal{I}^{(5)}_{jk}x^j x^k \tag{5.42}$$

where $\mathcal{I}_{jk}$ is the reduced mass quadrupole moment tensor, and the superscript represents the number of time derivatives. We find that the reaction force on the system evaluates to $F_{\text{react}} = -(8G/15c^5)mL^2\hat{q}^{(5)}$. Since the reaction force is dependent on $\hat{q}$ itself, it serves to modify the response of $\hat{q}$ to radiation pressure force. Here we are interested only in the backaction effects of GW interaction and have therefore ignored the input GW field. In its absence, and since the probe is operating under steady state, we may solve the probe EOM in the Fourier domain

$$\hat{q}(\Omega) = \left[\chi_q^{(0)} + \delta\chi_q\right]\frac{\omega_0\bar{\alpha}}{L}\hat{\alpha}_1(\Omega) \tag{5.43a}$$

for the free test mass response function and its modification

$$\chi_q^{(0)} = -\frac{1}{m\Omega^2}, \quad \delta\chi_q = -i\frac{8G}{15c^5}mL^2\Omega^3\chi_q^{(0)} \tag{5.43b}$$

In the Newtonian gauge the optical mode does not interact gravitationally, and the Heisenberg EOM for its quadratures depends only on the input optical field and the test mass dynamics, given by

$$\hat{\alpha}_1(\Omega)(\gamma - i\Omega) = \sqrt{2\gamma}\hat{\alpha}^{(1)}_{\text{in}}(\Omega) \tag{5.44a}$$

$$\hat{\alpha}_2(\Omega)(\gamma - i\Omega) = (\omega_0\bar{\alpha}/L)\hat{q}(\Omega) + \sqrt{2\gamma}\hat{\alpha}^{(2)}_{\text{in}}(\Omega) \tag{5.44b}$$

Substituting Eq. (5.43) into the expression for α_2, we find

$$\hat{\alpha}_1 = \frac{\sqrt{2\gamma}}{\gamma - i\Omega}\hat{\alpha}^{(1)}_{\text{in}}, \quad \hat{\alpha}_2 = \frac{\omega_0^2\bar{\alpha}^2}{L^2}\left(\chi_q^{(0)} + \delta\chi_q\right)\frac{\hat{\alpha}_1}{\gamma - i\Omega} + \frac{\sqrt{2\gamma}}{\gamma - i\Omega}\hat{\alpha}^{(2)}_{in} \tag{5.45}$$

where $\chi_q^{(0)} = -(m\Omega^2)^{-1}$ is the free test mass response and $\delta\chi_q$ is the GW correction. Making the substitution $-i\Omega \to s$, we find that modification to test mass response deriving from Φ_{react} exactly corresponds to the GW backaction term in Eq. (5.37) for $\Delta \to 0$

$$\left(\frac{\omega_0\bar{\alpha}}{L}\right)^2\frac{\delta\chi_q}{\gamma - i\Omega} \to \frac{\epsilon_{GW}s}{s+\gamma} \tag{5.46}$$

From here it follows that identical input-output relations to Eq. (5.40) may be obtained (ignoring the input fluctuations).

We have confirmed that in both gauges the same backaction effect appears in the output field that is being measured, as must be the case. However, there are some

interesting points that arises from comparing the different interpretations offered by each gauge. First, in the Newtonian gauge, the underlying physical mechanism for the backaction is the modification of test mass response to radiation pressure due to the radiative damping. Thus, the GW backaction can be interpreted as a correction to the ponderomotive backaction. But the ponderomotive backaction is understood to depend on the mass as evident in $\mathcal{K}_{pd}$ where m appears in the denominator, and becomes 0 in the limit that $m \to \infty$. However, as demonstrated in the TT gauge, the GW backaction appears without consideration of test mass dynamics, and without regard to its mass. Although this seems paradoxical, we find that the two viewpoints are nevertheless consistent, since the mass m appears in the denominator of the $\chi_q^{(0)}$ and the numerator of the GW modification factor, such that $\delta\chi_q$ is independent of mass. Therefore, even when the test mass is infinitely massive, the test mass still has a non-zero response to external forces due to the radiation reaction potential.

The second point of contrast is that in the Newtonian gauge, damping occurs because energy is radiated away from the probe in the form of gravitational waves. However, in the TT gauge, neither the test mass nor the optical mode experiences damping. Again, this seemingly paradoxical observation may be resolved when one recognizes that the energy that drives the test mass motion is from the optical pump, which also provides the energy radiated away in GWs. This is clear from Eq.s (5.33) and (5.37), where the generation of GWs is shown to depend on $T_{ij} \sim \hat{\alpha}_1$ which depends only on the input optical field, as shown in Eq. (5.45).

Detuned Configuration

While the energy radiating away from the probe can be traced back to the optical pump, it is nevertheless possible for GWs to change the damping of the optical mode if the phase and amplitude quadratures rotate into each other, as is the case in the detuned configuration. As discussed in the previous section, the GW backaction is independent of the mirror mass, and so for simplicity we can take $m \to \infty$ and eliminate the purely pondermotive term ϵ_q in ξ_B of Eq. (5.38). Then, solving the optical mode EOM in Eq. (5.37) for $\Delta \neq 0$, we find

$$\hat{\alpha}_1 = \sqrt{2\gamma}\left[\chi_1\hat{\alpha}_{\text{in}}^{(1)} - \chi_2\hat{\alpha}_{\text{in}}^{(2)}\right] - \frac{\omega_0\bar{\alpha}}{2}\chi_2\left(\hbar_s + \hat{\hbar}\right) \tag{5.47}$$

$$\hat{\alpha}_2 = \sqrt{2\gamma}\left[\left(1 + \frac{\epsilon_{GW}s}{\Delta}\right)\chi_2\hat{\alpha}_{\text{in}}^{(1)} + \chi_1\hat{\alpha}_{\text{in}}^{(2)}\right] + \frac{\omega_0\bar{\alpha}}{2}\chi_1\left(\hbar_s + \hat{\hbar}\right) \tag{5.48}$$

for response functions

$$\chi_1 = \frac{s+\gamma}{(s+\gamma)^2 + \Delta^2 + \epsilon_{GW}\Delta s}, \quad \chi_2 = \frac{\Delta}{(s+\gamma)^2 + \Delta^2 + \epsilon_{GW}\Delta s} \tag{5.49}$$

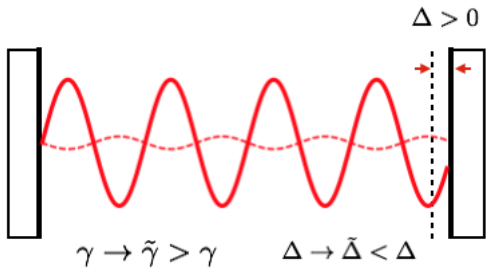

Figure 5.4: Illustration of quantum coherent backaction effects onto the cavity mode due to GW interaction in the presence of detuning. The GWs generated by the $\hat{\alpha}_1$ acts back on $\hat{\alpha}_2$ in such a way that causes the field to beat coherently with itself. The above shows the case for red-detuning where $\Delta > 0$. The solid red line represents the cavity mode in the absence of backaction, while the dotted red line represents the contribution due to GW backaction. This effect is quantified by changes to the cavity's effective damping and detuning rate/ so that $\tilde{\gamma} = \gamma + \epsilon_{GW}\Delta/2$ and $\tilde{\Delta} = \Delta - \epsilon_{GW}\gamma/2$.

Thus in the detuned case we see that the GW backaction additionally modifies the optical mode's response to external drive, encapsulated by shifts in the effective damping and detuning of the optical mode:

$$\tilde{\gamma} = \gamma + \frac{\epsilon_{GW}\Delta}{2}, \quad \tilde{\Delta} = \Delta - \frac{\epsilon_{GW}\gamma}{2} \tag{5.50}$$

It is straightforward to see that an analysis of radiative damping for the detuned configuration in the Newtonian viewpoint will yield the same results, since the only difference in the EOMs for $\hat{\alpha}_1$ and $\hat{\alpha}_2$ between the tuned and detuned cases in the Newtonian gauge would be the addition of the terms $-\Delta\hat{\alpha}_2$ and $\Delta\hat{\alpha}_1$ to the right hand sides respectively for the expressions in Eq. (5.45), which will yield identical solutions as Eq. (5.37) in the absence of the GW input field.

Since Δ can take positive or negative values, radiative damping from GWs can either augment or reduce the effective cavity damping rate γ. Although counterintuitive, this is simple to understand. We know that $\hat{\alpha}_1$ drives GWs, which in turn affects the evolution of $\hat{\alpha}_2$ through the GW dependence in its Heisenberg EOM. But since $\hat{\alpha}_1$ and $\hat{\alpha}_2$ rotate into each other, the amplitude quadrature is then coherently added to itself through the $\Delta\hat{a}_2$ term in its own EOM, which, depending the the sign of Δ, can either be destructively ($\Delta > 0$ or red-detuned), or constructively ($\Delta < 0$ or blue-detuned). Another way to say this is that the GW backaction changes how the optical field in a detuned cavity beats with itself, thereby changing the amplitude.

Necessity of Quantized GWs for Radiation Reaction on Quantum Matter

We'd like to emphasize the point that although radiation reaction can be traced back to the classical radiation reaction potential, in order include its effects on quantum matter, one must necessarily quantize GW fluctuations. This is clear from Eq.s (5.47) and (5.48), where including the ϵ_{GW} backaction effect without also including the $\hat{\hbar}$ fluctuations will result in

$$[\hat{\alpha}_1(t), \hat{\alpha}_2(t)] = i\hbar \left[1 - \frac{\epsilon_{GW}\Delta}{2\gamma}\left(1 - e^{2\tilde{\gamma}t}\right)\right] \tag{5.51}$$

and only by also including $\hat{\hbar}$ will we recover the canonical commutation relation $[\hat{\alpha}_1(t), \hat{\alpha}_2(t)] = i\hbar$.

5.8 Conclusion

In this paper, we studied the interaction of LIGO with weak quantum gravity consistent with Einstein's theory of General Relativity using the canonical formulation of quantization for both the perturbative gravitational field and quantum matter system comprising the LIGO detector. In particular, we study processes in which gravitons are emitted or absorbed, thereby restricting the gravitational field to its physical modes and with the use of Ward's identity enables us to fix the gauge prior to quantization with errors of $O(h^2)$, instead of taking the usual Hamiltonian approach that imposes restrictions on the physical Hilbert space. Choosing the TT gauge, we derive a Hamiltonian showing that the GWs interact with the probe via the optical mode, instead of the usual Newtonian viewpoint where the GWs predominantly affects the test mass. While all measurable quantities are the same in both viewpoints due to gauge invariance, the former allows for a straightforward calculation of LIGO's maximum sensitivity (qCRB) to a GW signal following the method of Ref. [66].

In our formulation, both the gravitational perturbations and the quantum matter operators are dynamical quantities, and their mutual interaction allows each component to act on the other, in contrast to the standard treatment where the gravitational field experiences no perturbations from matter. The probe→GW direction gives the quantum analogue of Einstein's field equations, while the GW→probe direction gives the input-output relations between LIGO's pump and output fields, as well a master equation for the state of the probe when the GW field is viewed as an external bath. Under unitary evolution, their mutual interaction leads to coherent backaction effects that in LIGO's tuned configuration enlarges its noise ellipse, and in the detuned configuration modifies the detuning frequency and damping rate.

The quantum nature of the GW field also plays an essential role in the GW backaction. The GW backaction onto the quantum probe is equivalent to the effect of the classical radiation reaction damping potential, but including this effect without also including the input quantum GW fluctuations in the tuned case results in the output phase quadrature no longer commuting in time, and in the detuned case results in a violation of commutation relations between the amplitude and phase of the optical mode. Therefore gravity must be quantum in order to consistently account for radiation reaction effects on quantum matter. Additionally, these fluctuations point to the necessity of reformulating the qCRB for signals deriving from quantum fields, since a naive calculation of the qCRB may give a result in which the maximum sensitivity for a probe to a signal increases when one increases the signal's own quantum fluctuations. This may be relevant when backaction effects are significant. We note that the backaction effects correspond to the graviton propagator between in and out matter states, which generally may not be restricted to the physical TT modes. However, contributions from non-physical gravitons in the propagator result in time-symmetric self-gravity effects that is separate from the GW backaction.

Chapter 6

QUANTUM MEASUREMENT, DECOHERENCE, AND RADIATION IN LIGO

6.1 Preface

In the previous chapter we derived the equations for motion for the quantum interactions between the LIGO detector and gravitational waves, which can be generalized to apply to the interactions with linearized metric perturbations with optomechanical systems on a flat background. From a measurement point of view, the equations of motion for the outgoing field to the detector tell us about the quantum noise as a function of the parameters of the cavity (i.e. transmissivity and detuning) and readout scheme (e.g. homodyne angle), but they do not tell us the the *limit* of measurement sensitivity. We can search through the parameter space of our system to obtain the best outcome, but it is also helpful to understand the fundamental limits to detection sensitivity in order to guide the design for a better detector. In this chapter, we discuss the fundamental limit to quantum measurement in a general way and apply it to the LIGO detector, using the canonical formulation of its interactions with gravitational waves in the TT gauge that we developed in the previous chapter. Interestingly, we shall see that the bound on measurement is fundamentally related to the radiation of gravitational waves by the detector, as well as the decoherence to the detector due to a GW bath.

6.2 Introduction

As improvements and upgrades are made to Advanced LIGO, its noise floor is increasingly pushed towards its quantum limit. Fundamentally speaking, the quantum noise in LIGO comes from the vacuum fluctuations of the electromagnetic field which is injected into the interferometer in its antisymmetric port. The fluctuations are divided into two types: radiation pressure noise which acts on the cavity mirrors and mimic the effect of GW strain force, and shot noise which is the photon counting noise derived from discreteness of the photon whose arrival time at the detector can be modelled as a Poissonian process. Since the signal to noise ratio for a Poisson process goes as $1/\sqrt{N}$, to decrease shot noise one would have to increase laser power. However, doing so would increase the radiation pressure noise. Thus, we see that there is a tradeoff between the two types of quantum noise which implies that we

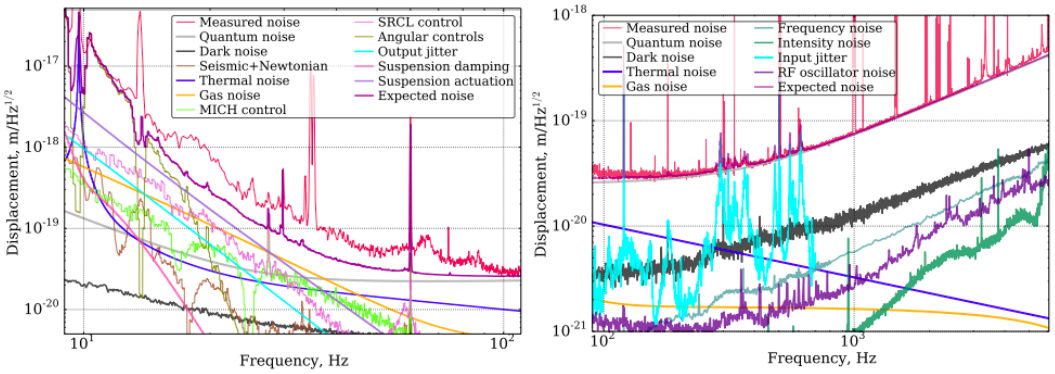

(a) LIGO Livingston Observatory (b) LIGO Hanford Observatory

Figure 6.1: Noise budgets from the LIGO Livingston and Hanford sites, taken from [42]. Figure a) shows the noise budget for the Livingston observatory in the low frequency range (<100Hz), and figure b) shows that for the Hanford observatory in the high frequency range (>100Hz). At low frequencies, classical sources of noise such as seismic noise dominate, but the detected is quantum shot noise limited at high frequencies. Reducing quantum noise such as the high frequency shot noise is possible by building quantum correlations in the electromagnetic vacuum that gets injected into the detector.

cannot make both arbitrarily small. This is in fact a manifestation of the Heisenberg uncertainty principle, since the radiation pressure and shot noise are associated with conjugate quadratures of the cavity mode (phase and amplitude, represented by $\hat{\alpha}_1$ and $\hat{\alpha}_2$) which satisfy the canonical commutation relation $[\hat{\alpha}_1, \hat{\alpha}_2] = i\hbar$. In LIGO, radiation pressure noise dominate at low frequencies while shot noise dominates at high frequencies. Heuristically speaking, this frequency dependence can be attributed to the fact that radiation pressure follows the frequency response of the test mass, which goes as $1/\Omega^2$, while the shot noise is frequency independent. The transfer function for a GW signal onto the light quadrature has inverse frequency dependence, and therefore the signal referred noise (or noise/signal) goes as $1/\Omega$ for radiation pressure, and as Ω for shot noise. This behaviour is shown in the noise budge plot in Fig.[6.1] taken from Ref. [42]. We also see that while classical sources of noise, notably seismic noise, still dominate at low frequencies, the detector is already limited by quantum shot noise above 100Hz [42]. More recently broadband radiation pressure noise has been measured in a frequency range relevant to GW detection (10kHz to 50kHz) [21]. Therefore it is crucial to understand the the behaviour of quantum noise well as methods to manipulate the noise over different frequency bands as LIGO becomes quantum limited.

For a pure vacuums state of the electromagnetic field, the tradeoff between radiation

pressure and shot noise gives one the standard quantum limit. However, it has been shown theoretically that injecting a squeezed vacuum into the detector can reduce the quantum noise floor at certain frequencies, and when the squeezing quadrature is frequency dependent this can result in broadband improvement to quantum limited sensitivity [38]. Most pertinent for LIGO is the shot noise above $\sim$ 100Hz, and indeed there are ongoing efforts to introduce squeezed vacuum into Advanced LIGO in to combat this. The idea behind squeezed vacuum injection is that, due to the backaction of the test mass onto the cavity mode in LIGO (also known as the ponderomotive squeezing effect), the output phase quadrature which carries the signal carries the noise of both phase and amplitude quadratures of the input vacuum. Uncorrelated, their fluctuations add in quadrature, but when correlated they can beat to cancel each other, thereby reducing noise. Building correlations among the noise quadratures to improve sensitivity is not limited to the squeezed vacuum injection scheme. Other proposals have been made to implement the same concept (e.g. [41]).

The question then is how much better can one do, and what are the fundamental limitations? The answer lies in the so-called quantum Cramer Rao Bound (qCRB), which is a general lower bound on the minimum variance of an the optimal estimator for the classical parameter of a quantum probe. In LIGO's case, the quantum probe is the cavity mode and the classical parameter is the gravitational wave.

One key point in the formulation of the qCRB is that the parameter is classical. Since the formalism introduced in the previous chapters allows for the quantization of gravitational waves, it is then interested to ask what happens when the classical parameter being estimated has its own quantum fluctuations (such as a displaced coherent state with a large classical amplitude and small fluctuations). This is in fact quite a general situation, since fundamental all signals should have a quantum source. We find that, while from the classical part one obtains the qCRB, from the quantum part one obtains decoherence to the probe and radiation into the GW field. Then, we find that there exist fundamental relations between LIGO's qCRB, its GW-induced decoherence, and its GW radiation. Specifically, we find that the qCRB appears both both the rate of GW radiation from the LIGO as well as the rate of its decoherence under GW vacuum fluctuations. That the radiation and decoherence rates are related in not surprising, since decoherence is caused by exchange of fluctuations between the system and bath. The reciprocity between GW radiation and detection (qCRB) furthermore has a classical analogy to radio antenna

[17]. However, the relationship between the fundamental bound on measurement sensitivity and the quantum decoherence of the measurement device has not, to the best of our knowledge, been pointed out before. We note that ours is a specific case of a what should be a more general statement that applies to any quantum probe detecting a signal which is associated with its own quantum field: that the qCRB of the probe is proportional to the radiation by the probe into the signal field, as well as the decoherence of the probe under vacuum fluctuations of the signal field.

6.3 A general discussion of the Quantum Cramer Rao Bound

In this section we will briefly discuss the quantum Cramer Rao Bound (qCRB), presenting some of its formal derivation and try to provide some intuitive understanding of the bound from the formalism. More details can be found in standard references [33, 72].

As suggested by its name, the qCRB can be viewed as an extension of the classical Cramer Rao bound, which states that given a probability distribution over $p(x;\theta)$ over sample space x and parametrized by the unknown deterministic parameter θ, that the variance $\sigma_{\hat{\theta}}$ of an unbiased estimator $\hat{\theta}$ is bounded by the inverse Fisher information $F(\theta)$, or

$$\sigma_{\hat{\theta}}^2 \geq \frac{1}{F(x;\theta)} \tag{6.1}$$

Formally, $F(\theta)$ is given as

$$F(\theta) = \int dx\ p(x|\theta) \left(\frac{\partial \ln p(x|\theta)}{\partial \theta} \right)^2 = -\left\langle \frac{\partial^2 \left(\ln[p(x;\theta)] \right)}{\partial \theta^2} \right\rangle \tag{6.2}$$

where the expectation value is taken over $p(x,\theta)$. The intuition for this definition of the Fisher information and its relation to the bound on the variance of the estimator is as follows: as the value of the true parameter varies, $p(x;\theta)$ gives us the likelihood function $p(x;\theta) = L(\theta|x)$, which tells us that, given the set of measurements x, how likely that the true value of the parameter is θ. The maximum likelihood estimator $\hat{\theta}_{ML}$ is the value of θ which, true to its name, is the maximum of $L(\theta|x)$. Then if $L(\theta|x)$ is a Gaussian, its second derivative gives us the inverse of the Gaussian's spread. It is sensible that is the spread of $L(\theta|x)$ is small (corresponding to large $F(\theta)$), then as we vary over the sample space x the resulting likelihood functions $L(\theta|x')$ will yield similar values of $\hat{\theta}_{ML}$, thereby reducing the variance σ_θ. We note that the bound in Eq. (6.1) is saturated to the optimal estimator $\hat{\theta} = \hat{\theta}_{ML}$.

An equivalent way to view this is through the notion of statistical distance between the distributions $p_1(x;\theta_1)$ and $p_2(x;\theta_2)$. From sampling each probability distribu-

tion we can find the maximum likelihood estimators $\hat{\theta}_1$ and $\hat{\theta}_2$, but this has some uncertainty since we can only approximate the p_1 and p_2 due to our limited sample size, and different samplings will in general gives us different values for the estimators. Then, each true value of θ engenders its own distribution of estimators, let's call them $\hat{\theta}_1(\theta_1)$ and $\hat{\theta}_2(\theta_2)$, and the distinguishability of $\hat{\theta}_1(\theta_1)$ and $\hat{\theta}_2(\theta_2)$ is related to $F(\theta)$. Then, the statistical distance ΔS can be understood as the distance between the distributions as compared to the uncertainty, or how many distinguishable distributions fit between $\hat{\theta}_1(\theta_1)$ and $\hat{\theta}_2(\theta_2)$ as compared to $\theta_1 - \theta_2$. But the uncertainty of the maximum likelihood estimator is simply the inverse of the Fisher information, and therefore

$$dS = \frac{d\theta}{\delta\hat{\theta}}, \quad \left(\frac{dS}{dX}\right)^2 = \frac{1}{\delta\theta^2} = \frac{1}{\sigma^2_{\hat{\theta}}} = F(\theta) \tag{6.3}$$

where we've taken the differential limit.

Let us now try to extend these classical notions for quantum measurements. The question we are asking is, given quantum states $\hat{\rho}_\lambda$ which are parametrized by a classical and deterministic quantity λ, how well can be know λ through measurements on $\hat{\rho}_\lambda$. In other words, what is the variance of our estimator $\hat{\lambda}$?

Immediately we can recognize that ρ_λ resembles a probability distribution, and in analogy to Eq. (6.2) we define the Fisher information as

$$F(\lambda) = \int dx \frac{\Re\left(\mathrm{Tr}\left[\rho_\lambda \Pi_x L_\lambda\right]\right)^2}{\mathrm{Tr}[\rho_\lambda \Pi_x]} \tag{6.4}$$

where the superoperator (an operator which acts on operators) L_λ is defined such that it takes the derivative of the quantum state with respect to λ, or

$$\frac{L_\lambda \rho_\lambda + \rho_\lambda L_\lambda}{2} = \frac{\partial \rho_\lambda}{\partial \lambda} \tag{6.5}$$

and Π_x is the POVM of the quantum measurement (or, in the simplest case, the basis onto which the quantum state is projected). When $\mathrm{Tr}[\rho_\lambda \Pi_x] = p(x|\lambda)$, the Eq. (6.4) becomes

$$F(\lambda) = \int dx \, \frac{1}{p(x|\lambda)} \left(\frac{\partial p(x|\lambda)}{\partial \lambda}\right)^2 \tag{6.6}$$

which, as the reader can check, is equivalent to the classical $F(\theta)$. However, our bound on estimator variance is not quite complete, since we have to also maximize $F(\lambda)$ over all possible POVMs on ρ_λ. Doing so then gives us the upper bound on $F(\lambda)$ which we denote by H_λ and which takes the form [49]

$$F(\lambda) \leq H(\lambda) \equiv \mathrm{Tr}[\rho_\lambda L_\lambda^2] \tag{6.7a}$$

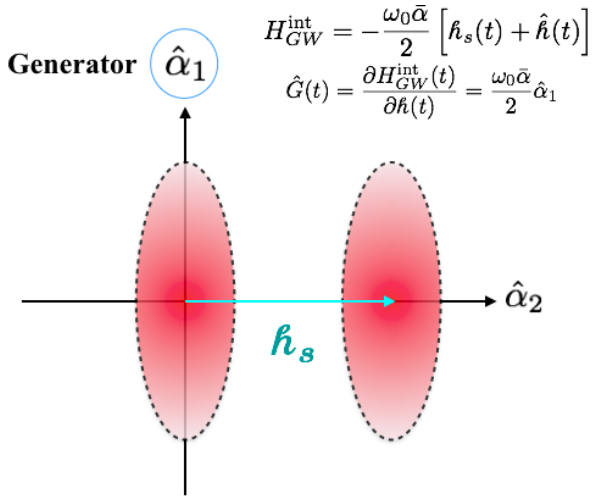

Figure 6.2: An illustration for a pictorial understanding of the qCRB using LIGO's interaction Hamiltonian. Here, the signal is $\hbar_(t)$, and the generator associated with quantum state translation in phase space is given by $\partial H/\partial \hbar_s$, and in this case is the amplitude quadrature of the cavity mode $\hat{\alpha}_1$. Upon receiving the signal, the quantum state shift in phase space along the quadrature *conjugate* to the generator. In other words, the state is displaced along the phase quadrature $\hat{\alpha}_2$. Measurement sensitivity improves if the quantum states are more distinguishable along $\hat{\alpha}_2$ by squeezing the fluctuations along this quadrature. For a pure quantum state, antisqueezing along the generator $\hat{\alpha}_1$ quadrature implies squeezing along the phase, and therefore an improved measurement sensitivity. This provides a heuristic justification for why the minimum estimation error is inversely proportional to the fluctuations of the generator.

and thus we have

$$\sigma_\lambda^2 \geq \frac{1}{MH(\lambda)} \tag{6.7b}$$

where M is the number of measurements, or identical quantum states on which we perform the same measurement.

The above discussion is rather formal, but the essential point is to identify the operators $L\lambda$ which gives us the gradient of the quantum state with respect to λ. Once we find find L_λ then the qCRB is straightforwardly given by Eqs. (6.7). To see this in an example, let's consider the unitary transformation parametrized by λ on an initial pure state

$$\rho_\lambda = e^{-iG\lambda\hbar}\rho_0 e^{iG\lambda\hbar} \tag{6.8}$$

Then straightforwardly taking the derivative gives us

$$\frac{\partial \rho_\lambda}{\partial_\lambda} = -\frac{i}{\hbar}[G, \rho] \tag{6.9}$$

Writing $L = -2i[G, \rho_\lambda]/\hbar$, we can check that this solution satisfies (recall that ρ_λ is a pure state)

$$\frac{L_\lambda \rho_\lambda + \rho_\lambda L_\lambda}{2} = -\frac{i}{\hbar}[G, \rho] = \frac{\partial \rho_\lambda}{\partial_\lambda} \tag{6.10}$$

Then the qCRB states that

$$\sigma_\lambda^2 \geq \frac{1}{\mathrm{Tr}[\rho_\lambda L_\lambda^2]} = \frac{\hbar^2}{4\langle \Delta G^2 \rangle} \tag{6.11}$$

for $\langle \Delta G^2 \rangle = \langle G^2 \rangle - \langle G \rangle^2$. In this very simple example, we can also very easily find the optimal estimator which saturates the bound, which is simply the variable Q conjugate to the generator G of the transformation, so that $[Q, G] = \pm i\hbar$. To see this, note that by Heisenberg uncertainty and for a pure state ρ_λ, we have

$$\langle \Delta Q \rangle^2 \langle \Delta G \rangle^2 = \frac{\hbar^2}{4}, \quad \langle \Delta Q \rangle^2 = \frac{\hbar^2}{4\langle \Delta G \rangle^2} \tag{6.12}$$

This makes sense intuitively because since G is the generator of a unitary transformation the quantum change experiences a shift λ along the conjugate direction Q (e.g. the unitary $e^{ip\lambda}$ will transform $|x\rangle \to |x + \lambda\rangle$). In terms of statistical distance and assuming that quantum states have a representation in the Q and G phase space, we see since the translation of the state in phase space is along the Q quadrature, we can maximize the information we obtain if we also measure along this quadrature, and therefore Q is the optimal estimator (as opposed to, for example, G, which will give us no information). Additionally, if we squeeze the quantum state to increase the fluctuations in G while preserving the area of the noise ellipse, we can obtain a better sensitivity because the fluctuations along Q are now smaller and quantum state with different values of λ are now more distinguishable (Fig.[6.3])

In summary, we have presented a plausibility argument in analogy with the classical Cramer Rao Bound the lower bound on measurement uncertainty in the determination of a classical parameter using a quantum measurement device. The result, known as the quantum Cramer Rao Bound, states that the minimum variance of the optimal estimator is the inverse of the device's quantum Fisher information, maximized over all possible POVMs (Eq. (6.7)). This bound gives us the fundamental limit to measurement by a quantum device in most quantum measurement schemes (there are situations for which the assumptions underlying the qCRB do not hold. In these situations a different bound on parameter estimation would apply. For a discussion of such cases see [61]).

6.4 The QCRB for continuous waveforms

The general discussion of the qCRB above concerned itself with the determination of a single value. However, to obtain a fundamental limit of LIGO requires one to adapt the results to the estimations of a continuous gravitational waveform which arrives at LIGO over some time. The general results for this type of measurement were derived by Tsang, Wiseman, and Caves [66] and we present a brief overview below.

The strategy is to discretize the signal into a vector and perform multi-parameter estimation, where the parameters are all independent and their estimators commute. This allows for the construction of a Fisher information matrix (as opposed to a scalar Fisher information function for single parameter). Subsequently one takes the continuous limit, and for a quantum device measuring a classical waveform $x(t)$ and which system's total dynamics is governed by the Hamiltonian $H(t)$ that is *linear* in $x(t)$, one obtains the result

$$F(t,t') = \frac{4}{\hbar^2}\langle \Delta q(t)\Delta q(t')\rangle_{\text{sym}} \tag{6.13}$$

where $\delta q(t) = q(t) - \langle q(t)\rangle$, and $q(t)$ is the operator given by

$$\tilde{q}(t) = \lim_{\delta t\to 0}\tilde{q}_k = \frac{\partial H(t_k)}{x_k}, \quad q(t) = U^{\dagger}(t)\,\tilde{q}(t)\,U(t) \tag{6.14}$$

where the k subscript denotes quantities at discretized time t_k and $U(t)$ is unitary evolution operator with respect to $H(t)$. Note that the two time correlator in Eq. (6.13) is symmetrized.

We point out that $q(t)$ is analogous to the generator G in our earlier example (Eq. (6.8)), and indeed, we find that the quantum Fisher information is given by its fluctuations.

To put $F(t,t')$ into a useable form, Tsang et. al constructs the cost function

$$C \equiv \int dt\ dt'\ \Lambda(t,t')\Sigma(t,t') \geq \int dt\ dt'\ \Lambda(t,t')F^{-1}(t,t') \tag{6.15}$$

The integration limits are taken to the $\pm T/2$. In the above, $\Sigma(t,t')$ is the estimation error covariance matrix and $F^{-1}(t,t')$ is the inverse of the Fisher information, satisfying

$$\int dt''\ \Sigma(t,t'')F(t'',t) = \delta(t-t') \tag{6.16}$$

The left hand side of the inequality is the estimation error given in different forms, depending on the choice of the kernel $\Lambda(t,t')$, while the righthand side is the

corresponding representation of the minimum bound, and any choice of $\Lambda(t,t')$ would result in a valid form of the qCRB. Since the noise curve in LIGO is expressed as a power spectral density in frequency, we choose

$$\Lambda(t,t') = \lim_{T\to\infty} \frac{1}{T} e^{i\Omega(t'-t)} \tag{6.17}$$

for which

$$C = S_x(\Omega) \geq \frac{\hbar}{4} \frac{1}{S_q(\Omega)} \tag{6.18}$$

In obtaining Eq. (6.18) we've assumed that $x(t)$ and $q(t)$ are stationary processes for which noise spectral densities can be defined. The meaning of the equation is clear: the minimum noise power resulting from estimation error of x is bound by the inverse of the of the noise power in the fluctuations of q.

6.5 QCRB for LIGO

From our Hamiltonian derived in the previous chapter we can follow the formalism of [66] to calculate the qCRB for LIGO for each k-modes. Recall that the interaction Hamiltonian is

$$H_{GW}^{int} = -\frac{\omega_0 \bar{\alpha}\hat{\alpha}_1}{2} \int d^3\mathbf{k}\; J_\lambda(\mathbf{k}) \hat{h}_\lambda(t,\mathbf{k}) \tag{6.19}$$

for

$$J_\lambda(\mathbf{k}) = \frac{\tau_{xx}(\hat{\mathbf{k}})}{\sqrt{(2\pi)^3}} \mathrm{sinc}\left(\frac{k_x L}{2}\right) e^{ik_x L/2} \tag{6.20}$$

for the sinc function $\mathrm{sinc}(x) = \sin x/x$. Since the k-modes of the GW field are independent, we may find the qCRB for each. However, recall that $\hat{h}_\lambda(t,\mathbf{k})$ is the Fourier transform of the real field $\hat{h}_{ij}(t,\mathbf{x})$ and is in general complex. Therefore, we must first identify the Hermitian k-mode operator which in the classical limit corresponds to a real signal. This is

$$\hat{h}_\lambda^R(\mathbf{k}) = \frac{1}{2}\left[\hat{h}_\lambda(\mathbf{k}) + \frac{i}{\omega_k M_G}\hat{\Pi}_\lambda(\mathbf{k})\right] e^{ik_x L/2} + h.c \tag{6.21}$$

with the corresponding canonical momentum

$$\hat{\Pi}_\lambda^R(\mathbf{k}) = \frac{1}{2}\left[\hat{\Pi}_\lambda(\mathbf{k}) - i\omega_k M_G \hat{h}_\lambda(\mathbf{k})\right] e^{ik_x L/2} + h.c \tag{6.22}$$

It can shown that this canonical transformation gives the interaction Hamiltonian

$$H_{GW}^{int} = -\frac{\omega_0 \bar{\alpha}\hat{\alpha}_1}{2} \int d^3\mathbf{k}\; |J_\lambda(\mathbf{k})|\, \hat{h}_\lambda^R(\mathbf{k}) \tag{6.23}$$

From here on, we will redefine $\hat{h}_\lambda(\mathbf{k}) = \hat{h}_\lambda^R(\mathbf{k})$ and drop with λ subscript with the understanding that we are summing over the + and $\times$ polarizations. In the classical

limit where $\hat{h}_\lambda(\mathbf{k}) \to h_\lambda(t, \mathbf{k})$, The quantum Fisher information for each mode corresponding to the optimal POVM is given by the fluctuations in the operator

$$\hat{G}(t) = \frac{\partial H_{GW}^{int}}{\partial h(t, \mathbf{k})} = -\frac{\omega_0 \bar{\alpha} \hat{\alpha}_1}{2} |J(\mathbf{k})| \tag{6.24}$$

from which we obtain (Eq. (6.13))

$$F_{\mathbf{k}}(t, t') = \frac{4}{\hbar^2} \left(\frac{\omega_0 \bar{\alpha}}{2} \right)^2 |J(\mathbf{k})|^2 \langle \hat{\alpha}_1(t) \hat{\alpha}_1(t') \rangle_{\text{sym}} \tag{6.25}$$

Then, choosing the kernel $\Lambda(t, t') = e^{i\Omega(t-t')/T}$, we find the Fisher information in spectral density form

$$F_{\mathbf{k}}(\Omega) = \frac{4}{\hbar^2} \left(\frac{\omega_0 \bar{\alpha}}{2} \right)^2 |J(\mathbf{k})|^2 S_{\alpha_1}(\Omega) \tag{6.26}$$

so that the measurement noise is bound by

$$S_{hh}^{\mathbf{k}}(\Omega) \geq \frac{\hbar^2}{(\omega_0 \bar{\alpha})^2 |J(\mathbf{k})|^2 S_{\alpha_1}(\Omega)} \tag{6.27}$$

This bound is independent of whether the interferometer is operating in the tuned or detuned configuration, since the relevant quantity for calculating the quantum Fisher information, and therefore the qCRB, is the interaction term H_{GW}^{int}, which is the same in either case. Increasing the maximum sensitivity for LIGO for all modes now reduces to tuning three independent quantities: the resonant frequency of the cavity ω_0, the average amplitude of the optical mode $\bar{\alpha}$, and the fluctuations of the amplitude quadrature $S_{\alpha_1}(\Omega)$. There is also the mode dependent parameter $J_\lambda(\mathbf{k})$, through which the length of the cavity L becomes relevant in selecting for which modes the detector is sensitive to (those for which $k_x L < 1$). Lastly, we point out that the bound is independent of test mass properties to $O(v^2/c^2)$, which is intuitive in the TT gauge where there the interaction between GWs and the probe is via the optical mode.

The bound in Eq. (6.27) is the most useful form of the qCRB for understanding the sensitivity of the LIGO detector, since LIGO's noise curve is given by the noise spectral density, as in Fig. 6.1, and the cavity is always strongly pumped when in operation, making it possible to linearize the Hamiltonian. However, as we will demonstrate, the qCRB has a relation to decoherence that is simplest to understand in the absence of external optical pumping, so that the GW field is the sole external environment to the probe. In this case we cannot make the linearizing approximation, and the interaction Hamiltonian takes on the full form

$$H_{GW}^{int} = -\frac{\hbar \omega_0}{2} \hat{n} \int d^3\mathbf{k} \, |J(\mathbf{k})| \, \hat{h}(\mathbf{k}) \tag{6.28}$$

where $\hat{n} = \hat{a}^\dagger \hat{a}$ is the number operator. In this case, the quantum Fisher information for estimating the parameter $h(t, \mathbf{k})$, denoted by $\mathcal{F}_{\mathbf{k}}$, is now

$$\mathcal{F}_{\mathbf{k}} = \left(\frac{\omega_0}{2}\right)^2 4\left\langle \Delta\hat{n}^2 \right\rangle |J(\mathbf{k})|^2 \tag{6.29}$$

We note that in the absence of external pumping, the probe degree of freedom $\hat{n}$ has no time dependence and we are unable to place a bound on the noise spectral density as in Eq. (6.27). Thus, the form of the Fisher information in Eq. (6.29) offers a different interpretation of measurement. One can verify that the above expression is also the Fisher information for the time integrated signal $h_t(\mathbf{k}) \equiv \int_0^t d\tau\, h(\tau, \mathbf{k})$, and therefore can be understood as a bound on the detectability of signal presence in the time interval $\tau \in (0, t)$, or equivalently a bound on the error of hypothesis testing $\sigma^2_{h_t}$

$$\sigma^2_{h_t} \geq \frac{1}{\omega_0^2 |J(\mathbf{k})|^2 \left\langle \Delta\hat{n}^2 \right\rangle} \tag{6.30}$$

Limitation of qCRB for signals deriving from a quantum field

The qCRB is the ultimate bound on sensitivity for the optimal estimator and simply having a quantum-limited measurement device does not entail achieving the bound (for a discussion on the conditions for achieving the qCRB for a linear probe formulated in terms of conditions on noise spectral densities, see Ref. [43]). In fact, allowing the signal to have its own fluctuations appears to result in situations where the bound cannot be obtained. To see this, we express S_{α_1} in terms of input fields:

$$S_{\alpha_1} = 2\gamma \left[|\chi_1|^2 S^{in}_{\alpha_1} + |\chi_2|^2 S^{in}_{\alpha_2} - 2\Re\{\chi_1 \chi_2 S^{in}_{\alpha_1 \alpha_2}\} \right] + \left(\frac{\omega_0 \bar{\alpha}}{2}\right)^2 |\chi_2|^2 S_{\hbar} \tag{6.31}$$

where $S_{\hbar}$ is spectral density for quantum GW fluctuations. Here the response functions χ_1, χ_2 take the same form as Eq. (5.49) with $s \to -i\Omega$. In tuned case, $\chi_1 \to (\gamma - i\Omega)^{-1}$ and $\chi_2 \to 0$, and the only contribution to S_{α_1} comes from the input amplitude quadrature $S^{in}_{\alpha_1}$. In this case, holding all other experimental parameters constant, increasing the qCRB amounts to antisqueezing the amplitude fluctuations of the input light across the detection bandwidth. Attaining the qCRB is in principle possible if one counters ponderomotive backaction effects by correlating $\hat{\alpha}^{in}_1$ and $\hat{\alpha}^{in}_2$, such as with frequency dependent squeezing techniques, or by using variational readout [38]. In either case, one must be have access to the external optical modes in order to perform unitary transformations or measurements. In the detuned case, the GW field's own quantum fluctuations drive the cavity's amplitude quadrature,

leading to an unclear interpretation of the bound where greater quantum uncertainty in a particular signal quadrature appears to increase maximum achievable sensitivity, to which one must furthermore have independent access in order to attain the bound. Evidently, since the qCRB for formulated for a quantum probe measuring a deterministic classical signal, it is unequipped to precisely account for situations where the quantum fluctuations and backaction effects of the signal field is taken into account.

6.6 Reciprocity between qCRB, GW radiation, and decoherence

The quantum Cramer Rao bound gives the minimum estimation error on a classical signal which is measured by a quantum probe, where the fundamental source of error lies in the quantum uncertainty of the probe and cannot be eliminated. In the scenarios in which the qCRB is studied, only the measurement device is quantum while the signal is pre-given and purely classical, and as such is not affected by the probe's quantum behaviour. However, in our formalism we view the "classical signal" as a large excitation of a fundamentally quantum field, which for large amplitude signals and be separated into a classical component with quantum fluctuations. Evidently, this means that the classical signal and its quantum fluctuations couple to the probe in the same way, as shown explicitly in Eq. (5.19). While the classical interaction is characterized by the qCRB, the quantum interactions results in radiation and decoherence, as discussed in the previous section. It is interesting then to consider whether there are fundamental relations between these quantities.

QCRB and GW Radiation

Far away from the source where the GWs are radially propagating, the power carried by GWs crossing a sphere at radius $r \gg L$ is given by

$$P_{\rm rad}^{GW} = \int d\mathbf{\Omega}\, r^2 \langle \dot{\hat{h}}_{jk}^{TT} \dot{\hat{h}}_{jk}^{TT} \rangle \tag{6.32}$$

for the solid angle element $d\mathbf{\Omega}$. Using Eq. (5.33) for generation of GWs by the probe and Eq. (5.34) for the TT projection operator for radially propagating waves, we find

$$P_{rad}^{\rm GW} = \frac{32G}{15c^5} \int \frac{d\Omega}{2\pi} \Omega^2 \left(\frac{\omega_0 \bar{\alpha}}{2}\right)^2 S_{\alpha_1}(\Omega) \tag{6.33}$$

where the numerical factor includes the effect of TT projection. This can be put into a more suggestive form by explicitly writing the TT projection as an integral over the angular dependence of $\mathbf{k}$. Noting that $J(\mathbf{k})$ is simply the TT projection tensor

in the large r limit where we can take $k_x L \ll 1$, Eq. (6.33) takes the form

$$P_{rad}^{\mathrm{GW}} = 4\pi^2 \frac{\hbar G}{c^5} \int d\hat{\mathbf{k}} \int \frac{d\Omega}{2\pi} \hbar\Omega^2 \, |J(\mathbf{k})|^2 \left(\frac{\omega_0 \bar{\alpha}}{2}\right)^2 \frac{4}{\hbar^2} S_{\alpha_1}(\Omega) \tag{6.34}$$

where $d\hat{\mathbf{k}}$ is the integration measure over the angular dependence of $\mathbf{k}$. Comparing this with the Fisher information given in Eq. (6.26), we finally have

$$\frac{dP_{rad}^{\mathrm{GW}}}{d\hat{\mathbf{k}}\, d\Omega} = (2\pi)\, \Omega E_g \, F_{\mathbf{k}}(\Omega) T_p^2 \tag{6.35}$$

where $T_P = \sqrt{\hbar G/c^5}$ is the Planck time and $E_g = \hbar\Omega$ is the graviton energy. To interpret Eq. (6.35), we note that $\Omega\, E_g \sim E_g/T$ is the power carried by a graviton of frequency Ω and that $F_{\mathbf{k}}(\Omega)T_P^2$ is a frequency dependent gain function for radiation that is given by the quantum Fisher information for a pumped cavity. This means for any mode channel $(\hat{\mathbf{k}}, \Omega)$, the power radiated across the channel is proportional to LIGO's sensitivity to a signal sent across the same. We emphasize that this is a fundamental relation: for all channels the gain function for GW radiation is exactly LIGO's ultimate measurement sensitivity (modulo fundamental constants). This means that improving LIGO's ultimate sensitivity at any frequency necessarily implies more GW power radiated at the same frequency. The connection shown here between LIGO's qCRB and its radiated GW power offers the viewpoint of LIGO as an antenna or a transducer between gravitons and photons, capable of both sending and receiving GW signals with the same transmission efficiency when optimal measurement is achieved.

QCRB and Decoherence

Let us now consider the evolution of the probe (the system) in state $\rho_s(t)$ upon interaction with a GW field (the bath) in state ρ_B which we cannot measure. Denoting the total state (system and bath) by ρ, the evolution of the probe's density matrix in the interaction picture is given by

$$\rho_s(t) = \mathrm{Tr}_B \left\{ U(t)\rho(0)U^\dagger(t) \right\} \tag{6.36}$$

where a partial trace is performed over the bath modes. The unitary operator $U(T)$ is given by

$$U(t) = T\left\{ \exp\left[-\frac{i}{\hbar} \int d\tau \, H_I(\tau) \right] \right\} \tag{6.37}$$

where T in the front of the exponential denotes time ordering and

$$H_I(t) = U_0^\dagger(t) H_{int} U_0(t) \tag{6.38}$$

for the free evolution operator $U_0(t)$ is the interaction picture Hamiltonian. Expanding the system state in the Fock state basis and assuming $\rho(0) = \rho_s(0) \otimes \rho_B(0)$, for matrix element $\rho_{nm}(t) = \langle n|\rho_s(t)|m\rangle$ we have

$$\rho_{nm}(t) = \sum_{n'm'} \rho_{n'm'}(0) \mathrm{Tr}\left\{\langle n|U(t)|n'\rangle \rho_B(0) \langle m'|U^\dagger(t)|m\rangle\right\} \tag{6.39}$$

Since Fock states are eigenstates of the system operator for the Hamiltonian in Eq. (6.28), $\langle n|U(t)|n'\rangle$ takes on the simple form

$$\langle n|U(t)|n'\rangle = T\left\{\exp\left[\frac{i\omega_0 n}{2}\int d^3\mathbf{k}\,|J(\mathbf{k})|\int_0^t d\tau\,\hat{h}(\tau,\mathbf{k})\right]\right\}\delta_{nn'} \tag{6.40}$$

Furthermore, since the different time commutator of the argument in the exponential is a c-number, we can remove the time ordering operator (with an overall c-number phase shift which we ignore) so that $\rho_{nm}(t)$ becomes

$$\rho_{nm}(t) = \rho_{nm}(0)\left\langle \exp\left[\frac{i\omega_0}{2}(n-m)\int d^3\mathbf{k}|J(\mathbf{k})|\int_0^t d\tau\,\hat{h}(\tau,\mathbf{k})\right]\right\rangle \tag{6.41}$$

where the angular brackets signify averaging over the bath state. Let us denote the argument of the exponential by $\hat{\Gamma}(t)$ so that we can write

$$\rho_{nm}(t) = \rho_{nm}(0)\left\langle e^{\hat{\Gamma}(t)}\right\rangle \equiv \rho_{nm}(0)e^{\Gamma(t)} \tag{6.42}$$

It can be shown that for Gaussian bath state (e.g. vacuum, thermal) that

$$\left\langle e^{\hat{\Gamma}(t)}\right\rangle = \exp\left[\frac{1}{2}\left\langle\hat{\Gamma}^2(t)\right\rangle\right] \tag{6.43}$$

Explicitly, we have

$$\Gamma(t) = -\frac{1}{2}\left(\frac{\omega_0}{2}\right)^2(n-m)^2\int d^3\mathbf{k}\int d^3\mathbf{k}'\,|J(\mathbf{k})||J(\mathbf{k}')| \int_0^t d\tau\int_0^t d\tau'\left\langle\hat{h}(\tau,\mathbf{k})\hat{h}(\tau',\mathbf{k}')\right\rangle \tag{6.44}$$

We can define a noise special density function for the correlation function

$$S_{\mathbf{k}\mathbf{k}'}(\omega) = \int_{-\infty}^{\infty} dT\left\langle\hat{h}(\tau,\mathbf{k})\hat{h}(\tau-T,\mathbf{k}')\right\rangle e^{i\omega T} \tag{6.45}$$

Since the different k-modes have δ-function commutators, Eq. (6.45) evaluates to

$$S_{\mathbf{k}\mathbf{k}'}(\omega) = S_h^{\mathbf{k}}(\omega)\delta^3(\mathbf{k}-\mathbf{k}') \tag{6.46}$$

for some $S_h^{\mathbf{k}}(\omega)$ which now depends only on $\mathbf{k}$ and ω. Substituting Eqs. (6.45) and (6.46) into Eq. (6.43), we find

$$\Gamma(t) = -\frac{1}{2}\left(\frac{\omega_0}{2}\right)^2 (n-m)^2 \int d^3\mathbf{k}\, |J(\mathbf{k})|^2 \int \frac{d\omega}{2\pi} S_h^{\mathbf{k}}(\omega) W_t(\omega) \tag{6.47}$$

where the window function $W_t(\omega)$ derives from the double time integral

$$W_t(\omega) = \int_0^t d\tau \int_0^t d\tau'\, e^{-i\omega(\tau-\tau')} = \frac{4}{\omega}\sin^2\left(\frac{\omega t}{2}\right) \tag{6.48}$$

To see how this relates to the qCRB, let us evaluate the decoherence for the system in an initial superposition of Fock states

$$|\psi_+(0)\rangle = \frac{1}{\sqrt{2}}\left(|n\rangle + |m\rangle\right) \tag{6.49}$$

for which

$$\left\langle \Delta\hat{n}^2 \right\rangle = \frac{1}{4}(n-m)^2 \tag{6.50}$$

Note that in the above the averaging may be with respect of the probe state at any time and its value is unaffected by the GW interaction. Then for this initial Fock state superposition, its decoherence may be expressed by

$$\Gamma(t) = -\frac{1}{2}\left(\frac{\omega_0}{2}\right)^2 4\left\langle \Delta\hat{n}^2 \right\rangle \int d^3\mathbf{k}\, |J(\mathbf{k})|^2 \int \frac{d\omega}{2\pi} S_h^{\mathbf{k}}(\omega) W_t(\omega) \tag{6.51}$$

and comparing this to the quantum Fisher information $\mathcal{I}_{\mathbf{k}}$ for an undriven cavity given in Eq. (6.29), we have finally

$$\Gamma(t) = -\frac{1}{2}\int d^3\mathbf{k}\, \mathcal{I}_{\mathbf{k}} \int \frac{d\omega}{2\pi} S_h^{\mathbf{k}}(\omega) W_t(\omega) \tag{6.52}$$

The relation in Eq. (6.52) states that the decoherence to an initial Fock state superposition of the cavity mode depends only its quantum Fisher information and the noise spectrum of the GW bath. In other words, the minimum measurement error for a signal using a quantum state is inversely related to the decoherence to the state due to the quantum fluctuations of the signal field. This appears to be a general relation and should apply in some form for any linear quantum measurement where the signal is a large excitation of an underlying quantum field. While it seems like we have chosen a very specific initial state to arrive at this result, our choice is not arbitrary and is instead determined by the probe's pointer basis. If we limit our Hilbert space to the basis states $|n\rangle$, $|m\rangle$, then $|\psi_+(0)\rangle$ is maximally coherent. We therefore make the following statement: in the interaction of a system with an

external quantum field, the decoherence of a maximally coherent state with respect to the pointer basis in a $d = 2$ Hilbert subspace is determined by the state's quantum Fisher information for estimating a large amplitude excitation of the field (a classical signal) and the quantum bath's noise spectrum. Heuristically, this means that increasing measurement sensitivity necessarily causes stronger decoherence.

For concrete examples, we calculate the decoherence to $|\psi_+\rangle$ due to vacuum and thermal states of the bath given by the density matrices

$$\rho_B^{(0)} = |0\rangle\langle 0| \tag{6.53a}$$

$$\rho_B^{\text{th}} = \otimes_{\mathbf{k}} \left(1 - e^{\hbar\beta\omega_{\mathbf{k}}}\right) \sum_{n_{\mathbf{k}}} e^{-\hbar\beta n_{\mathbf{k}}\omega_{\mathbf{k}}} |n_{\mathbf{k}}\rangle\langle n_{\mathbf{k}}| \tag{6.53b}$$

where $\beta = (k_B T)^{-1}$ for temperature T. Note we've discretized the k-modes in the representation of the thermal state, and will take the continuum limit in our calculations. In the absence of interaction, the GW field evolves freely with the mode dispersion relation $\omega_{\mathbf{k}} = c|\mathbf{k}|$. For these states then, we find the noise spectral densities (taking the large T limit for the thermal state)

$$S_h^{\mathbf{k}(0)}(\omega) = \frac{\hbar}{2M_G\omega_{\mathbf{k}}}(2\pi)\delta(\omega_{\mathbf{k}} - \omega) \tag{6.54a}$$

$$S_h^{\mathbf{k}(\text{th})}(\omega) = \frac{1}{2M_G\omega_{\mathbf{k}}}\frac{1}{\beta\omega_{\mathbf{k}}}(2\pi)\left[\delta(\omega_{\mathbf{k}} - \omega) + \delta(\omega_{\mathbf{k}} + \omega)\right] \tag{6.54b}$$

from which, upon substitution into Eq. (6.52), we obtain the decoherences

$$\frac{d\Gamma^{(0)}(t)}{d\hat{\mathbf{k}}\, d\Omega} = -\frac{1}{2}\left(\frac{\hbar\Omega}{2M_G c^3}\right)\mathcal{F}_{\mathbf{k}}\, W_t(\Omega) \equiv -\frac{1}{2}g^{(0)}(\Omega)\mathcal{F}_{\mathbf{k}}\, W_t(\Omega) \tag{6.55a}$$

$$\frac{d\Gamma^{(th)}(t)}{d\hat{\mathbf{k}}\, d\Omega} = -\frac{1}{2}\left(\frac{1}{M_G\beta c^3}\right)\mathcal{F}_{\mathbf{k}}\, W_t(\Omega) \equiv -\frac{1}{2}g^{(th)}(\Omega)\mathcal{F}_{\mathbf{k}}\, W_t(\Omega) \tag{6.55b}$$

where we've rewritten the integration measure $d^3\mathbf{k} = d\hat{\mathbf{k}}\, d\Omega\, \Omega^2$ for $\Omega \equiv c|\mathbf{k}| = \omega_{\mathbf{k}}$. The Eqs. (6.55) can be interpreted as the decoherence across each channel $(\hat{\mathbf{k}}, \Omega)$ and depends only on its quantum Fisher information weighted by the bath spectrum $g(\Omega)$ (in contrast to the noise spectral density, $g(\Omega)$ also contains information about the density of modes). Of course, this is not an entirely accurate interpretation since $W_t(\Omega)$ is sinusoidal and therefore the coherence will experience "revival", which is a reflection of the general principle that true decoherence does not occur over a single channel and instead requires a trace over a continuum of modes. In particular, when $g(\Omega)\mathcal{F}_{\mathbf{k}}$ is approximately white over the interval $\Omega \in (0, 2\pi/t)$ where $W_t(\Omega)$ has support, the trace over the continuum gives

$$\frac{d\Gamma(t)}{d\hat{\mathbf{k}}} = -\pi\left[g(\Omega)\mathcal{F}_{\mathbf{k}}\right]\Big|_{\Omega=0} t \equiv -\gamma_{\hat{\mathbf{k}}}\, t \tag{6.56}$$

and the system's coherence decays at a constant rate. This is known as the Markovian regime and applies in our case for the thermal bath state when $t \gg L/c$, for which $\mathcal{F}_{\mathbf{k}} \to \mathcal{F}_{\hat{\mathbf{k}}}$ becomes independent of Ω over the support of $W_t(\Omega)$, giving the decoherence rate

$$\gamma^{th}_{\hat{\mathbf{k}}} = \frac{\pi}{M_G c^3 \beta} \mathcal{F}_{\hat{\mathbf{k}}} \tag{6.57}$$

When $g(\Omega)\mathcal{F}_{\mathbf{k}}$ is colored the decoherence $d\Gamma(t)/d\hat{\mathbf{k}}$ has more complicated time dependence, but the key point is that the only relevant quantities in determining the decoherence is the quantum Fisher information and parameters of the bath state, as shown in Eq. (6.52). For the special case where the bath is in the vacuum state, the decoherence depends only on the Fisher information and fundamental constants, as shown in Eq. (6.55a).

Discussion of Reciprocity

To summarize, the quantum Fisher information relates the maximum achievable sensitivity for LIGO to detect a GW signal (which is simply its inverse), its GW radiation, and its decoherence due to GW bath fluctuations. To show this, we considered two forms of the quantum Fisher information: first for the case of a strongly pumped cavity operating in the linear regime (Eq. (6.26)), and second for the case of an undriven cavity whose only external environment (with respect to the probe) is the GW field (Eq. (6.29)). The first form is useful to constrain LIGO's noise floor $S^{\mathbf{k}}_{hh}(\Omega)$ at all frequencies for each k-mode of the signal, while the second is the bound on the error of hypothesis testing $\sigma^2_{h_T}$ for whether a signal is present. These relations, given in Eqs. (6.35) and (6.55), are fundamental in the sense that these processes *only* depend on the Fisher information and fundamental constants (for decoherence due to the vacuum state). Thus, LIGO's ultimate noise floor (as determined by the qCRB) is precisely the inverse of gain function for graviton radiation, while the lowest bound on hypothesis testing error is inversely proportional to the decoherence of a maximally coherent state in the pointer basis in the $d = 2$ Hilbert subspace. These relations are shown pictorally in Fig. 6.3 and suggest an equivalence of information gain and loss, although further investigation is necessary to more precisely formulate this claim.

6.7 Conclusion

We found there there exist fundamental relationships between LIGO's qCRB and its GW radiation and vacuum decoherence rate. Specifically, the radiated energy and the qCRB obey a reciprocity relation that offers the interpretation of LIGO as an photon-

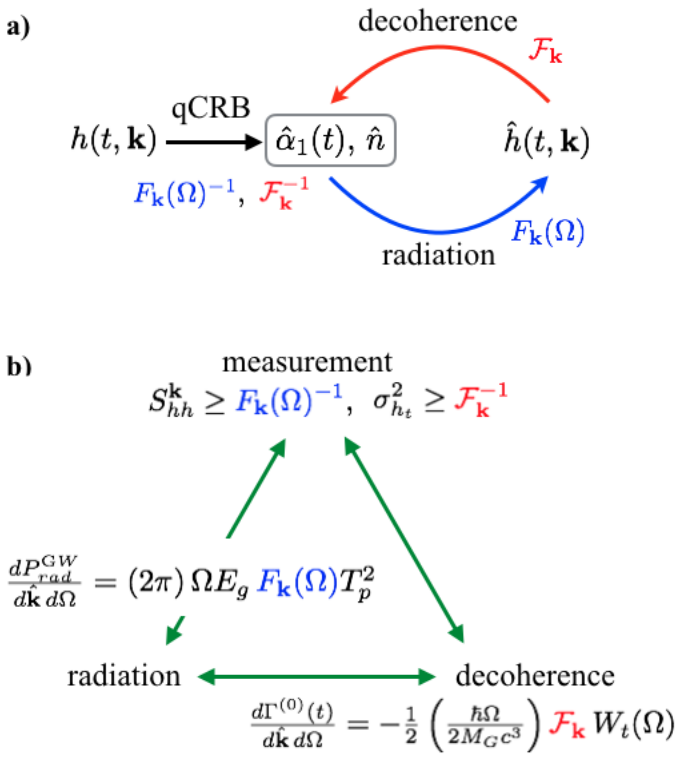

Figure 6.3: Figure a) elucidates the interactions between the GW field and the probe. For each k-mode we separate the GW field into a large classical amplitude $h(t,\mathbf{k})$ and quantum fluctuations $\hat{h}(t,\mathbf{k})$, and denote the probe degree of freedom by $\hat{\alpha}_1(t)$ (strongly pumped cavity) and $\hat{n}$ (no pumping) with the associated quantum Fisher information $F_{\mathbf{k}}(\Omega)$ and $\mathcal{F}_{\mathbf{k}}$. The action of the external classical amplitude $h(t,\mathbf{k})$ onto the probe is a measurement process characterized by the qCRB which is the inverse of the quantum Fisher information in either scenario, while action of the quantum fluctuations $\hat{h}(t,\mathbf{k})$ results in decoherence. The reverse quantum process in which the probe acts onto $\hat{h}(t,\mathbf{k})$ results in radiation. Figure b) quantifies the reciprocity relations between the three processes through the quantum Fisher information.

graviton transducer. We find a similar reciprocity relation for decoherence, where for particular initial states of the probe the qCRB appears in the vacuum decoherence rate, such that reducing the error of hypothesis testing for signal presence will necessarily increase decoherence due to its quantum component, which cannot be eliminated by assuming zero temperature. Since measurement is information gain and decoherence represents information loss, these relations suggest an equivalent exchange of information between a probe and a quantum field which merits further study. Additionally, the qCRB is formulated under the assumption that signals are purely classical. However, all signals derive from underlying quantum fields, and therefore an extension of theory may be necessary to account for how the quantum

fluctuations many effect measurement sensitivity in the regime where the signal strength is comparable to fluctuations.

Chapter 7

CONCLUSIONS

In this work we have constructed frameworks for analyzing quantum systems in classical or linear quantum gravity in a way that is consistent with Einstein's theory of general relativity, in order to provide a more rigorous foundation for studying gravitational effects in quantum systems. In Chapters 2 and 3, we developed a covariant formulation for different implementations of quantum free fall experiments, specifically for diffracting matter waves and the Mach Zehdner atom interferometer, and noted the differences in the interpretation from the covariant versus Newtonian viewpoint. This difference highlights the usefulness of the general relativistic viewpoint as a comparison to the predictions made in non-relativistic quantum theory.

In Chapters 4 and 5 , we developed a canonical formulation of LIGO's interactions with linear quantum gravity, and observed that, in addition to being consistent with known equations of motion, these interactions also give rise to quantum backaction effects that have not been previously discussed. Additionally, the canonical formulation in the TT gauge resulted in an Hamiltonian in which the GWs appear explicitly, such that LIGO's quantum Cramer Rao bound (qCRB, which represents the fundamental limit to sensitivity) can be straightforwardly obtained. This is in contrast to the standard Newtonian viewpoint, in which GWs act unilaterally on LIGO without back-action effects, and in which the GWs do not appear in the quantum Hamiltonian governing LIGO's dynamics (rather, GWs are added "by hand" as an external force on the test mass). Additionally, as we discuss in Chapter 5, by allowing the GW field's quantum fluctuations to interact with those of LIGO's cavity mode, we find that LIGO's measurement sensitivity, decoherence, and GW radiation are fundamentally related through its quantum Fisher information. While these relationships were calculated specifically for LIGO, they appear generalizable.

The interface of quantum mechanics and gravity is an exciting and subtle area that, with improvements in experimental techniques, may offer insight into how to reconcile the numerous paradoxes between quantum mechanics and general relativity. Despite the various challenges in adapting quantum theory to general relativistic language, it is worthwhile to build a strong theoretical foundation upon which to proceed. The author hopes that she has made a contribution to this effort.

BIBLIOGRAPHY

[1] B. P. Abbott et al. Observation of gravitational waves from a binary black hole merger. *Phys. Rev. Lett.*, 116(6), 2016.

[2] B. P. Abbott et al. Gw170104: Observation of a 50-solar-mass binary black hole coalescence at redshift 2.0. *Phys. Rev. Lett.*, 118(22), 2017.

[3] B. P. Abbott et al. Gw170814: A three-detector observation of gravitational waves from a binary black hole coalescence. *Phys. Rev. Lett.*, 119(14), 2017.

[4] S. Adler and A. Bassi. Gravitational decoherence for mesoscopic systems. *Physics Letters A*, 380(3), 2016.

[5] G. Amelino-Camelia. Gravity-wave interferometers as quantum-gravity detectors. *Nature*, 398(216-218), 1999.

[6] C. Anastopoulos and B. L. Hu. A master equation for gravitational decoherence: Probing the textures of spacetime. *Class. Quantum Grav.*, 30(165007), 2012.

[7] K. G. Arun and C. M. Will. Bounding the mass of the graviton with gravitational waves: effect of higher harmonics in gravitational waveform templates. *Class. Quantum Grav.*, 26(155002), 2009.

[8] M. Aspelmeyer, T. J. Kippenberg, and F. Marquardt. Cavity optomechanics. *Rev. Mod. Phys*, 86, December 2014.

[9] A. Bassi, K. Lochan, S. Satin, T. P. Singh, and H. Ulbricht. Models of wavefunction collapse, underlying theories, and experimental tests. *Rev. Mod. Phys*, 85, April 2013.

[10] M. P. Blencowe. Effective field theory approach to gravitationally induced decoherence. *Physical Review Letters*, 111(2), 2013.

[11] Y. Bonder, E. Okon, and D. Sudarsky. Can gravity account for the emergence of classicality? *Physical Review D*, 92(12), 2015.

[12] A. Bonnin, N. Zahzam, Y. Bidel, and A. Bresson. Characterization of a simultaneous dual-species atom interferometer for a quantum test of the weak equivalence principle. *Phys. Rev. A*, 92, 2015.

[13] H. P. Breuer and F. Petruccione. *The Theory of Open Quantum Systems*. Oxford University Press, 2002.

[14] D. E. Bruschi, T. C. Ralph, I. Fuentes, T. Jennewein, and M. Razavi. Spacetime effects on satellite-based quantum communications. *Physical Review D*, 90(4):045041, 2014.

[15] A. Buonanno and Y. Chen. Scaling law in signal recycled laser-interferometer gravitational-wave detectors. *Phys. Rev. D*, 67(062002), 2003.

[16] M. Carlesso and A. Bassi. Decoherence due to gravitational time dilation: Analysis of competing decoherence effects. *Phys. Lett. A*, 380, July 2016.

[17] J. R. Carson. A generalization of the reciprocal theorem. *Bell Labs Technical Journal*, 3(3), 1924.

[18] J. Chan, M. T. P. Alegre, A. H. Safavi-Naeini, J. T. Hill, A. Krause, S. Gröblacher, M. Aspelmeyer, and O. Painter. Laser cooling of a nanomechanical oscillator into its quantum ground state. *Nature*, 478:89–92, October 2011.

[19] Y. Chen. Macroscopic quantum mechanics: theory and experimental concepts of optomechanics. *J. Phys. B: At. Mol. Opt. Phys.*, 46(104001), 2013.

[20] C. Cohen-Tannoudji, J. Dupont-Roc, and G. Grynberg. *Photons and Atoms: Introduction to Quantum Electrodynamics*. John Wiley and Sons, 1989.

[21] J. Cripe et al. Observation of a room-temperature oscillator?s motion dominated by quantum fluctuations over a broad audio-frequency band. *arXiv:1802.10069*, Feb 2018.

[22] T. Damour and G. Esposito-Farese. Tensor-multi-scalar theories of gravitation. *Class. Quantum Grav.*, 9(2093), 1992.

[23] S. Dimopoulos, P. W. Graham, J. M. Hogan, and M. A. Kasevich. General relativistic effects in atom interferometry. *Phys. Rev. D*, 78(042003), August 2008.

[24] L. Diósi. A universal master equation for the gravitational violation of quantum mechanics. *Physics Letters A*, 120(8), 1987.

[25] L. Diósi. Centre of mass decoherence due to time dilation: paradoxical frame-dependence. *arXiv preprint arXiv: 1507.05828*, 2015.

[26] L. Diósi. Centre of mass decoherence due to time dilation: paradoxical frame-dependence. *J. Phys.: Conf. Ser.*, 800, 2017.

[27] P. A. M. Dirac. Generalized hamiltonian dynamics. *Can. J. Math*, 2(129), 1950.

[28] J. F. Donoghue. General relativity as an effective field theory: The leading quantum corrections. *Physical Review D*, 50(6), 1994.

[29] T. G. Downes, J. R. van Meter, E. Knill, G. J. Milburn, and C. M. Caves. Quantum estimation of parameters of classical spacetimes. *Phys. Rev. D*, 96(105004), 2017.

[30] P. W. Graham, J. M. Hogan, M. A. Kasevich, and S. Rajendran. Resonant mode for gravitational wave detectors based on atom interferometry. *Phys. Rev. D*, 94, November 2016.

[31] S. N. Gupta. Theory of longitudinal photons in quantum electrodynamics. *Proc. Phys. Soc. A*, 63(681), 1950.

[32] S. N. Gupta. Quantization of einstein's gravitational field: Linear approximation. *Proc. Phys. Soc. A*, 65(161), 1952.

[33] C. W. Helstrom. Quantum detection and estimation theory. *Journal of Statistical Physics*, 1(2):231–252, Jun 1969.

[34] D. Kafri, J. M. Taylor, and G. J. Milburn. A classical channel model for gravitational decoherence. *New J. Phys.*, 16(065020), 2014.

[35] M. A. Kasevich. *Atom Interferometry in an Atomic Fountain*. PhD thesis, Stanford University, 1992.

[36] S. Khorasni. Higher order interactions in quantum optomechanics: Revisiting theoretical foundations. *Applied Sciences*, 7, June 2017.

[37] C. Kiefer. *Quantum Gravity*. Oxford University Press, 2012.

[38] H. J. Kimble, Y. Levin, A. B. Matsko, K. S. Thorne, and S. P. Vyatchanin. Conversion of conventional gravitational-wave interferometers into quantum nondemolition interferometers by modifying their input and/or output optics. *Phys. Rev. D*, 65(022002), 2001.

[39] D. Kleckner, I. Pikovski, E. Jeffrey, L. Ament, E. Eliel, J. van den Brink, and D. Bouwmeester. Creating and verifying a quantum superposition in a micro-optomechanical system. *Phys. Rev. Lett.*, 116(161303), 2016.

[40] C. K. Law. Interaction between a moving mirror and radiation pressure: A hamiltonian formulation. *Phys. Rev. A*, 51, March 1995.

[41] Y. Ma et al. Proposal for gravitational-wave detection beyond the standard quantum limit via epr entanglement. *Nature Phys*, 13, May 2017.

[42] D. V. Martynov et al. The sensitivity of the advanced ligo detectors at the beginning of gravitational wave astronomy. *Phys. Rev. D*, 93, June 2016.

[43] H. Miao, R. X. Adhikari, Y. Ma, B. Pang, and C. Yanbei. Towards the fundamental quantum limit of linear measurements of classical signals. *Phys. Rev. Lett.*, 119(050801), 2017.

[44] C. W. Misner, K. S. Thorne, and J. A. Wheeler. *Gravitation*. W. H. Freeman and Company, 1973.

[45] H. Müller, A. Peters, and S. Chu. A precision measurement of the gravitational redshift by the interference of matter waves. *Nature*, 463, 2010.

[46] T. Oniga and C. H.-T. Wang. Quantum dynamics of bound states under space-time fluctuations. *J. Phys. Conf. Ser.*, 845(012020), 2016.

[47] T. Oniga and C. H.-T. Wang. Quantum gravitational decoherence of light and matter. *Phys. Rev. D*, 93(044027), 2016.

[48] B. H. Pang, F. Y. Khalili, and Y. Chen. Universal decoherence under gravity: A perspective through the equivalence principle. *Phys. Rev. Lett*, 117, 2016.

[49] M. G. Paris. Quantum estimation for quantum technology. *Int. J. Quant. Inf.*, 7, 2009.

[50] R. Penrose. On gravity's role in quantum state reduction. *Gen. Rel. and Grav.*, 28, May 1996.

[51] R. Penrose. On gravity's role in quantums state reduction. *General Relativity and Gravitation*, 28(5), 1996.

[52] M. E. Peskin and D. V. Schroeder. *An Introduction to Quantum Field Theory*. Perseus Books, 1995.

[53] A. Peters. *High precision gravity measurements using atom interferometry*. PhD thesis, Stanford University, 1998.

[54] A. Peters, K. Y. Chung, and S. Chu. High-precision gravity measurements using atom interferometry. *Metrologia*, 38(25), 2001.

[55] I. Pikovski, M. R. Vanner, M. Aspelmeyer, M. Kim, and Č. Brukner. Probing planck-scale physics with quantum optics. *Nature Physics*, 8(5):393–397, 2012.

[56] I. Pikovski, M. Zych, F. Costa, and Č. Brukner. Time dilation in quantum systems and decoherence: Questions and answers. *arXic preprint arXiv:1508.03296*, 2015.

[57] I. Pikovski, M. Zych, F. Costa, and C. Brukner. Universal decoherence due to gravitational time dilation. *Nature Physics*, 11:668, 2015.

[58] T. P. Purdy, R. W. Peterson, and C. A. Regal. Observation of radiation pressure shot noise on a macroscopic object. *Science*, 338:801–804, February 2013.

[59] N. F. Ramsey. *Molecular Beams*. Oxford University Press, 1956.

[60] G. Rosi et al. Quantum test of the equivalence principle for atoms in coherent superposition of internal energy states. *Nature Communications*, 8, June 2017.

[61] L. Seveso, M. A. C. Rossi, and M. G. A. Paris. Quantum metrology beyond the quantum cramer-rao theorem. *Phys. Rev. A*, 95, 2017.

[62] K. Stannigel, P. Rabl, A. S. Sorensen, M. D. Lukin, and P. Zoller. Optomechanical transducers for quantum-information processing. *Phys. Rev. A*, 84, October 2011.

[63] P. Storey and C. Cohen-Tannoudji. The feynman path integral approach to atomic interferometry. a tutorial. *Journal de Physique II*, 4(11), 1994.

[64] The LIGO Scientific Collaboration and the Virgo Collaboration. First search for nontensorial gravitational waves from known pulsars. *Phys. Rev. Lett.*, 120(3), 2018.

[65] M. Toroš, Großardt, and A. Bassi. Quantum mechanics for non-inertial observers. *arXiv:1701.04298*, Jan 2017.

[66] M. Tsang, H. M. Wiseman, and C. M. Caves. Fundamental quantum limit to waveform estimation. *Phys. Rev. Lett.*, 106(090401), 2011.

[67] W. G. Unruh. Notes on black-hole evaporation. *Phys. Rev. D*, 14, August 1976.

[68] L. Viola and R. Onofrio. Testing the equivalence principle through freely falling quantum objects. *Physical Review D*, 55(2):455, 1997.

[69] D. F. Walls and G. J. Milburn. *Quantum Optics*. Springer, 2008.

[70] S. Weinberg. Photons and gravitons in s-matrix theory: Derivation of charge conservation and equality of gravitational and inertial mass. *Phys. Rev.*, 135(4B), 1964.

[71] C. M. Will. The confrontation between general relativity and experiment. *Living Rev. Relativity*, 4, 2014.

[72] H. Wiseman and G. Milburn. *Quantum Measurement and Control*. Cambridge University Press, 2010.

[73] P. Wolf, L. Blanchet, C. J. Bordé, S. Reynaud, C. Salomon, and C. Cohen-Tannoudji. Does an atom interferometer test the gravitational redshift at the compton frequency? *Nature*, 463, 2010.

[74] E. E. Wollman, C. U. Lei, A. J. Weinstein, J. Suh, A. Kronwald, F. Marquardt, A. A. Clerk, and K. C. Schwab. Quantum squeezing of motion in a mechanical resonator. *Science*, 349:952–955, August 2015.

[75] H. Yang, H. Miao, D.-S. Lee, B. Helou, and Y. Chen. Macroscopic quantum mechanics in a classical spacetime. *Physical review letters*, 110(17):170401, 2013.

[76] Z.-q. Yin, W. L. Yang, and L. M. Duan. Quantum network of superconducting qubits through an optomechanical interface. *Phys. Rev. A*, 91, January 2015.

[77] N. Yunes, K. Yagi, and F. Pretorius. Theoretical physics implications of the binary black-hole mergers gw150914 and gw151226. *Phys. Rev. D*, 94(084002), 2016.

[78] M. Zych and u. Brukner. Quantum formulation of the einstein equivalence principle. *arXiv:1502.00971*, February 2015.

[79] M. Zych, F. Costa, I. Pikovski, T. C. Ralph, and Č. Brukner. General relativistic effects in quantum interference of photons. *Classical and Quantum Gravity*, 29(22):224010, 2012.